Tobias Stegk

Establishment, implementation and operation of a High-Throughput Experimentation (HTE) plant for dry ceramic powders

Cuvillier Verlag Göttingen
Internationaler wissenschaftlicher Fachverlag

Establishment, implementation and operation of a High-Throughput Experimentation (HTE) plant for dry ceramic powders

Vom Promotionsausschuss der
Technischen Universität Hamburg-Harburg
zur Erlangung des akademischen Grades

Doktor-Ingenieur (Dr.-Ing.)

genehmigte Dissertation

von
Tobias Stegk
aus Kronberg

2009

Bibliografische Information der Deutschen Nationalbibliothek
Die Deutsche Nationalbibliothek verzeichnet diese Publikation in der Deutschen Nationalbibliografie; detaillierte bibliografische Daten sind im Internet über http://dnb.ddb.de abrufbar.
1. Aufl. - Göttingen : Cuvillier, 2009
Zugl.: (TU) Hamburg-Harburg, Univ., Diss., 2009

978-3-86955-032-9

1. Gutachter:	Prof. Dr. rer. nat. Gerold A. Schneider
2. Gutachter:	Prof. Dr. Dr. h.c. Frerich J. Keil

Tag der mündlichen Prüfung: 16. Juni 2009

Nonnenstieg 8, 37075 Göttingen
Telefon: 0551-54724-0
Telefax: 0551-54724-21
www.cuvillier.de

1. Auflage, 2009
Gedruckt auf säurefreiem Papier

978-3-86955-032-9

"*You look at where you´re going and where you are and it never makes sense, but then you look back at where you´ve been and a pattern seems to emerge. And if you project forward from that pattern, then sometimes you can come up with something.*"

- Robert M. Pirsig: *Zen and the Art of Motorcycle Maintenance*

Danksagung

Zu allererst möchte ich mich bedanken bei Herrn Prof. Dr. Gerold Schneider für das Interesse an der Durchführung und die Betreuung dieser Arbeit sowie für geduldige Geburtshilfe bei zentralen Ideen und schwierigen Formulierungen.

Herrn Prof. Dr. Frerich Keil gilt mein Dank für die Übernahme des Zweitgutachtens.

Ein herzliches Dankeschön an Herrn Dr. Rolf Janssen für fachliche Betreuung und gute Vorschläge zur richtigen Zeit.

Bei allen anderen Mitarbeitern im Institut für Keramische Hochleistungswerkstoffe bedanke ich mich für das ausgezeichnete Arbeitsklima, die gute Stimmung, Freundlichkeit, Hilfsbereitschaft, für kulturelle Herausforderungen sowie für viele schöne Erinnerungen.

Diese Arbeit wäre nicht möglich gewesen ohne den Einsatz und den Einfallsreichtum von Thomas Pomfrett und Michael Agthe. Tausend Dank auch Euch Beiden.

Ich danke meinen Eltern Brigitte und Dr. Arno Stegk, die mir eine lange, sorgenfreie Ausbildungszeit ermöglicht haben und diese durch ihre stets zuversichtliche moralische und materielle Unterstützung erleichtert und bereichert haben.

Schließlich ein großer Dank an meine liebe Katrin, die meine Freuden teilt, meine Sorgen halbiert und die versteht, wenn ich hier und heute schreibe: “And now for something completely different!”

Roskilde im Juni 2009.

Contents

Nomenclature

α	Level of significance of statistical test
β_0	Regression coefficient
β_1	Regression coefficient
$\Delta\overline{p_Y}$	[%] Relative deviation of mean values of yttria concentration between sample and reference
$\hat{\mathbf{c}}$	Vector containing six molar fractions of masterbatches as a result of algebraic model
$\overline{\Delta w_M}$	[%] Mean of differences between monoclinic phase content of high-throughput library samples and reference library samples
$\overline{p_Y^{reference}}$	[scale − %] Mean value of yttria concentration of reference sample taken from library MB4
$\overline{p_Y}$	[scale − %] Mean value of yttria concentration
σ_0^2	Reference variance for F-Test
σ_i^2	Variance to be F-tested against reference for heteroscedasticity
$CVar$	[%] Coefficient of Variance
d_{50}	[m] Median of grainsize distribution
H_0	Null-hypothesis of statistical test
H_A	Alternative hypothesis of statistical test
I_M	Intensity of an XRD peak resulting from monoclinic phase
$I_{C,T}$	Intensity of an XRD peak resulting from cubic and tetragonal phase
$L1, L2, L3$	[m] Characteristic length scale for diffusion mechanisms while sintering
N	Number of distinguishable compositions resulting out of theoretical combinatoric assumptions
n_C	Number of incremental compositions in combinatorial model
n_E	Number of chemical elements for combinatorial model
n_p	Number of process factors in combinatoial model
n_r	Combinatorial range for combinatorial model
n_{pv}	Number of parametic values in combinatorial model

N_{sc}	Number of starting compounds in Single Sample Concept [HA05]
P	Probability distribution
P_0	Probability distribution to be tested against in hypothesis test
p_Y	[scale − %] Yttria concentration
q	Number of distinguishable solid phases in Single Sample Concept [HA05]
w_M	[weight − %] Mass fraction of monoclinic phase from polymorph-method
x, y, z	Stoichiometric coefficients
x_M	[%] Fraction of monoclinic phase from polymorph-method
$\mathbf{p}$	Vector containing n minimization parameters
$\mathbf{S}$	Vector containing m data points of investigated XRD pattern
$\mathbf{x}$	Matrix containing m data points of n XRD patterns stored in a database to be compared to patterns under investigation
ANN	Artificial Neural Network
CHTE	Combinatorial High-Throughput Experimentation
DOE	Design of Experiments
HTE	High-Throughput Experimentation
KNN	Sodium Potassium Niobate, $K_{0.5}Na_{0.5}NbO_3$
LTKNN	Sodium Potassium Niobate modified by Li and Ta, $(K_xNa_{1-x})_{1-y}Li_y(Ta_zNb_{1-z})O_3$
MB	Masterbatch
MC	Monte Carlo algorithm
MPB	Morphotropic Phase Boundary
PCA	Principal Component Analysis
PZT	Lead Zirconate Titanate, $Pb(Ti_xZr_{1-x})O_3$
TZP	Tetragonal Zirconia Polycrystal
XRD	X-Ray Diffraction
YTZ	Yttria-toughened Zirconia

1 Introduction

The most conventional production route towards an advanced ceramic material consists of the conditioning, shaping and heat-treatment of dry precursor powders. This procedure is traditionally time-consuming, taking up one or more days per batch of material. Fortunately, this process can be scaled up arbitrarily and considerations of time recede in an industrial environment. For scientific work however, the mentioned time frame is often a hindrance since in contrast to industrial materials production where the emphasis frequently lies on a maximum batch size, the materials scientist seeks to synthesize and learn about as many distinct materials as possible. Thus, the experimental effort scales with the duration of one synthesis cycle.

An opportunity to conduct materials research in a more efficient way is high-throughput experimentation (HTE). The fundamental idea of this scientific paradigm is to maximize the density of information gained from an experiment with respect to experimental time by means of parallelization and automation of synthesis and analysis procedures.

HTE had seen extensive use in pharmaceutical research [MSS07] as well as organic chemistry [Sch04, MSS07], frequently supported by a design of experiments based on combinatorial models as well as elaborate data mining approaches to filter experimental results for valuable knowledge. An adaption to material science with its multi-parameter experimental spaces was obvious and since the 1990s HTE has been common practice also in ceramics research [Sie98, MSS07].

For ceramics however, the vast majority of works reported in literature are based on thin-film technology or use liquid-phase, colloidal processing techniques, both of which allow for an easy, continuous change of composition between samples. Frequently though, samples resulting out of such HTE campaigns fail to allow conclusions with respect to the behaviour of the respective bulk material. Conse-

quently, in this work an attempt is made to implement an HTE setup emulating a conventional powder metallurgical synthesis route that yields ceramic bulk materials.

In the beginning of the work an illustrative part describes the HTE setup as well as the necessary equipment. Requirements leading to the acquisition or adaption of the equipment are illucidated.

Subsequently, the setup is validated by using yttria-toughened zirconia, a well-known ceramic material system. Conventionally produced reference samples are compared to sample libraries from the HTE setup and their difference is evaluated statistically.

Finally, the setup is applied to a novel piezoelectric materials system, namely sodium potassium niobate (KNN). Starting from a well-known subsidiary KNN system, it is shown that the presented HTE-approach allows for an efficient and reliable detection of phase boundaries. Phase boundaries constitute areas of amplified interest in piezoceramics due to the possibility of finding maximum piezoelectric behaviour in their vicinity. The successful employment of a software-based data mining approach for this purpose is demonstrated.

Due to the parallelized handling of small amounts of dry powders the samples from the HTE setup show an inferior composition homogeneity compared to conventionally prepared ceramics. In the course of the work the reasons underlying this effect are closely examined and consequential guidelines for operation and experimental planning are developed.

2 Fundamentals

2.1 Origins

Since its development in the 19th century by Russian chemist Dimitriy Mendeleyev the Periodic Table of Elements has been used for the purpose of classification and comparison of chemical compounds with respect to the positions of their elements in this ingenious tabular arrangement. Few scientists have been capable of perceiving it in addition as a well-ordered catalogue of building blocks to synthesize new and useful substances in a systematic manner. Among these visionaries were people like the German chemist Alwin Mittasch who in the beginning of the 20th century undertook 20000 experimental runs while systematically trying to develop an efficient catalyst for Haber-Bosch-synthesis of Ammonia [Caw03a]. Paul Ehrlich synthesized several hundred trivalent arsenic compounds and finally succeeded in finding Salvarsan, a drug against syphilis [Caw03a]. In the late 19th century US-American inventor Thomas Edison tested several thousand substances until he came up with an optimal material for the filament inside the light bulb. Edison is probably the most renowned of the scientists using this systematic approach and consequently has lent his name to a class of experiments conducted in his spirit [AXZ02, Caw03a].

To understand the scope the Periodic Table offers as a mere record of potential modular blocks one can use the basic models of combinatorics, a subset of discrete mathematics that deals with quantification of combinations of distinguishable and indistinguishable objects. Assuming 50 elements out of the Periodic Table to be useful and stable and, for a start, equimolar compositions of those 50 elements the combinatoric model of a disordered and unreclined sample can be used. The total number of different combinations in this case would be [BB95]

$$N(n_E, n_r) = n_E! / \left[n_r! \, (n_E - n_r)! \right] , \tag{2.1}$$

where n_E is the number of elements (i.e. 50), n_r is the combinatorial range (e.g. 2 for binary) and N is the number of possible combinations. It follows that there are theoretically 1225 possible binary, 19600 ternary and 230000 quaternary molecules or compositions.

Dropping the restriction of equimolarity one can make use of the model of a disordered, reclined sample [BB95]:

$$N(n_C, n_r) = (n_C + n_r - 2)!/\left[(n_C - 1)!\,(n_r - 1)!\right]. \tag{2.2}$$

n_C here is the number of different incremental compositions. Molecules are thus treated as ordered partitions of n_C parts into words of length $n_r - 1$, where the subtraction of 1 is due to stochiometry. Of course equation 2.2 pertains to each of the combinations calculated by equation 2.1. For example for a hypothetical binary combination AB $n_C = 11$ (concentration increments of 10%) would mean A_0B_1, $A_{0.1}B_{0.9}$, $A_{0.2}B_{0.8}$,..., A_1B_0. Hence, the size for this concentration space can be estimated by

$$N(n_E, n_C, n_r) = N(n_E, n_r) \cdot N(n_C, n_r). \tag{2.3}$$

Table 2.1 shows the numbers of some possible combinations.

$\mathbf{n_C}$	$\mathbf{n_r = 2}$	$\mathbf{n_r = 3}$	$\mathbf{n_r = 4}$
6	7350	411600	12.9×10^6
11	13475	1.3×10^6	65.8×10^6
21	25725	4.5×10^6	0.4×10^9

Table 2.1: Estimate of possible molecules from 50 starting elements according to equation 2.3.

It is obvious though that the number of actual experimental runs would be even higher. In addition to formulation factors mentioned so far the experimental space is spanned by all variables in the system [Caw03b]. Thus process factors like for example annealing temperature or mixing time can not be neglected. In fact including these factors will make the experimental space grow geometrically,

$$N(v_{pv}, n_p) = N(n_C, n_r) \cdot n_{pv}^{n_p}, \tag{2.4}$$

with growth factor n_{pv} being the number of parametric values of all n_p process factors. For applications in materials science the numbers resulting from these thought experiments can be put into perspective when one considers the number of known inorganic phases in the late 1980s to be approximately 24000 [AXZ02]. The experimental space mentioned above therefore constitutes both a challenge and a chance for modern materials development. The challenge can be met by combinatorial high-throughput experimentation (CHTE) and high-throughput experimentation (HTE) .

CHTE and HTE can be defined as "*a set of techniques for creating a multiplicity of compounds and then testing them for activity*" [Caw01]. The earliest antecedents of this paradigm fell together with the development of what is known today as Design of Experiments (DOE) [Caw03a] and can be found in the field of agriculture where due to the extreme running times of experiments (typically multiples of years) a parallelization became inevitable. The distinction between HTE and CHTE is not well-defined. In general, the former refers to the parallelized and/or automatized sequential synthesis and analysis of a high number of samples, where preconceptions about the sample behaviour and the analytic results lead to a pre-experimental containment of the experimental space. In the latter this containment does not exist to the same degree which explains the necessity for different procedures for the design of experiments and the evaluation of their results mentioned later in this chapter.

Like many other technologies, HTE and CHTE was only made possible on a larger scale for industry and academia by the advent of affordable and user-friendly computer technology in the 50s of the last century [PM07]. The 60s and 70s brought an interest in the quantitative assessment of biochemical structure-activity relationships and also saw the development of the first autosampling units which effectively introduced robotics into a laboratory work field. Consequently, pharmaceutical companies started putting more and more effort into utilizing CHTE for their needs to lower their time to market [PM07, Caw01]. CHTE-prepared compound sets, so-called "libraries", with up to 10^6 distinct samples are produced

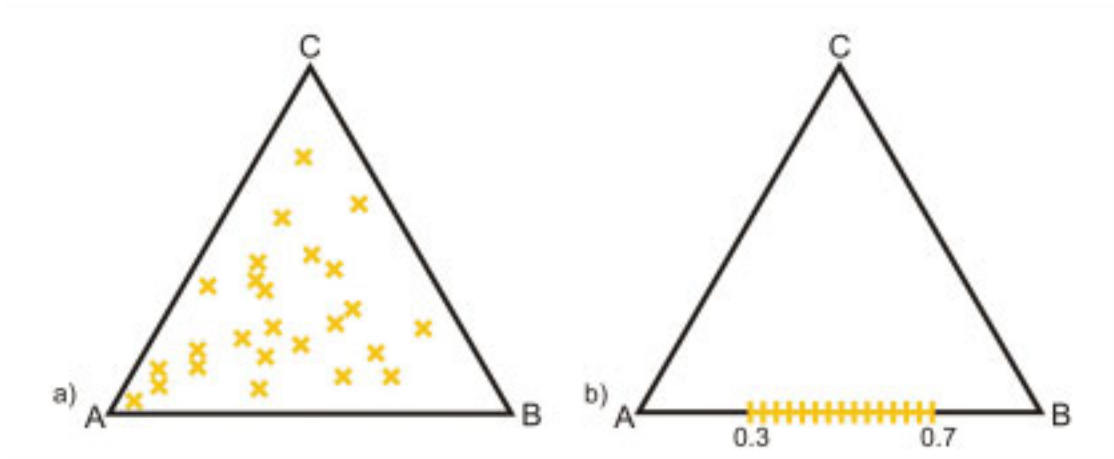

Figure 2.1: Scheme exemplifying the difference between CHTE and HTE concepts with a) showing a typical experimental space in case of a CHTE and b) of an HTE approach.

routinely by most pharmaceutical manufacturers these days [Caw01].

The first works in CHTE of materials science surprisingly go back to the 60s of the last century. Kennedy *et al.* [KSD+65] and Miller and Shirn [MS67] used cosputtering techniques to produce the first multiple-component phase libraries in materials science. Kennedy *et al.* were able to demonstrate agreement between their "proto"-HT phase diagrams and the respective conventional ones by means of electron diffraction. Miller and Shirn succeeded in measuring the electrical resistivity over the full range of composition in the binary Au-SiO_2-system.

In 1970 Hanak published his work on the Multiple-Sample-Concept [Han70] which many authors claim to be the forerunner of modern day CHTE materials science. Hanak made a strong case for dealing with the topic of efficiency in materials development when he wrote "*The present approach to the search for new materials suffers from a chronic ailment, that of handling one sample at a time in the processes of synthesis, chemical analysis and testing of properties*" [Han70]. He suggested to implement a radio frequency sputtering device with two or three different targets that could be sputtered simultaneously onto one substrate. Varying film thickness on the substrate as a function of their position relative to the respective target sections on the substrate was responsible for the varying local

compositions. Hanak later blamed a lack of computing power at the time to have prevented his concept from having broad success in the materials community [Han03]. Consequently, the HT-strategy was not implemented on a larger scale until this problem was relieved.

More than two decades later Schultz *et al.* published a paper that marked the beginning of modern combinatorial and HTE materials science [XSB+95]. Catalysed by the developments in biochemistry and pharmaceutical industry mentioned above numerous high-throughput synthesis and screening schemes had been implemented. This newly emerging discipline called combinatorial chemistry also brought the ideas of spatially addressable libraries and gene chips [XT03] and thus the trend to parallelize and minimize experiments. These ideas were taken up by Schultz *et al.* when they deposited metal oxides on top of each other using a masking scheme. The major difference with respect to Hanak's work was the spatial addressability of the samples. The experiments yielded various cuprate superconductors.

CHTE has since developed rapidly spanning the whole field of materials development as it has been applied to all major classes of materials incorporating all possible aggregate states of educts and a plethora of processing and analysis concepts.

2.2 Industrial and academic potential

Industrial HTE originated from academic backgrounds, e.g. at UC Berkeley [Xia98, CTX99, CGT+98], which lead to the foundation of Symyx as the first commercial supplier of hardware and service in the field. Parallely several hundred million US-dollars worth of HT-technologies were being implemented in various projects in large scale industry aiming for the most part at the optimization of known materials and processes. In the US, federal agencies like NIST (National Institute of Standards and Technologies), North Dakota State University or University of Iowa followed. Service providers like Symyx also spawned the interest in the European industrial environment and European start-ups followed in Symyx'

footsteps. Examples were hte (Germany), Avantium (Netherlands) and Accelab (Germany). These developments in turn allowed for collaborations between industry and academia which produced among others DPI (Netherlands), FLAMAC (Belgium) and Insight Faraday (UK) [DAHfM06]. At the time of writing it is estimated that by 2010 a yearly turnover of US-$ 400 million will result from sales of HT-equipment in Western Europe alone. The world market for HT-technologies and services is estimated to be at US-$ 1 billion per year with growth rates of 7% [FS03].

The automatized parallel or rapid sequential execution of large numbers of experiments has also remained attractive to academia where money and manpower are traditionally even more limited than in industrial environments. Hence the exceeding presence of HTE- and CHTE-related topics in the respective scientific journals. Potyrailo and Maier [PM07] state that in 2007, the growth-rate of HTE-related publications in materials research has exceeded that of rational materials development publications. About 70% of those publications deal with synthesis and measurement, another 11% with the design of experiments and 8% with the organization and mining of the reaulting data [PT05]. It is obvious from these figures that HTE needs a variety of academic orientations to be impelled.

Indeed the absolute numbers of publications in the field of materials have seen a strong incline within the 10 years leading up to 2004 as can be seen from a search in *ISI Web Of Science* (http://portal/isiknowledge.com/).

Interestingly enough, the search for "High-Throughput" *AND* various materials groups does not sum up to the numbers for "High-Throughput" *AND* "Materials" with the difference increasing over the years. It is possible that workers in the field are actually starting to perceive themselves as "High-Throughput Material Scientists" instead of, say, ceramists using HTE. Although the main reason for this phenomenon is supposedly the rising use of a common terminology of HTE that now reaches back to the sources of HTE, namely various disciplines of what is nowadays termed "life sciences". Their works would surface under the keyword "Materials" but not under any of the material classes mentioned above.

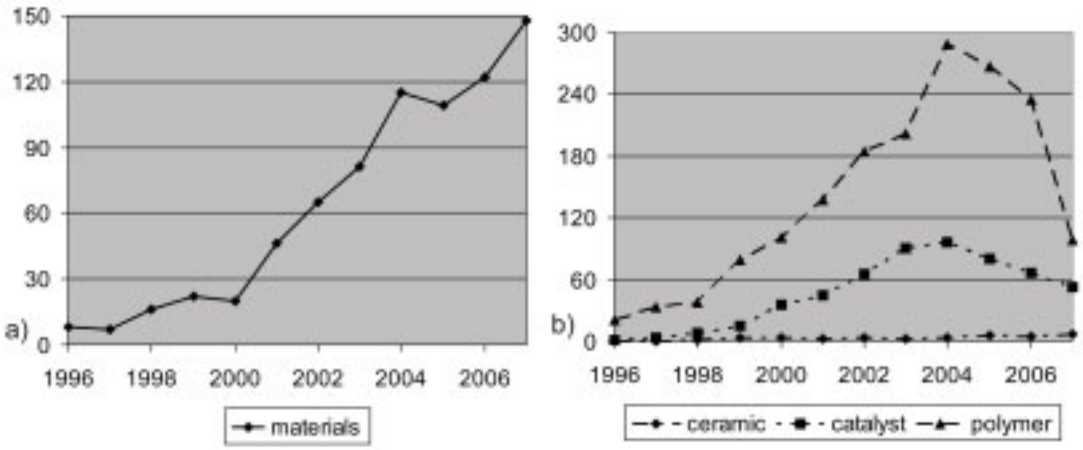

Figure 2.2: Number of publications from literature research with keywords "High-Throughput" AND "Materials" (a) and "High-Throughput" AND "Ceramics", "Catalyst" and "Polymer" respectively (b).

2.3 CHTE and HTE in Materials Science

It has been claimed that "*chemistry has now accelerated to approach the speed of early computers*" [Caw03a]. The same would hold for materials science as vital part of chemistry and indeed a look at CHTE in materials science can verify this quote. The conventional and still dominant approach in the development of materials can be classified as "one-at-a-time", i.e. the scientist synthesizes a batch of material and subsequently tests it for one or more specific properties (activity). This procedure will be repeated with changed synthesis and/or testing parameters until a satisfactory result is obtained. Parametrical change in each iteration is done according to previous knowledge or just according to educated guessing. Therefore new materials or material properties are being discovered more often than once by serendipity and it is obvious that for scientific endeavors in a large experimental space this strategy holds high risk of missing optima and hence is disadvantageous.

As mentioned earlier the goal of any CHTE effort is to synthesize and scan large experimental spaces by allowing a more efficient use of time and material. It is obvious from these preconceptions that materials science is predestined for this kind of experimental approach. Materials and their behaviour, much like pharmaceuticals, depend largely on an abundance of formulation factors. Additionally a plethora of process parameters affect the activity. CHTE and HTE allow the

materials scientist to systematically analyse phase diagrams as a whole and not only manoeuvre within them. Subsequent data mining using software or database tools allows for the exploration of new structure-property-relationships. As a result the scientist is capable of deducing necessary descriptors to move from qualitative space, e.g. “good”, “better”, “best” material behaviour, to a quantitative space that constitutes true knowledge.

In pharmaceutical research the goal is usually for one compound with a specified bio-chemical activity often resulting out of an organic reaction in a liquid-medium whereas materials scientists seek to find systems meeting physical, chemical and structural prerequisites all at once. This fact creates additional challenges for the implementation of HTE in materials science. Firstly, unlike for pharmaceutical substances the “similar property principle” stating that similar structure implies similar behaviour does not necessarily hold for materials [Sch04]. The most evident documentation of this fact is the use of phase diagrams as graphical representations of non-linear physical behaviour. In particular, the concept of similarity is misleading in materials science. In organic and pharmaceutical technology certain molecular features like, say, the amount of C-atoms in the longest chain, can be used as descriptors, directly linking molecular structure to activity [Ran90]. Materials behaviour is frequently dominated by an interaction of molecular and supra-molecular characteristics. Secondly, materials synthesis paths are only rarely downscalable to the dimensions of one sample without problems. Very often this shortcoming will result out of the necessity for good homogeneization which gets more and more problematic when reaching towards smaller dimensions. Finally, resulting out of the facts mentioned above, in pharmaceutical research, activity can usually be detected optically by e.g. measuring the turbidity of a titre. Optical analysis methods though, can be parallelized and automated easily as the measured quantity is usually homogeneous over the sample. In materials the desired activities usually result out of an interplay of structural properties like e.g. microstructural defects and analysis methods for those generally require frequent interference of an experienced operator.

Among the materials classes the objections just outlined are the most valid for ceramic materials. The very nature of HTE states that every sample pro-

duced is ideally supposed to be a distinct material, different from its neighboring samples. Consequently, the homogeneity, purity and reproducibility demands the HT-scientist has concerning one sample are the same the conventional scientist has concerning a whole batch of material. As a result polymers and also catalytic materials lend themselves a lot better to HTE-procedures. Often they are synthesized from liquid or viscous precursors and the reactions involved will proceed under more or less ambient conditions. Advanced ceramics in turn pose a greater challenge. Due to their powdery raw state and the aggressive synthesis conditions, notably highly elevated temperatures, their pure and reproducible synthesis is a complex matter even when utilizing conventional approaches. Ceramic materials are more liable to impurities, as their influence very often does not scale with their concentration and can lead to non-linear effects, like phase changes. Furthermore the ceramic material structure consists of crystallites. Thus any homgenization of the ensuing material is superimposed by interfacial influences. This dilemma is reflected in the inferior numbers of publications. It is also the topic and the motivation of this work.

2.3.1 Synthesis of HT-libraries in ceramics technology

The two principally different approaches to synthesize HT-libraries in materials science can be seen from the schematic sketch in figure 2.3. For spatially addressable libraries the individual samples should be homogeneous within but should differ in concentration from their neighboring samples. Very often these libraries are set up in the format of microtitre plates with 96 samples, a remnant from the life-science background of CHTE.

In contrast, the composition spread approach usually allows for far fewer samples, most often just one varying the concentration of the respective components gradually. It is obvious that a liquid phase library synthesis route does not lend itself to the preparation of composition spread samples as a well-defined gradual change of component concentration is not possible using liquid precursors.

The most frequently applied process for liquid phase prepared libraries is the robot-assisted dosage of mostly aqueous solutions of the respective salts to be com-

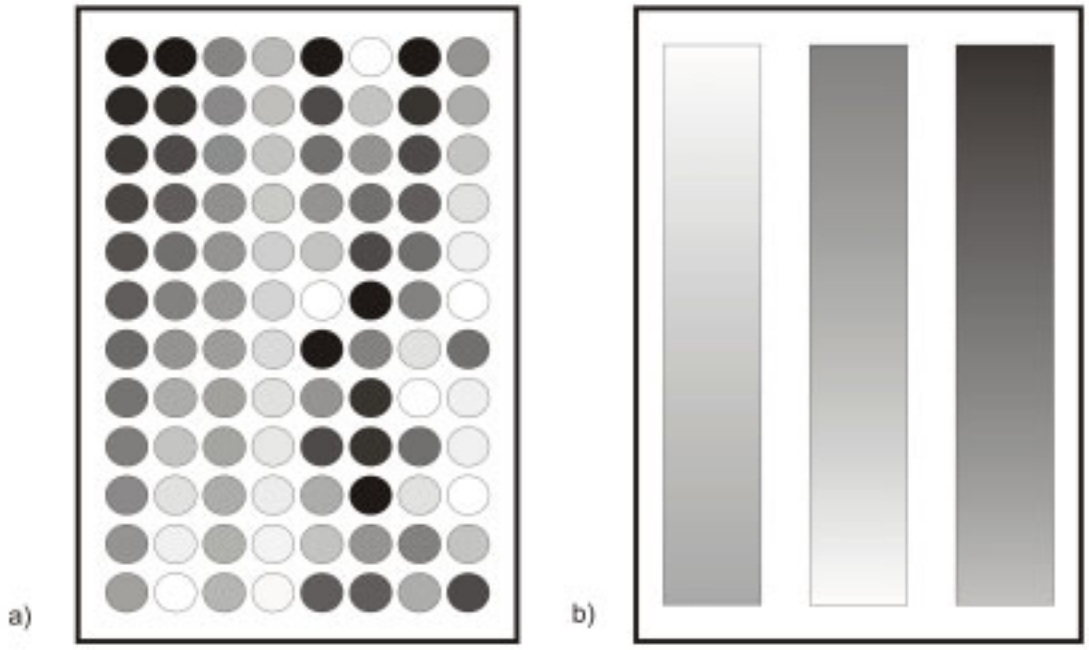

Figure 2.3: Schematic of spatially addressable (left) and a composition spread or concentration gradient (right) HT-library. Color change is correlated with respective composition.

bined. Fujimoto *et al.* used a commercial liquid handling robot to dose and mix aqueous precursors [FTSW04, FW05]. They produced libraries in three pseudo-ternary oxide systems by subsequent heat treatment and tested for solubility limits of 3d elements. Reichenbach *et al.* used a slightly different approach which they called polymerizable-complex method (PCM) [RM01]. After mixing, their aqueous precursor solutions were used to form complexes with citric acid. In a second step these complexes were polyesterified to form organo-metallic networks which could be transformed into a homogeneous ceramic material by a pyrolysis step. The resulting materials were tested for variations in their surface area and also for their capacity to catalyze diesel soot combustion [RAM03].

In the case of ceramic suspensions the dosing can be achieved by ink-jet printing techniques that allow the drop-on-demand deposition of suspensions with up to 40 vol-% of ceramic powders where typically waxes are used as suspension media [EECE01]. Much work has been done on the development and optimization of ceramic inks for use in CHT and HT ceramics research [TEE97, TE98] and on the

development of respective technologies to mix and precisely dispense those inks [ME02, EECE01].

Several conventional techniques for liquid phase synthesis of ceramics were adapted for HTE. Henderson *et al.* used two different forms of sol-gel synthesis on their quest for transparent, conductive ceramic materials [HAHW05]. Alcoholic precursor solutions were gelled by solvent removal and by water addition respectively. Parallel precipitation under elevated temperatures of up to 48 samples was reported by Wendelbo *et al.*. They used a so-called *MultiAutoclave* [ADKW98] to study phase structure of perovskites and the influence of various A-site cations, pH-value and organic additives thereupon [WAK$^+$06].

Most of the liquid phase techniques mentioned above yield libraries of samples in thin-film dimensions. Few lead to bulk samples with very minute sample masses. Pullar *et al.* presented an HT-approach that produced libraries of bulk ceramic samples with size of a few millimetres [PZC$^+$07a, PZC$^+$07b]. They were synthesized from aqueous inks highly loaded with the educts $BaTiO_3$ and $SrTiO_3$. The samples were to be printed directly onto suitable substrates on which they were supposed to undergo all further synthesis and analysis steps. Even though samples were generated and analyzed, Pullar reports that different substrates had to used for each processing step, making it necessary to transfer samples manually and one by one. The search for such a suitable substrate posed a problem that remained unresolved [ZCYE07].

Various means of physical vapour deposition (PVD) can be used for the vapour phase route of ceramic HT-library synthesis. All those techniques differ only in the form of energy that is used to release the respective ions from the target. This energy creates in vacuum a plume of vaporized material which is accelerated towards a substrate. Thus, the main challenge here lies in banning the material onto clear-cut spots. Usually physical or lithographic masking techniques are applied to this end [Sun03]. For instance, Xiang used pulsed laser deposition (PLD) and radio frequency sputtering to create spatially addressable as well as linear-gradient libraries of oxide materials [Xia99]. The author raised awareness to the fact that when depositing multiple layers of material on top of each other, instead of single-

phase material only a set of binary phases is formed. This problem has to be met by heat-treatment cycles tailored respectively and is only suitable for materials with high diffusivity.

Laser molecular beam epitaxy (MBE) was employed by Jin *et al.* to fabricate a set of of epitaxial zinc oxide films doped with 3d transition metal elements to study their solution behaviour in an oxide matrix [JMF+00]. The adjustment of concentrations was achieved by varying the respective numbers of ablation pulses. Ohkubo *et al.* solved this problem by translating a heated substrate in front of the target plume which was focussed by a physical slit mask [OCK+04]. Van Dover *et al.* successfully optimized electric charge density in the Zr-Sn-Ti-oxide system [vDSFH99]. These workers arranged sputter guns with the respective elements as targets in an angle towards an Si-wafer substrate.

2.3.2 Preparation of solid phase HT-libraries

For the solid phase preparation of libraries only few approaches exist in literature at present. Mohebi *et al.* described a setup in which powders were dosed via reversible destruction of solids bridges in glass hopper outlets [MYE06]. By means of acoustic energy which was transferred into the hoppers via steel rods the powder flow was initialized and could be inhibited by stopping the influx of acoustic energy [YE04a]. Using an automatic x-y-table this setup had been conceived for solid freeforming using metal powders but was also used in the preparation of powder metallurgic libraries [YE04b].

Zhao came up with a very different approach for a solid phase library synthesis. Bulk wedges of pure elements were combined, exposed to hot-isostatic pressing (HIP) and subsequent heat treatment at ambient pressure to promote interdiffusion and oxidation. Various diffusion couples and multiples have been studied both mechanically by nano-indentation and structurally by X-ray diffraction [Zha01]. Zhao's work showed that it was possible to very densely scan multi-phase areas of the diffusion couples with a distance between measuring points of 25 µm translating into a concentration resolution of <0.7 at-%. Nevertheless, the sample preparation involved an assembly by welding, hot-isostatic pressing, slicing as well as a final

heat-treatment. Also substantial amounts of pure metals were necessary as raw materials. A modular and flexible use was hence impossible.

Referring to Hanaks Mutliple-Sample-Concept [Han70] mentioned above, Hulliger *et al.* subsumed their work under the name Single-Sample-Concept [HA04]. The workers claimed that one sample of $1cm^3$ volume made up of a random mixture of N_{sc} starting compounds, e.g. metallic oxides provided access to a high dimensional phase space [HA05]. Randomly constituted neighbourhoods of grains within this sample termed local configurations will lead to a set of q solid phases with $q \leq N_{sc}$ where q and N_{sc} are linked by a combinatorial function. Hence each sample of randomly mixed starting compounds that has subsequently undergone heat treatment is in fact a combinatorial material library in its own right. Hulliger *et al.* reported on experimental evidence of their approach in the fields of magnetic oxides [HA04] as well as cuprate superconductors [HDS06].

Cardin *et al.* reported a parallel solid state synthesis route using parallelized ball milling of up to eight masterbatches each of which was later split into five samples of the same concentration [CWS+07]. This procedure yielded libraries of bulk ceramic samples of roughly 0.5g mass. Unfortunately they encountered a serious bottleneck in their procedure due to the unability to dose the educt powders automatically and thus had to revert to manual dosage. Nevertheless they point out a promising idea that also formed a rationale for the present work, namely the possibility to combine the mentioned bulk approach with other HT-technologies in the quest for new materials. This thought shall be elaborated on in a later section.

2.3.3 Characterization of HT-libraries

For CHTE and HTE it holds that one should be able to "*analyse in a day what is made in a day*" [PM07] to avoid bottlenecks and hence narrow the high-throughput capacities present. This prerequisite can be met in two different ways, namely by parallelized as well as by sequential and automated screening methods.

For ceramic materials many workers have used x-ray diffraction (XRD) [Xia99, WAK+06, FTSW04, GNK99, HAHW05, VGKM04]. Due to area detection devices

that speed up the screening greatly and also due to automated positioning of samples and evaluation of resulting patterns this technique is especially attractive for HT-operation.

Researchers in the field of ceramic catalysts frequently have resorted to gas chromatography/mass spectroscopy (GC/MS) setups. Catalyst libraries have been subjected to reaction conditions either in a series of miniature reactors or as a whole library in parallel. Reaction products are then collected either by sequentially switching a set of valves [HBL+02, HLF+03] or by a flexible gas probe [RIL+03, CDF+99] and subsequently fed into conventional GC/MS equipment.

Wendelbo *et al.* reported the use of a scanning electron microscope (SEM) in combination with a wavelength dispersive microprobe [WAK+06]. Samples were positioned and scanned in an automated procedure. Hence imaging and element mapping could be performed parallelized.

Lately, publications showed a rapid sequential, automated characterization by use of scanning probe microscopy equipment in both Atomic Force and Piezo Force mode (AFM/PFM) [RSR+07, HSWS08]. Adapted or custom-made solutions of various scanning probe techniques are also in use in CHTE- and HTE-laboratories active in ceramic materials research [Xia99, CGT+98, Xia98]. Warren *et al.* advertised nano-indentation for the rapid sequential determination of micromechanical properties in composition spread combinatorial or high-throughput samples [WW05].

Parallel screening methods are most often conventional optical technologies adapted to the special HT-demands. Parallel photoluminescence imaging has been used for red phosphor materials on the basis of yttria ceramics [CKL+07], this endeavour being part of the development of new light-emitting diodes (LEDs). Reddington *et al.* managed to apply the same technology to assess electrocatalytic quality for methanol oxidation, a reaction that is important for the yield of alternative energy [RSG+98]. In this case the catalytic quality had to be translated into fluorescence by an additional indicator in the reaction chamber. A direct way to parallely measure reaction activity is IR-thermography which has also been ap-

plied in catalytic HT-research, most often on grounds of model gas phase reactions [VGKM04, RM01, RAM03].

Configuration	**Processes**	**References**
	liquid phase	
spatially addressable	hydrothermal synthesis	[KLSM98] [WAK+06]
	solution mixture	[AKAW04] [FUK04] [FW05]
	ink-jet printing	[SWY+97] [EECE01] [ME02] [PZC+07a] [PZC+07b]
	solution-polymerization	[GNK99] [RM01] [HAHW05]
	sol-gel synthesis	[HAHW05] [RSR+07]
	impregnation/incipient wetness	[RIL+03] [HBL+02]
	vapour phase	
composition spread spatially addressable	pulsed laser deposition	[CGT+98], [Xia99], [OCK+04]
	radio frequency sputtering	[Han70] [CDF+99]
	molecular beam epitaxy	[JFK+01]
	electrostatic atomization	[FTI+06]
	cosputtering	[KSD+65] [MS67] [vDSFH99]
	solid phase	
spatially addressable composition spread	acoustic deposition	[YE04b]
composition spread	diffusion multiples	[Zha01]
spatially addressable	mixed oxide route	[CWS+07]
n.a.	single sample concept	[HA04]

Table 2.2: Classification of library synthesis paths

2.3.4 Data management

From what was said so far it should be obvious that CHTE and HTE have the potential to create massive amounts of possibly complex raw data. The qualitative assessment of these data can no longer be performed by pure inspection and hence statistical hypothesis tests are applied, a rough introduction to which is given below. These data demand means of storage that allow their retrieval and organization. They also demand ways to value and rank them such that the desired scientific progress is actually possible. The former task is achieved by database setups, the latter, usually termed data mining, can be tackled in multiple ways shortly outlined subsequently.

Observations in scientific experiments are realizations of usually random variables. The specific realization (i.e. the observed value) cannot be anticipated before it actually manifests in a measurement and all possible realizations of the respective variable in a population will occur with a certain probability. Hence there will be a distinct probability distribution P over the realizations of the variable. The hypothesis being tested in the experiment can also be phrased as a probability distribution P_0 and it is then of interest whether the experimental realizations can be reconciled with the hypothetical distribution.

The branch of statistical inference that deals with this question is hypothesis testing. The customary wording of a testing problem is in terms of a null-hypothesis ($H_0 : P = P_0$) and some form of alternative hypothesis (e.g. $H_A : P \neq P_0$). The statistical test is arranged such that it aims at reclining the null-hypothesis under a certain level of confidence α with α being the probability to untruly recline H_0 (Type I error).

Two special hypothesis tests frequently used are the T-test for equality of location parameters and the F-Test for equality of variation parameters. Hence, a potential null-hypothesis for a T-test could be the equality of mean values of two sets of experimental data and an F-test could be used to test for equality of variance of the same two sets.

An F-test is also used in a more versatile statistical procedure called analysis of

variance (ANOVA). This procedure is applied to compare experimental data to a theoretical model for that data. E.g. an ANOVA can be used to test whether an experimental data set can be approximated by a linear regression. The fundamental idea is to split the overall scattering of data (variance) into a component that can be explained by the model (linear regression in the aforementioned example) and one that cannot be explained. These two contributions of variance can be evaluated using an F-test.

For a more concise explanation of hypothesis testing and its practical explanation the reader is referred to basic literature for scientific data evaluation [Ste04, Mor91] or statistics textbooks [KKMN98, FKPT99].

As for the data mining the progressive tactic advertised by most workers in HT materials science is to selectively pick members of an initial library by means of data mining tools. Those will then be used as the base for a subsequent library, possibly employing experimental design procedures mentioned earlier. In the course of the ensuing cyclic process, the researcher is supposed to limit the amount of samples per library and increase the analytic effort, such that at the end ideally only a handful of the best formulations, phases or materials remain as so-called "leads". Subsequent conventional analytic techniques can be used to identify the single best member as a "hit" [Caw03a, JSP+99, Har03]. Sometimes though this "zooming" procedure is not appropriate, e.g. when a partially known material system is supposed to be scanned for more active regions [WAK+06, vDS04, RSG+98].

Several combined solutions for storage and data mining have been presented in literature. Adams and Schubert reported on several commercial software packages specifically designed for HT materials research [AS04]. Custom made integrated solutions that include storage, data mining and also control of related instruments were presented by Harvey *et al.* and Zhang *et al.* [HSC06, ZFKA05], where Zhang advertised the use of open-source components to facilitate modification due to easy procurement and transparent design.

Principal component analysis (PCA) , Monte Carlo algorithms (MC) and artificial neural networks (ANN) are among the software based approaches exclusively

suitable for data mining purposes. PCA is a mathematical tool to identify patterns in big data sets depending on many factors, i.e. data that can no longer be visualized easily. It is in fact a form of data compression as it reduces the dimensions of the data set, such that a projection into two- or three-dimensional space is possible. Andersson *et al.* used PCA extensively upon structuring of an in-house library of chemical compounds [ASWL01].

Various forms of Monte Carlo algorithms are in wide use in various scientific disciplines. They are randomized algorithms that may - with a certain probability - yield a wrong result. They are alluring for the screening of large data sets in materials science as they do not exclusively converge towards one global optimum but also yield local optima. The aforementioned wrong results can be understood to "lie on the path" towards these local optima. Falcioni and Deem describe an MC scheme for structural inspection of zeolites [FD99].

Artificial Neural Networks are software designs that model organic network functionality like it can be found within brains of higher forms of life. They consist of layers of "neurons", elementary processing units, which are linked by "synapses". Provided sufficient and suitable training data, ANNs allow the transcribing of, say, a catalyst system's structural factors into its activity. An ANN thus trained can subsequently be used to optimize other catalyst systems [CLT+03].

A more specialized data mining approach exclusively used on XRD-patterns is the one by Barr *et al.* [BDG04b] obtainable through the commercial software tool PolySNAP that has seen extensive employment in the course of this work. It provides the possibility to compare numerous XRD-patterns using a full pattern matching approach. This means that patterns are compared in pairs on a point-by-point basis along the 2θ axis. By means of various statistical correlation tests it is thus possible to determine a degree of alikeness between patterns that allows conclusions towards groups of structurally equal materials and hence towards phase diagrams. This procedure is termed clustering.

Clustering, also known as automatic classification, comprises a variety of methods to detect similarity in multivariate datasets and group those datasets accord-

ingly [Wil90]. The data is hence hierarchically nested according to a measure of distance or similarity and a customary way to report a clustering outcome is a tree-diagram or dendrogram with as many branches as there are objects in the dataset [Gor81]. The position "down" the tree (along an axis of similarity) at which two branches are linked (referred to as nodes or vertices in mathematical graph theory) are each marked by a specific distance or similarity value that states the limit for the two linked objects to be in the same cluster. Numerous algebraic algorithms can be used to determine how many clusters are present in one dataset which is conterminous with determining a cut-off distance or similarity at which the clustering is stopped. It is generally assumed that cutting a dendrogram at a specific similarity will create clusters of comparable homogeneity [Gor81].

A second feature of the program is to determine fractions of patterns that are accounted for by other patterns from a database. Provided the database contains patterns of pure substances, it is therefore possible to determine the composition of a material from its diffraction signal. This is a procedure that is analogous to the standard procedure for quantitative phase analysis, namely Rietveld's method [GBP04]. In comparison to Rietveld though, the method described above does not rely on the repetitive calculation of a comparative pattern for the minimization but only on a set of stored patterns and is therefore HT-compatible. On a point-by-point basis it is possible to quantitatively compare patterns when minimizing

$$\chi^2 = \mid \mathbf{x} \cdot \mathbf{p} - \mathbf{S} \mid \tag{2.5}$$

by a least squares algorithm [GBP04]. $\mathbf{x}$ is an $(m \times n)$ matrix consisting of n XRD-patterns with m data points each and $\mathbf{S}$ is a vector in $\mathbb{R}^m$ that was formed by the m data points of the XRD pattern under investigation. $\mathbf{p}$ in turn is a vector in $\mathbb{R}^n$ holding m parameters for the minimization which are constrained by

$$\sum_{i=1}^{n} p_i = 1. \tag{2.6}$$

It is thus possible to express any of the patterns $\mathbf{S}$ detected from a green body made from a powder mixture by a linear combination of n stored patterns and quantify this combination by the values of p_i. In the present work this feature was used to quantitatively assess the distribution of two raw powders ($n = 2$) in a green body. The respective composition is reported in $\mathbf{p}$.

2.4 Motivation

The usual synthesis approach for advanced ceramics at the Institute of Advanced Ceramics at Hamburg University of Technology is the very common powder metallurgical processing route which consists of the conditioning, shaping and heat-treatment of dry powders, most often oxide or carbonate salts of relevant metal ions. The conditioning subsumes concentration and grain size homogenization of various powder species in one batch. This takes place in attrition mills under an organic solvent (e.g. ethanol) at batch sizes in the order of 100g. After drying the shaping of the resulting powder mixtures is done by a combination of uniaxial and hydrostatic dry pressing. If carbonate raw powders were used the shaping would only take place subsequent to a calcination heat-treatment followed by further milling. The final heat-treatment takes place in industrial furnaces capable of a multitude of gas atmospheres. Frequently though, sintering in air is sufficient. Ultimately, the products are dense ceramic bulk samples.

The idea that lead to the work presented here was that it should be possible to apply all the advantages of a CHTE/HTE procedure outlined above and still remain close to the conventional synthesis cycle. Firstly, because analytical data should be comparable to results gained from conventional synthesized samples. Secondly, the resulting samples should be in bulk form and not in one or other form of thin film as in the majority of approaches presented so far. The preference for bulk ceramics is justified by the fact that the institute's focus of the research is on piezoelectric materials and relevant properties, like the piezoelectric coefficient d_{33} can only be determined reproducibly on bulk materials [CWS+07].

These preliminary considerations also confirmed that none of the strategies presented in literature could be utilized. The approaches by Hulliger [HA04] and Zhao [Zha01] yielded bulk samples. But in the case of Zhao the composition spread did not allow for discrete samples and the library synthesis procedure was too complex to be feasible for application-aimed research. As for Hulliger's concept, only one

bulk sample ensued which was in fact assembled out of the different materials. This sample needed to be crushed and subsequently separated according to the desired property. Thus the resulting materials were no longer bulk but in fact in powdery state again. Additionally, even though their activity in terms of, say, magnetic behaviour could be determined by the respective separation procedure, one would need some form of element analysis to determine the exact composition of the hits to verify which material yielded the desired behaviour. An analytic procedure with sufficient resolution was not accessible to the author.

The strategies outlined by Cardin [CWS+07] and Pullar [PZC+07a, PZC+07b] indeed produced bulk ceramics. Nevertheless, that was achieved via a liquid-phase route. It is well known that colloidal processing of ceramic materials is complex technology that needs detailed optimization for any material/liquid combination. Slight changes in either the liquid or the solid for example, can change the rheology of these systems completely [Lew00]. Hence, an HTE-approach based on colloidal processing was deemed not versatile enough for the desired goal.

Mohebi's concept was the only one in literature that actually dealt with samples directly synthesized from dry powders [MYE06]. Nevertheless, these were very coarse (particle size 90-212 µm) metal powders and the diameters of the powder hoppers for acoustic dosing as well as the respective frequencies were triggered directly to those powders [YE04a]. The powders used for ceramic synthesis however, are commonly in the range of 1 µm particle size.

It followed that a completely new approach had to be conceived. When trying to categorize experimental approaches in this field, the information in table 2.3 can be proposed. For the conceived setup the subsumption under the HTE group is obvious. Since samples were supposed to be in bulk state, spatial addressability was necessary. Furthermore, conventional screening techniques that showed potential to be adapted for the apprach (e.g. XRD) were sequential. Finally, transferring the conventional bulk ceramic synthesis it became clear that really only a medium number of samples could be processed in each cycle.

It is obvious that one of the main challenges to be dealt with in the course of

	Conventional	**HTE**	**CHTE**
Synthesis / Preparation	Materials batch: one-at-a-time	Library: Spatially addressable	Library: Spatially addressable Composition spread
Screening	one-at-a-time	Rapid sequential (automatized)	Rapid sequential (automatized) Highly parallel
Evaluation	Classical: Compare sequentially	Classical: Compare parallely or rapid sequential (automized)	Data Mining: ANN MC PCA ...
Throughput / Amount of data	Low	Medium or high	Very high
Cyclic decrease of sample numbers	n.a.	Possible	Yes

Table 2.3: Comparison between conventional experimentation, HTE and CHTE (ANN: Artificial Neural Network, MC: Monte-Carlo-Algorithm, PCA: Principal Component Analysis).

this work was to achieve an acceptable mixing of dry powders. The mixing of powders is a highly empirical field of science. Due to the particulate nature any attempt to approach the matter analytically is necessarily subject to variance and hence descriptive statistics will be used to estimate the quality of samples if indeed sampling is possible. The interaction between single particles is well understood and the various mechanisms (e.g. van der Waals' forces, electrostatic forces etc.) can be described individually by general mechanics equations. Nevertheless, the superposition of the multitude of mechanisms as well as as the high number of particles make an analytical solution impossible for all but exemplary mixtures [LRWE04].

Two difficulties may occur in powder mixtures, namely segregation and agglom-

eration [Sta82, VW01]. Segregation or demixing is advantaged by disparities in the grains size and the density of mixed powder species [VW01]. An additional factor is the shape of particles [Sta82]. Agglomeration is the tendency of smaller primary particles to stick together and form larger secondary particles due to cohesiveness. It can be stated very crudely that particles with a particle size lower than 30 µm will behave cohesively [Bri94] and hence agglomerates will be present in any powder batch in ceramics technology since particle sizes below 5 µm are the normal case. With respect to the unwanted effect of demixing this fact is actually beneficial as cohesive powders are less prone to segregation [Wil68].

From these very general remarks about powder mixing it follows directly that special care needed to be taken when preparing the masterbatches for the HTE-procedure. Obviously, the density of the species in use could not be tailored and hence control of the mixing quality over this route was impossible. Therefore, it was all the more important to ensure unified particle sizes and particle shapes of the masterbatches as very small aliquots of those masterbatches had to be mixed dryly. Hence when preparing the masterbatches by ball-milling it was necessary to continuously monitor the grain size distribution and generally try to mill all the batches in the same amount of time. This was especially true, since the quality of the mixtures in the final HTE-samples could not be assessed in a direct manner after the parallelized mixing procedure. Since in general the powders that are used in ceramics technology are all white a visual inspection for the homogeneity of the samples was impossible. Also it is common when judging the quality of the powder mixture to draw a multitude of samples from the the mixture, evaluate those and subsequently use statistical measures like a mean value and a standard deviation to report the homogeneity. This approach relies on the background of a size difference between observational unit (powder mixture) and experimental unit (sample) so as to be able to draw samples without disturbing the mixture (and thus any subsequent samples to be drawn). This notion is of course negligible on an industrial scale but for powder mixtures in the vicinity of a few hundred mg it meant that sampling in the common sense was made impossible and an alternative method had to be devised that will be explained in a chapter to come.

3 Experimental setup

3.1 Robot

The core piece of the setup that was used in all the experiments of this work was an industrial robot carrying a solid dosing unit (SDU). The demands that were posed to the robot were as follows:

1. *Capacity to reproducibly create a multitude of samples:* Since the dosing was supposed to feed an HTE-workflow a reliable and automatic dosage of powder samples in the order of magnitude of 50 samples per experimental run had to be possible.

2. *Possibility to dose powders masses of different magnitudes:* High resolution (possibly down to 0.1 mg) and precision (possibly $<1\%$). Especially for the creation of doped bulk samples dosing of powders masses in the gram- and in the microgram-regime had to be possible with the same accuracy and precision.

3. *Capacity to dose gravimetrically:* The used powders are prone to compaction and hence change their tapping density. A volumetric dosage was not acceptable for this reason.

4. *Possibility to dose ultrafine powders:* The handling of material with usual shortcomings of powders employed for ceramic synthesis had to possible. These powders are most often ball-milled mixtures of oxide powders with a grain size in the vicinity of 1 µm. They are not free flowing and due to their small grain size and high surface area they tend to agglomerate. Additionally, owing to their ceramic nature they are highly abrasive.

5. *Possibility for many-to-many-dosage:* Since ultimately, as explained above, each sample was supposed to be a distinct material, it was necessary to be able dose all the samples in one experimental run with a different concentration.

6. *Possibility to use various sample carriers:* Since the dosing unit was supposed to be a chain in a workflow of various synthesis and analysis tools, some of which were only to be adapted or acquired at a later time, the highest possible degree of flexibility was necessary. Especially the fixation onto normed carriers, e.g. in the micro titer plate format, was supposed to be avoided.

7. *Software control:* The dosing unit had to equipped with a software to plan and execute the dosing program. Specifically, it had to be possible to store previously planned experimental programs as files to later on reuse or modify them.

The device that was used was an Accelerator VLT-100 Dual Dispensing Station (Chemspeed Technologies AG, Augst, Switzerland). It allowed for the parallel dosage of powders and liquids but was only used in powder dosage mode for the presented work. The device was a 4-axis (x, y, z and α) robot where the robotic arm would drive the SDU.

The SDU consisted of two main parts. First it contained a class II (EN45501) precision balance with a measurement maximum of 10g and a precision of 0.1mg. Furthermore, it carried as a driving unit a 3.5W DC motor complete with a carbon PEEK holder for the respective powder containers. The containers were 15ml PE bottles that when in use where outfitted with a PE funnel and an extruder. The extruders came in various types (see figure 3.2) and could be used according to the respective powder properties. When dosing, the robotic arm made the SDU pick up the respective powder container by means of the PEEK holder attached

Figure 3.1: a) VLT-100 Dual Dispensing Station and b) Solid Dosing Unit (SDU)

to the motor. It then maneuvered the container over the goal position and start the dosing by activating the motor. The motor in turn would drove a gear wheel that turned the container relative to the extruder which induced powder ejection, the operation method being reminiscent of an Archimedean screw. The balance monitored the powder loss from the container and stopped the procedure when the set mass was reached.

Some of the powders used in the course of this work showed a high cohesiveness and as a result showed a tendency to get compacted inside the PE funnel and completely inhibit the powder dosing after a short time. To alleviate the problem a modified extruder was designed including a rake-like piece of thin wire. This rake allowed the powder in the funnel to be loosened and subsequently to be fed through the extruder.

In the default assembly the robot was set up to use micro titer plates as as a standard sample carriers. A new sample carrier format was devised that could be used in the parallelized mixing procedure explained below. The carriers were

Figure 3.2: Powder extruders used in the Chemspeed dosing robot. From left to right: Type II (wide thread), Type I (narrow thread) and modified Type I with wire rake to loosen compacted powder.

machined from ultrahigh molecular weight PE to minimize abrasion due to the ceramic powders. They had height and width of 30 mm and a length of 120 mm and contained five boreholes into which the powders were dosed (see figure 3.5). Up to seven of those carriers could be fixated in the field of work of the robot by means of a likewise custom made rack.

The robot was controlled by programs that could be compiled in a software with a graphical user interface. Within this software also the necessary control parameters of the dosing procedure could be set according to the nature of the powder in use. The main parameters were the fine dispensing amount (FD amount), the fine dispensing speed (FD speed) and the filter coefficient. The motor performing the dosing allowed for two speeds, one fast and one slow. The FD amount, a mass difference from the final dosing mass, set the point upon which the motor would switch to the slower turning speed. This speed was determined by FD speed as a percentage of the invariable fast speed. The filter coefficient finally, influenced the damping of the balance and hence the quickness the balance reacted on mass changes when weighing. A combination of the FD amount and speed on the one hand and filter coefficient on the other hence counterbalanced each other and al-

lowed to accurately meet the final dosing amount for a wide variety of powders. The programs were executed within a second software exclusively directed to that purpose. The final masses of all dosage steps were stored and written into a log-file after completion of the respective run.

3.2 Mixing

3.2.1 Premixing step in the robot

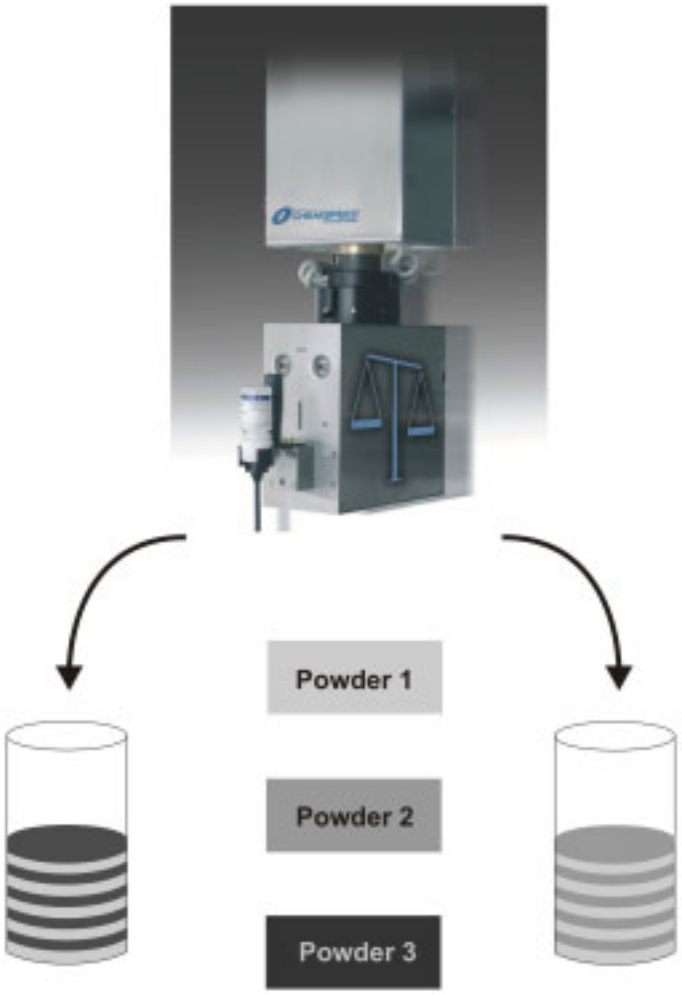

Figure 3.3: Scheme of layered dosing facilitating premixing of dry powders in HTE setup. 3 exemplary masterbatch powders (Powders 1-3) are shown.

The SDU participated in the overall mixing by means of a special dosage program. Instead of dosing the complete mass of the respective powder fractions all at once, the robot was programmed to dose only parts of these fractions and hence achieve a premixing by layering the powders. The extension of the dosing time by a factor of up to five was invalidated by the increase in homogeneity, since the robot ran unsupervised and could be left to dose over night if necessary.

3.2.2 Planetary mill

Figure 3.4: a) Customary planetary mill adapted to high-throughput usage by b) steel fixture to fix up to four powder containers.

The actual main mixing step was conducted after dosing in a conventional planetary mill in laboratory scale (Pulverisette, Fritsch, Idar-Oberstein, Germany). The carriers described in 3.1 could be mounted into one of the two baskets of the mill by means of a custom-made steel fixture (see figure 3.4). Each fixture held four containers and so it was possible to mill and hence mix up to 40 samples in parallel.

3.3 Shaping and densification of samples

For powder compact shaping and densification a conventional cold-isostatic press was used (KIPP200ES, Paul Weber, Remshalden-Brunbach, Germany). For the shaping silicone moulds were cast which were adapted to fit onto the sample carriers by means of groove-and-tongue-design. This assured transfer of the powders from the carriers into the dies without significant powder loss and cross contamination between neighbouring samples. Unfortunately, the press in use had a very small chamber (diameter 59mm). Hence only five samples (i.e. one mould) could be densified at a time. It is important to note that this did not constitute a principal bottleneck of the setup but was an individual shortcoming due to geometrical constraint.

The heat-treatment of the HTE-samples was conducted in a regular industrial furnace (HT 04/17, Naber, Germany) under air. The samples were sintered in Al_2O_3-crucibles on ZrO_2-balls (diameter 1mm) as sintering bed. As the amount of samples sintered parallely was high, a substantial part of the grate surface in the furnace was covered. Therefore, it was important to affirm a continuous temperature distribution over all samples. A set of 5 equal green bodies of sodium potassium niobate ($(K_{0.5}Na_{0.5})NbO_3$, KNN) were sintered parallely. The green bodies were placed on different locations within various crucibles and the crucibles themselves were placed in different sections of the furnace. Subsequently, the samples were subjected to 1075 °C for 1 hour. Only when it was assured that after the heat-treatment the samples showed minimum variation in density ($\rho = 4.3g/cm^3 \pm 0.01g/cm^3$) and sintering loss ($\Delta m = 0.25wt - \% \pm 0.01wt - \%$) the furnace was deemed practical for HTE processing.

3.4 Analytics - Powder X-ray diffraction

All analytic procedures were based on powder X-ray diffraction (XRD) on a D8 Discovery (Bruker AXS, Karlsruhe, Germany). It was equipped with a Göbel mirror to parallelize the incident beam as well as with a so-called general area diffraction detection system (GADDS). The latter was especially important as it allowed the concurrent detection of a 2θ-window instead of successive scanning

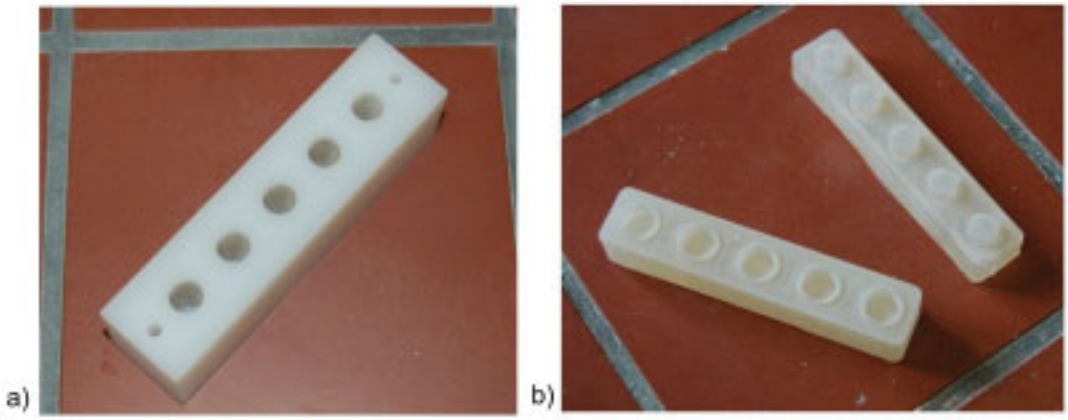

Figure 3.5: a) Custom-made powder container from UHMPE. Containers take up the powder from the SDU and also serve as mixing receptacle. b) Pressing mould adapted to powder container. Moulds take up powder samples losslessly before cold-isostatic pressing.

which lowered the necessary measuring time and hence increased the throughput. An xyz-table also helped that effort in that it allowed the automization and hence unsupervised scanning of multiple samples and even the scanning of different areas of those samples. The resolution pertaining to 2θ was set to $0.02°$.

3.5 Scanning Electron Microscopy

For visualization and size estimation of powder agglomerates, powders were dusted on a sample carrier to be scanned by electron microscopy (Leo 1530 Gemini, Carl Zeiss SMT AG, Oberkochen, Germany). An acceleration voltage of 20kV was applied.

4 High-throughput experimentation of a known material

4.1 Yttria-toughened zirconia

It was necessary to prove the functionality of the setup presented in the previous chapter by means of a proof of principle approach. Hence a material system that essentially formed a worst case example was asked for. This was found in the well-known $ZrO_2 - Y_2O_3$ system.

Zirconium oxide (ZrO_2, zirconia) exists in a monoclinic crystal structure (M) at room temperature and transforms into a tetragonal modification (T) at 1170 °C and further into cubic (C) at 2370 °C [SS07]. The phase transformations in the system take place diffusionless (martensitic) [RH84] and in the case of the T-M transformation is accompanied by an elongation in the unit cell and substantial shearing of 9% [SS07]. What would usually cause insurmountable difficulties when sintering, namely the volume increase of the unit cell through the martensitic phase change, can be put to use in transformation toughening of ceramics. Grains below a certain grain size will be retained in a metastable tetragonal state and this critical grain size can be adjusted by addition of rare earth oxides like for example yttrium oxide (Y_2O_3, yttria) [Lan82]. When the mechanical clamping of those grains is relieved, e.g. by a propagating crack, the phase transformation towards monoclinic will take place and the ensueing volume increase will retard the crack propagation [SS07]. Very beneficial for technological features, zirconia shows a high solubility for rare earth ions, e.g. the system remains single-phase up to an addition of 40 mol-% yttria [Yos88]. The resulting charge mismatch gives rise to an increasing concentration of oxygene vacancies. Hence, these materials can be used for functional applications that depend on a high selective diffusivity of oxygene ions, e.g. electrolytes in solid oxide fuel cells. The microstructure of the $ZrO_2 - Y_2O_3$ solid solution is usually fine-grained and consists almost completely

of the metastable tetragonal grains mentioned above, hence its name tetragonal zirconia polycrytsal (TZP) [HS94].

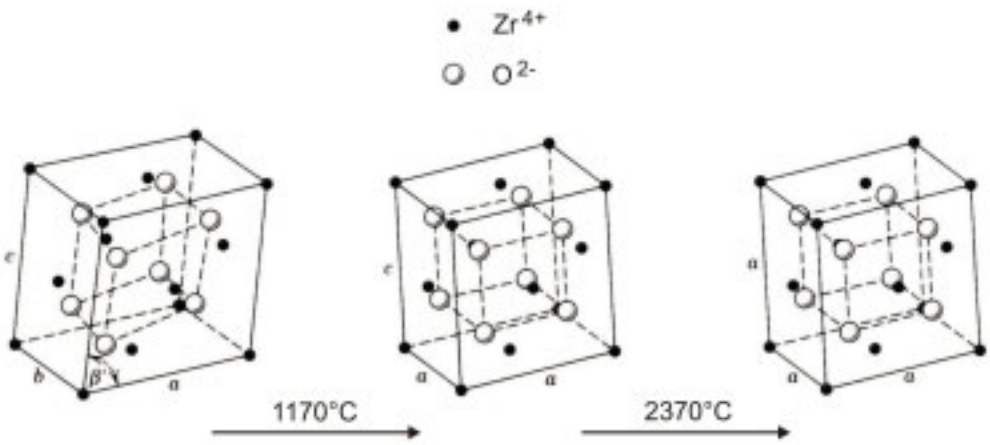

Figure 4.1: Phase changes of pure ZrO_2 [GHS89a].

The importance of a homogeneous distribution of Y_2O_3 in ZrO_2 has long been known and is the reason for the wet-chemical production technology of modern Y-TZP powders [RCH84, SCR84]. The basic driving force of concentration equalization during heat-treatment is diffusion which is a thermally activated process. Specifically,

$$D = D_0 \cdot e^{\frac{-Q}{RT}} \tag{4.1}$$

with D being a diffusion coefficient, D_0 a constant, Q the respective activation energy for 1 mol of diffusing species, R the universal gas constant and T the temperature. It is obvious that temperature influences diffusion exponentially in comparison to the linear contribution of the concentration difference in Fick's first law of diffusion. The diffusion of yttria in zirconia will be covered in more detail in a later section. However, it is important to understand that it takes place comparatively slow [KBL+02]. Furthermore, the competition between grain growth and densification that all ceramics have in common in view of heat-treatment is particularly problematic for this material class. The stabilization of the metastable tetragonal phase is strongly dependent on the grain size. In particular, there is a critical grain size, excess of which leads to M-T phase transformation in the mi-

crostructure upon cooling [Lan82]. The yttria-diffusion is hence further obstructed by the necessity to limit the sintering temperature with the objective of hindering grain growth while densification takes place [SCR84]. Therefore, the material essentially requires homogeneous powder compacts consisting of ZrO_2 and Y_2O_3 particles as green bodies and hence Y-TZP was well suited as a proof of principle system to achieve homogeneous powder compacts.

4.2 Experimental

4.2.1 Preparation of masterbatches

The raw materials for the Y-TZP experiments described in this chapter were yttrium (III) oxide (Y_2O_3, REacton, Alfa-Aesar, Karlsruhe, Germany) and monoclinic zirconium dioxide (ZrO_2, Carpenter/Z-Tech, Bow, NH, USA). These powders were used to produce 7 masterbatches (henceforth referred to as MB1-7) that contained 0, 1, 2, 3, 4, 5 and 10 mol-% yttria. The batches were produced applying a conventional mixed oxide route. The powders were weighed in in the respective ratios totalling 150g per batch. Homogenization was obtained by ball-milling in ethanol using 1200g of grinding balls (diameter 3mm, yttria-toughened zirconia, Tosoh, Tokyo, Japan). The grain size distribution of the mixtures was constantly monitored and the milling was stopped when a certain pre-defined median of d_{50}=0.9µm was reached which was usually approximately 5 hours into the milling procedure. Subsequent to milling, all the batches were dried by vacuum evaporation and homogenized by sieving over 200 µm mesh size.

4.2.2 Homogeneity investigations

The quality of the parallelized dry mixing procedure described in 3.2.1 and 3.2.2 was to be confirmed in preliminary experiments. The masterbatches MB1 and 6 (0 and 5 mol-% Y_2O_3) as well as MB1 and 7 (0 and 10 mol-% Y_2O_3) were used as boundary systems in the high-throughput setup to produce samples with a concentration of 3 mol-% yttria, termed 0-5/3 and 0-10/3 henceforth. As mentioned above the dosing took place by layering the respective powder fractions. For this purpose, the fractions of the masterbatches making up the respective samples were

split in five parts each and subsequently dosed alternately on top of each other. The robot's control software allowed for an easy implementation of this pre-mixing workstep by a five-fold repetition of the same dosing procedure. The samples had a final mass of 600mg and were endmixed in the parallelized planetary ball mill at varying intensities and mixing times. Homogeneous reference samples were pressed directly from MB4 (3 mol-% Y_2O_3). All homogeneity measurements were performed on green bodies to study the effect of the mixing not influenced by diffusion during heat treatment.

For the determination of the homogeneity it was necessary to determine the variation of the yttria concentration within one green HTE-sample and compare that to the variation within the reference sample from MB4. The yttria concentration itself could be determined from XRD-patterns using the software tool PolySNAP, already mentioned on page 20. Using the quantitative analyse feature of PolySNAP it was possible to express any of the patterns **S** detected from the $ZrO_2 - Y_2O_3$ green bodies by a linear combination of 2 stored patterns of pure yttria and zirconia raw powders respectively and quantify this combination by the values of p_i. For subsequent analysis steps the concentration value for yttria (p_Y) was used.

Ten XRD patterns were recorded on different areas of each of the samples in the range of 20-50° 2θ (detector distance 15 cm). Applying PolySNAP in the above mentioned way it was thus possible to determine ten independent yttria concentrations p_Y per sample. A mean value $\overline{p_Y}$ was formed and compared to the mean value of the reference sample from MB4 $\overline{p_Y^{reference}}$

$$\Delta\overline{p_Y} = \frac{\left|\overline{p_Y} - \overline{p_Y^{reference}}\right|}{\overline{p_Y^{reference}}} \times 100\%. \tag{4.2}$$

Furthermore, the normalized standard deviation (coefficient of variance)

$$CVar(p_Y) = \frac{\sqrt{\frac{1}{9}\sum_{i=1}^{10}(p_{Y,i} - \overline{p_Y})^2}}{\overline{p_Y}} \times 100\% \tag{4.3}$$

was taken as the measure of homogeneity of the sample.

Resulting out of the algebraic procedure outlined in equations 2.5 and 2.6, p_Y was reported in so-called scale-%. This percentage was merely the fraction of the pure yttria pattern in the analysed pattern. It was hence a purely mathematical value with no physical meaning as such. Even though a correlation between the reported scale-% and the physical yttria content in mol-% existed [GBP04], this correlation was dispensable for the evaluation mentioned above. Absolute physical values were not of interest and the results expressed by equations 4.2 and 4.3 were again percentages.

4.2.3 Preparation and characterization of Y-TZP HTE libraries

The HTE-libraries in the system $ZrO_2 - Y_2O_3$ consisted of ten samples of 600mg mass. They each covered a concentration range between 0 and 5 mol-% yttria with a concentration difference of 0.5 mol-% between two neighbouring samples. The libraries were mixed from either MB1 and MB6 (henceforth referred to as 0-5 library) or from MB1 and MB7 (0-10 library) according to figure 4.2. The approach outlined in section 4.2.2 resulted in an optimal set of mixing paramters for the parallelized planetary mill. Subsequent to the layered dosing explained above these mixing parameters were applied for library production. To shed light on the potential influence of mixing aids on the parallelized mixing procedure described in 3.2 three organic solvents, namely ethanol, cyclohexane and acetone were applied. A control group of libraries remained without mixing aids. The mixing aids were added directly into the powder containers right after the dosing such that the boreholes that held the individual powder lots were approximately half full.

Shaping took place cold-isostatically for 2 minutes at 400 MPa. Heat-treatment conditions were taken from [Lan82] with a heating ramp of 2 K/min, a dwelling time of 2 hours at 1500 °C and a cool-down to room temperature at 10 K/min.

Using the same synthesis conditions a reference library was produced by pressing and sintering samples using the masterbatches MB1-6.

As a parameter for the comparison between the reference and the HTE libraries the monoclinic phase content w_M after the heat-treatment was chosen. This pa-

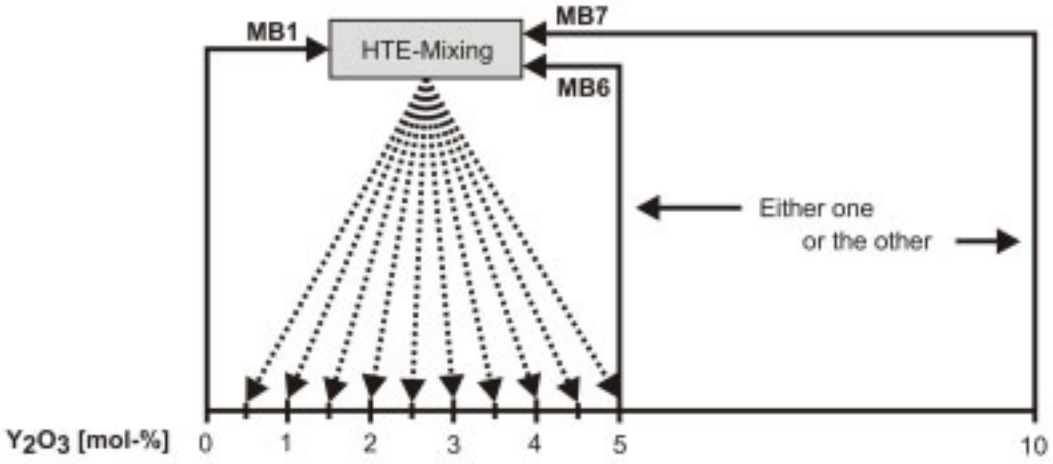

Figure 4.2: Scheme of the HTE library synthesis from masterbatches (MB) 1, 6 and 7 containing 0, 5 and 10 mol-% Y_2O_3 respectively.

rameter was determined by the so-called polymorph-method [GN72] and hence by a peak intensity ratio

$$x_M = \frac{I(111)_M + I(11\overline{1})_M}{I(111)_M + I(11\overline{1})_M + I(111)_{C,T}} \tag{4.4}$$

where the subscripts M, C and T are used for the peaks of the monoclinic, cubic and tetragonal phase in the XRD-pattern, respectively.

From the peak ratios a weight fraction of monoclinic phase w_M could be calculated according to [TYS84, HH91]:

$$w_M = \frac{1.311 \cdot x_M}{1 + 0.311 \cdot x_M}. \tag{4.5}$$

$\{111\}$ peaks of the tetragonal and the cubic ZrO_2 phases could not be resolved easily [HH91] and hence only monoclinic phase content could be determined. Ten XRD scans were performed on different areas of each sintered sample in a range of 20-50° 2θ. Therefore, ten monoclinic phase concentrations ($w_{M,i}$ for $i = 1, ..., 10$) could be determined for each member of both the reference and the HTE libraries.

The strategy to evaluate the comparability between the reference library and the

various HTE libraries were statistical tests for equal intercepts and parallelism of regression lines fitted to the reference library's and the HTE libraries' monoclinic phase concentration data.

The regression lines were fitted using a least-squares method according to

$$w_M([Y_2O_3]) = \beta_0 + \beta_1 \cdot [Y_2O_3] \tag{4.6}$$

and yielded regression coefficients β_0 (intercept) and β_1 (slope). An analysis of variance was performed to check whether the regression was capable of explaining most of the variance of the data. Provided the regression was sufficient two T-type test statistics with null-hypotheses $H_{0,1} : \beta_{0,reference} = \beta_{0,HTE}$ and $H_{0,2} : \beta_{1,reference} = \beta_{1,HTE}$ were applied, the subscripts of the regression coefficients denoting the respective library. Two-sided T-tests were performed, hence the alternative hypotheses $H_{A,1} : \beta_{0,reference} \neq \beta_{0,HTE}$ and $H_{A,2} : \beta_{1,reference} \neq \beta_{1,HTE}$. Acceptance of $H_{0,1}$ represented equality of intercepts and acceptance of $H_{0,2}$ parallelism.

Subsequently, to quantify the deviation between reference and HTE library, an arithmetic mean of the monoclinic phase content of each reference library member was calculated:

$$\overline{w_M} = \frac{1}{10} \sum_{i=1}^{10} w_{M,i}. \tag{4.7}$$

For each HTE library member j that had a counterpart in the reference library, a difference was formed between its mean monoclinic phase content and the mean monoclinic content of the reference library member with the same yttria concentration according to

$$\Delta\overline{w_M}_{,j} = \left| \left(\overline{w_M}_{,j}^{HTE} - \overline{w_M}_{,j}^{reference} \right) \right|. \tag{4.8}$$

Finally, where statistically opportune the arithmetic mean of the aforementioned differences was calculated

$$\overline{\Delta w_M} = \frac{1}{k}\sum_{j=1}^{k} \Delta\overline{w_M}_{,j} \tag{4.9}$$

and termed mean deviation $\overline{\Delta w_M}$ of the respective HTE library.

All statistical tests were performed on a level of significance α=0.05.

4.3 Results and discussion

Table 4.1 shows the results of the homogeneity investigations with varies mixing time and speed of the planetary mill. $\Delta\overline{p_Y}$ was supposed to be as small as possible. Additionally, a small variation within the sample ($CVar(p_Y)$) was necessary to suggest good homogeneity.

	mixing parameters					
sample	**time**[s]	**rpm**[min^{-1}]	$\overline{\mathbf{p_Y}}$[scale-%]	$\mathbf{\Delta\overline{p_Y}}$[%]	**CVar**($\mathbf{p_Y}$)[%]	
reference	n.a.	n.a.	4.2	n.a.	3.8	
0-5/3	60	340	5.2	23	2.9	
0-10/3	60	340	5.5	29	9.1	
0-5/3	10	340	4.6	8	2.1	
0-10/3	10	340	6.3	49	11.7	
0-5/3	600	80	4.4	5	10.7	*
0-10/3	600	80	4.4	5	17.7	*
0-5/3	10	80	3.5	17	36.4	
0-10/3	10	80	6.0	42	16.5	
0-5/3	60	80	5.2	22	27.4	
0-10/3	60	80	3.2	26	39.6	

Table 4.1: Results of the homogeneity tests done on green samples with constant concentration of 3 mol-% Y_2O_3. Asterisks mark the lines holding the mixing parameters that were used for later HTE library preparation.

Table 4.1 shows clearly that both demands could not be met simultaneously. Small $\Delta\overline{p_Y}$ as well as $CVar(p_Y)$ could only be achieved for 0-5/3 at 10s mixing

and 340 rpm. Nevertheless, the corresponding 0-10/3 mixture showed rather weak results. Also, while conducting the experiments it was found out that high rotational speeds of the mixer lead to massive frictional wear of the powder containers as well as increased agglomeration. A good matching of the mean values and an acceptable variance could be achieved for both samples at 600 s of mixing time and 80 rpm. Therefore, these mixing parameters were chosen for the ensuing HTE library preparation.

Table 4.2 shows the regression data. The linear regression was suitable to explain most of the data's variance as can be seen from the high coefficients of determination r^2 of all libraries. On a level of significance of α=0.05 neither equality of intercepts nor parallelism could be proved for any of the 0-10 libraries and the 0-5 library with cyclohexane as mixing agent. Since ceramic particles in suspension have a strong surface charge [Lew00], their interaction with the suspension medium is strongly dependent on the molecular structure of the medium. In contrast to ethanol and acetone, its ring-shaped structure causes cyclohexane to be non-polar. In the case of cyclohexane as mixing aid, a detrimental effect due to this non-polar nature was assumed. Furthermore, it could be supposed that that the concentration range between the two boundary systems for all 0-10 libraries was too wide to allow for sufficient homogenization using the parallelized mixing approach.

Only in the case of acceptance of $H_{0,2}$ (parallelism) could a normal distribution of the deviation of means be assumed and hence a mean deviation value $\overline{\Delta w_M}$ be reported which were in the same order of magnitude at approximately 7 wt-% monoclinic phase. The experimental error with respect to the Y_2O_3 concentration could be deduced from figures 4.3 and 4.4 showing the yttria contents versus the monoclinic phase of the libraries with accepted $H_{0,2}$ in comparison to the reference library. The range of interest is shaded gray and constitutes commercial composition of Y-TZP resulting out of the best mechanical performance in view of strength and fracture toughness [Lan82, GHS89b]. The HTE libraries' of figures 4.3 and 4.4 show that the phase content of 60 wt-% monoclinic phase corresponding to 3 mol-% Y_2O_3 in the reference system was met at approximately 2.5 mol-% Y_2O_3 in the investigated HTE systems which resulted in an experimental error with rela-

library	regression analysis					$\overline{\Delta w_M}$ [wt-%]
	β_0	β_1	r^2	equal intercepts	parallel	
reference	125.97	-22.99	0.98	n.a.	n.a.	n.a.
0-5, dry	107.20	-18.90	0.97	$H_{A,1}$	$H_{0,2}$	8.53
0-10, dry	103.50	-12.20	0.98	$H_{A,1}$	$H_{A,2}$	n.a.
0-5, acetone	109.20	-19.50	0.98	$H_{A,1}$	$H_{0,2}$	5.36
0-10, dry	100.90	-13.50	0.98	$H_{A,1}$	$H_{A,2}$	n.a.
0-5, ethanol	107.80	-18.80	0.98	$H_{A,1}$	$H_{0,2}$	7.79
0-10, ethanol	102.30	-12.00	0.97	$H_{A,1}$	$H_{A,2}$	n.a.
0-5, cyclohexane	104.60	-18.30	0.99	$H_{A,1}$	$H_{A,2}$	n.a.
0-10, cyclohexane	99.60	-11.70	0.95	$H_{A,1}$	$H_{A,2}$	n.a.

Table 4.2: Results of the regression analysis and mean deviation values of monoclinic phase content. The accepted hypotheses of the T-tests are given (H_0 null-hypothesis, H_A alternative hypothesis).

tive to yttria concentration of 0.5-1 mol-% Y_2O_3. It has to be stated that 60 wt-% of monoclinic phase only refers to the powder metallurgically produced reference synthesized in-house. Commercial 3Y-TZP powders contain virtually no monoclinic phase fraction and are purely tetragonal. They are nevertheless produced by a liquid-phase co-precipitation procedure that was neither possible within the Institute of Advanced Ceramics nor was it suitable for a high-throughput procedure for reasons mentioned in section 2.4.

Even though the three statistically relevant libraries showed roughly the same mean deviation, the system without any mixing additives was preferable, as the dosing and the drying of the mixing aid took approximately one extra day within the synthesis cycle.

It was apparent from both figure figures 4.3 and figure 4.4 and the results of the statistical analysis outlined in table 4.2 that an increase in deviation towards the yttria-poor side of the system occurred. To speculate on the reason for this effect, the diffusion behaviour facilitated by the heat treatment was studied using as a model a finite point source of matter (M moles) diffusing into an infinite volume

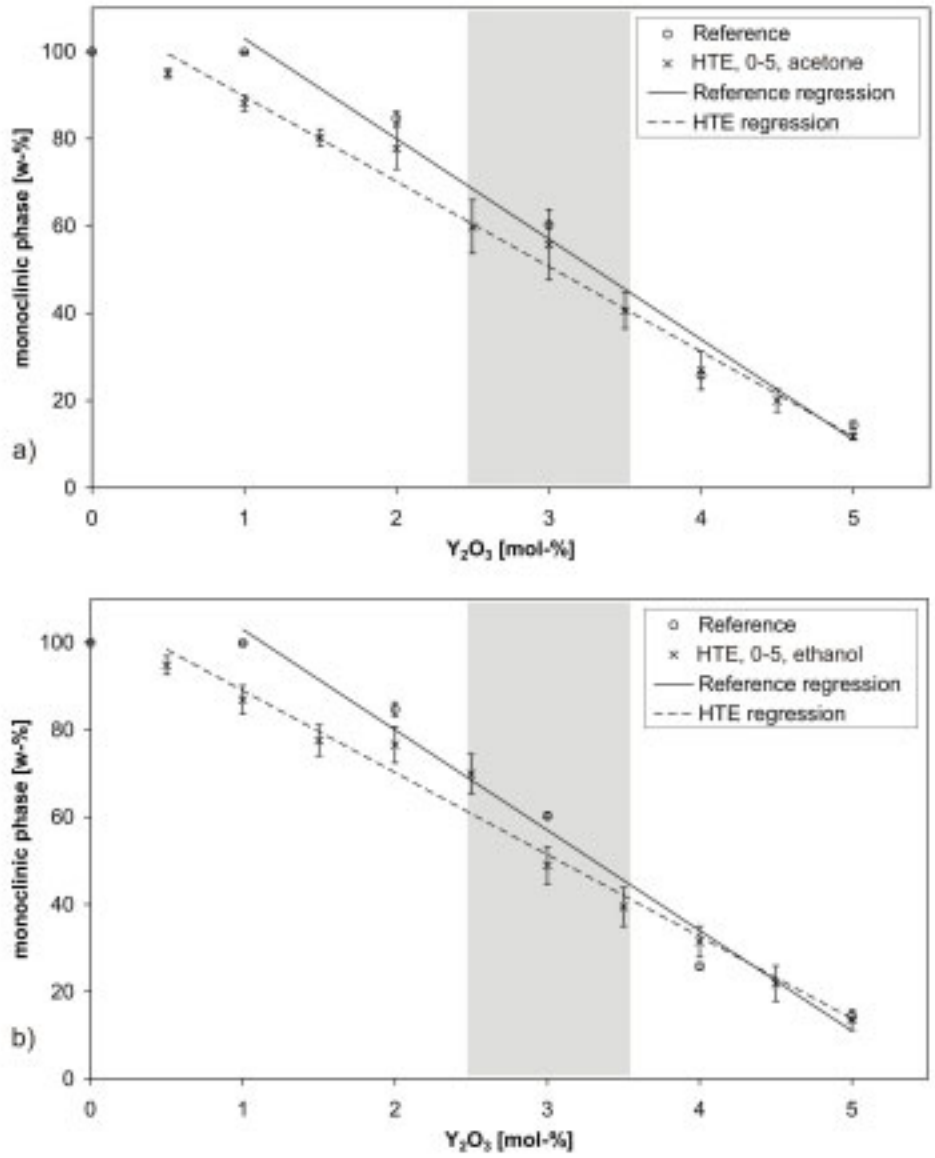

Figure 4.3: Y_2O_3 concentration vs monoclinic phase content for 0-5 libraries with a) acetone and b) ethanol as a mixing aid. The reference values as well as both regression lines are given for comparison. Scattering is shown as standard deviation. The grey area is the concentration range of commercial Y-TZP.

of zero initial concentration. The concentration is given as a special solution to Fick's second law of diffusion

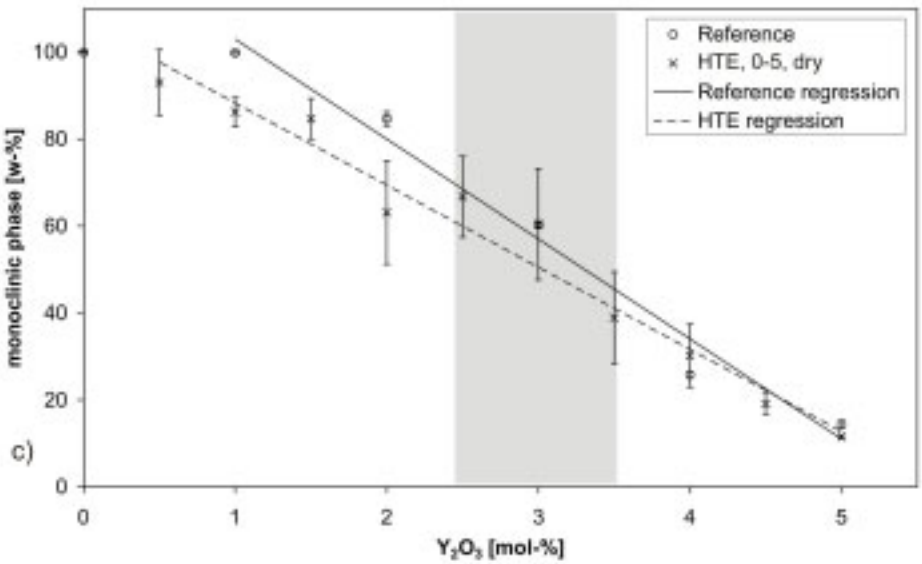

Figure 4.4: Y_2O_3 concentration vs monoclinic phase content for 0-5 libraries with no liquid mixing aid. The reference values as well as both regression lines are given for comparison. Scattering is shown as standard deviation. The grey area is the concentration range of commercial Y-TZP.

$$C(r,t) = M\frac{exp\left(-\frac{r^2}{4Dt}\right)}{8(\pi Dt)^{3/2}} \tag{4.10}$$

where r is the diffusion radius, t is the time and D is the diffusion coefficient [CBK97]. On the basis of this solution, the peak width at half height can be calculated to be

$$r_{0.5} = \sqrt{2.77Dt}. \tag{4.11}$$

This function of time constitutes the width of the concentration profile determined by equation 4.10 at half the peak concentration and is taken as an estimator for the homogenization potential through heat treatment induced diffusion. The microstructure of crystalline ceramics causes diffusion to take place in distinct regimes according to the respective material transport paths. It is evident that along grain boundaries the microstructural packing is less dense than within grains and consequentially the atom mobility yielding grain boundary diffusion is much

higher than that for transport within grains (lattice or bulk diffusion). This rather straight forward idea can be expressed formally by a difference in activation energies for diffusion under the two regimes resulting in a difference of diffusivities according to equation 4.1. For the sintering temperature of 1500 °C, diffusivity values of $D_B \approx 2 \times 10^{-18}\ m^2/s$ for bulk diffusion and $D_{GB} \approx 2 \times 10^{-12}\ m^2/s$ for grain boundary diffusion have been reported for diffusion of yttrium in yttria stabilized zirconia [KBL+02]. Assuming the diffusion of yttrium to be rate-limiting in the investigated system and furthermore using a sintering time $t = 7200$ s (experimental conditions), one can calculate $r_{0.5,B} \approx 2$ µm as well as $r_{0.5,GB} \approx 200$ µm. From figure 4.5 it is evident that the latter value exceeds the size of a typical agglomerate in the zirconia powder used. Furthermore it holds that $r_{0.5,B} \approx d_{50} \approx 0.5$µm for the respective powders. It is hence conceivable that grain boundary diffusion allowed a rapid global concentration equalization within each sample feeding a microscopic equalization within each grain through bulk diffusion. In other words, as a first theoretical approximation, homogenization should have been possible through a series connection of grain boundary diffusion with a characteristic length in the order of magnitude of the agglomerate size and bulk diffusion with a characteristic length in the order of magnitude of the grain size.

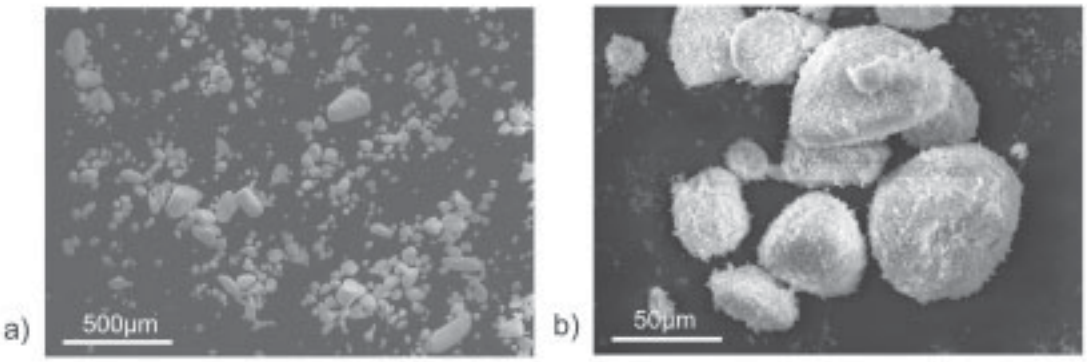

Figure 4.5: SEM pictures of zirconia agglomerates with a) 50- and b) 500-fold magnification.

These theoretical considerations contradicted the phenomenon of increasing deviation with decreasing yttria content mentioned above. It hinted to the existence of agglomerates that survived the mechanical offense of the mixing and pressing

and which, as a result, had the same yttria concentration for all samples of one library, namely the concentration of the masterbatch they descended from. However, the frequency of the yttria-rich agglomerates decreased with decreasing net yttria concentration in the sample, thus hindering more complete homogenization by longer diffusion paths. It could be followed that a third characteristic length in the homogenization process is the average distance between yttria-rich agglomerates. This distance (L3 in figure 4.6) would increase with decreasing net yttria concentration.

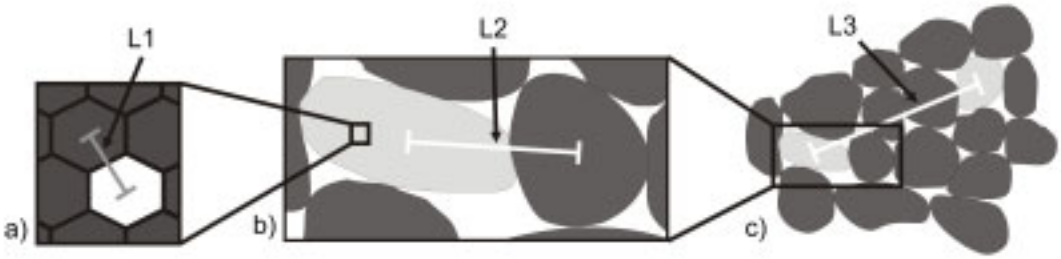

Figure 4.6: a) Scheme of microstructure with an yttria grain (bright) and several zirconia grains (dark) in an exemplified green body. b) and c) Scheme of agglomerate containing yttria and zirconia (bright) as well as zirconia only (dark). Characteristic lengths for homogenization through diffusion are in the order of magnitude of a) one grain size (L1), b) the agglomerate size (L2) and c) the average distance between two agglomerates of likewise concentration (L3). Note that L1<L2≤L3 always. Specifically, L2<<L3 for small overall concentrations of yttria.

4.4 Conclusions

In this initial study it could be shown clearly that high-throughput experimentation was applicable to ceramic bulk materials and that the setup described in chapter 3 was in fact a functioning HTE approach. Within one experimental run, the material system $ZrO_2 - Y_2O_3$ could be scanned in the concentration range between 0 and 5 mol-% yttria with a resolution of approximately 0.5 mol-%. Due to the importance of homogeneity of Y_2O_3 in ZrO_2 and the low interdiffusion rate in the material system used, the results stood as proof-of-principle that this setup was indeed a valuable help for development and optimization of materials

resulting out of solid state reactions. This discovery motivated the use of the HTE approach for a more realistic challenge in a partly unknown material system with a more topical frame of interest, which is the subject of the following chapter.

The considerations on the homogenization due to heat-treatment induced diffusion as well as the regression analysis helped to shed some light on the fundamentals of design of the masterbatches to be used in the HTE setup. The tertiary diffusion path length (L3 in figure 4.6) is directly dependent on the concentration difference that is spanned by the masterbatches. In the case of the 0-10 libraries this distance was too high as can be seen from the statistical refusal of all of them (see table 4.2) For the 0-5 libraries, L3 only had an impact on the yttria-poor side of the system. It is evident that if one perceives the higher concentrated component of the mixture (in this chapter zirconia) as matrix and the lower concentrated one (yttria) as dopant, the dopant's concentration difference spanned by the masterbatches (termed masterbatch range henceforth) should be as small as possible. In the case where the term dopant could be applied to more than one component of the mixture, the ion with the smallest diffusion coefficient in the respective matrix is crucial.

Additionally, the results on the dopant's lower concentration boundaries tend to be more error-prone. This has implications on the design of experiments for whole HTE-campaigns. When more than one library is necessary to scan a certain experimental space it make sense to prepare the masterbatches in such a way as to allow a sufficient overlap of the individual libraries pertaining to concentration. The redundant information thus generated will permit to spot and possibly correct larger experimental errors.

The advantages of the HTE approach protruded clearly in this proof-of-principle-study: The degree of automation involved in the setup made it possible to minimize the influence of human error on the accuracy and precision of the experiments. What is more, the complete cycle from masterbatch to evaluated results including the dosing, mixing, shaping and sintering was completed in approximately 3 days, the longest intervals of which were for sintering and the XRD analysis. Both of those ran unsupervised and further green body preparation could be performed

meanwhile. The experimental errors mentioned above were deemed acceptable against this background, since the tendency was obvious from the results and a subsequent more conventional experimental cycle would have revealed the errors in a real experimental setting.

5 High-throughput experimentation of a novel material

5.1 Sodium potassium niobate

A material class underlying, often invisibly, many of today's electronic appliances are so-called ferroelectric materials. Ferroelectric unit cells are always polar due to a permanent electrical dipole that aligns with the dipoles of neighbouring unit cells to form so-called domains. The polarization direction of these domains can be changed by means of an external electric field in several directions defined by certain geometric constraints dictated by crystallography. A second material property that always goes along with ferroelectricity is piezoelectricity. The linear extension of dipol moments inside the unit cells through an external field gives rise to a mechanical strain and, vice-versa, an applied mechanical force yields surface charges. Hence these materials are predestined for applications that rely on control of a mechanical force by an electric signal or on a rapid electric readout affected by a mechanical input. Evidently, applications will come frequently from the groups of actuators and sensors.

Presently, the material of choice for these applications is lead zirconate titanate ($Pb(Ti_xZr_{1-x})O_3$, PZT). PZT is a solid solution of $PbZrO_3$ and $PbTiO_3$. It was found that maximum piezoelectric behaviour can be achieved for x≈0.52 which is justified by a morphotropic phase boundary (MPB) [MH03]. An MPB is a temperature-independent phase boundary that separates in the case of PZT a rhombohedral and a tetragonal phase. The special properties result out of the fact that the free energies of the two adjacent phases are equal [CC92]. Hence the phase boundary can be perceived as a degenerated two phase field that allows for the coexistence of the two phases' piezoelectric domain orientation directions to coexist in a certain concentration area around the phase boundary [DZZ+07b]. This feature leads to a high number of thermodynamically equivalent states and hence a

high degree of ferroelectric alignment during poling. It is this high degree of alignment that results in the outstanding piezoelectric properties already mentioned. This knowledge has given rise to a multitude of cheap and ubiquitous appliances, e.g. for the automotive industry. In recent years though, a directive by the European Union on the restrictions of the use of toxic lead [Cou03] has spawned interest in finding a lead-free replacement for PZT ceramics. Under amplified investigation is the perovskite family of sodium potassium niobate ($K_{0.5}Na_{0.5}NbO_3$, KNN) [ZXS07] for which three MPBs are reported in literature so far, two in the system $K_xNa_{1-x}NbO_3$ [JCJ71] and one in the system $(K_{0.5}Na_{0.5})_{1-y}Li_y(Nb_{1-z}Ta_z)O_3$ [SHT+04]. For the sake of completeness it has to be stated that at the time of writing there is a dispute in literature as to whether the phase boundaries in the KNN-system are indeed morphotropic. Du *et al.* state that since they are strongly temperature dependent they are more likely polymorphic phase transitions [DZZ+07b]. However, for the desired increase in piezoelectric behaviour this controversy is marginal since according to Dai *et al.* any form of thermodynamically justified two-phase coexistence will increase material properties [DZZ07a]. The term morphotropic phase boundary will be used for the remainder of this thesis.

The potential of KNN as piezoelectric and hence as a potential lead-free replacement for PZT was mentioned already in 1975 by Kosec and Kolar [KK75]. However, the workers also reported KNN's biggest impediments to this day, namely the difficulties when sintering and its instability in air stemming from high reactivity with moisture [MYS+05]. Best known in this field are the works by Saito *et al.* [SHT+04, ST06]. The workers introduced Li on the A site of the perovskite into the system to improve sinterability. Furthermore, they inserted Ta on a B site to inhibit abnormal grain growth which would normally arise from just the addition of the sintering aid Li. Interestingly, in the resulting planar concentration section in $(K_{0.5}Na_{0.5})_{1-y}Li_y(Nb_{1-z}Ta_z)O_3$ with $y \in [0, 0.2]$ and $z \in [0, 0.6]$ (henceforth referred to as "Saito-plane") they found an MPB which proceeded approximately according to

$$y = 0.05 - 0.11z. \tag{5.1}$$

For compositions close to that MPB, Saito *et al.* found very promising piezoelec-

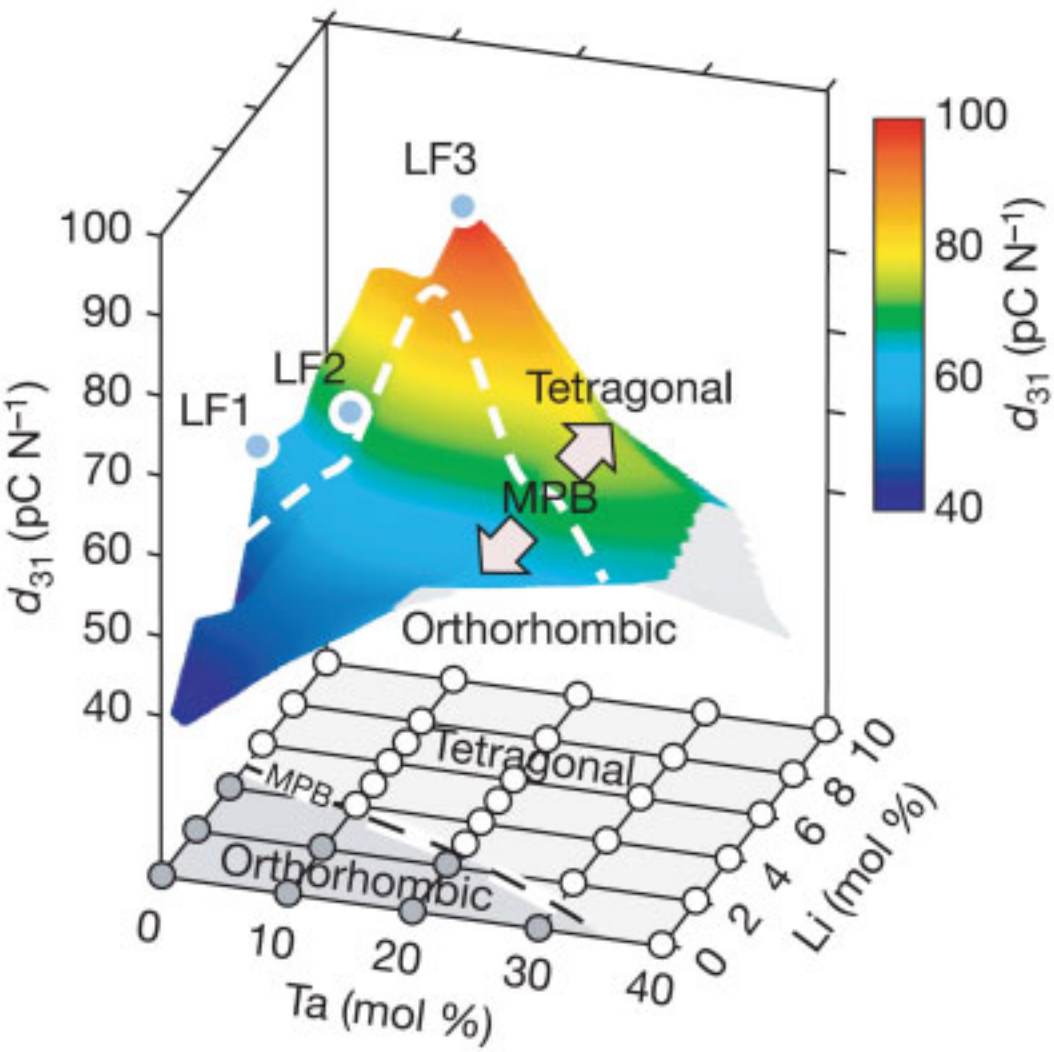

Figure 5.1: Piezoelectric sensor performances for the lead-free piezoelectric Li- and Ta-modified KNN (taken from [SHT+04]). The Li/Ta-plane is termed Saito-plane in this work.

tric properties as can be seen in table 5.1.

It is apparent that even though both sets of values for the KNN are promising, only the textured material can at the time of writing compete with PZT. However, the textured synthesis of ceramic materials is complex and an implementation in cheap mass production of, say, injection valves for the automotive industry is therefore questionable. Hence, further optimization is asked for with respect to function,

Piezoelectric properties	KNN (textured)	KNN	PZT
T_C [°C]	253	415	250
d_{33} [pCN^{-1}]	416	98	410
S_{max}/E_{max} [pmV^{-1}]	750	100	700

Table 5.1: Piezoelectric data of textured KNN and KNN with morphotropic concentration as compared to PZT according to [SHT+04] and [ST06].

synthesis and stability of KNN and HTE is a practical approach for this endeavour.

From what was said above it is evident that phase boundaries in a piezoelectric material are major targets due to the high likelihood of optimal behaviour and consequently the work described in this chapter was aimed at quickly and efficiently finding areas in the material system that showed abrupt structural changes. Several of those areas of interest could be detected in a concentration volume previously unknown as will be shown in the following. However, one of the reasons the KNN system was chosen for the experiments described here, was that the work could be started in the system that was already known to some extent from the works of Saito and could be expanded from there. Hence, the material system allowed a smooth transition from the proof of principle procedure described in the previous chapter towards an application within a real experimental campaign.

5.2 Preliminary experiments in the Saito-plane

5.2.1 Experimental

5.2.1.1 Preparation of masterbatches

The raw materials for all experiments in the KNN system were lithium carbonate (Li_2CO_3), sodium carbonate (Na_2CO_3) and potassium carbonate (K_2CO_3, all 99+%, ChemPur GmbH, Karlsruhe, Germany) as well as niobium oxide (Nb_2O_5) and tantalum oxide (Ta_2O_5, both 99.9%, ChemPur GmbH, Karlsruhe, Germany). In each case the raw powders were dried at 200 °C for 5 hours to remove all humidity and underwent pounding in a mortar prior to processing. After being weighed

in the respective batches were ball-milled for approximately 5 hours. The milling was stopped when a predefined median of the grain size distribution ($d_{50} \approx 0.5\mu m$) was reached. Each batch was 150 g and the milling took place in ethanol using 1000 g grinding balls (diameter 3 mm, yttria-toughened zirconia, Tosoh, Toyko, Japan). All batches were dried and homogenized after being milled. Subsequently, three calcination cycles ensued, conducted at 750 °C for 5 hours. In between calcination powders were repeatedly attrition milled to expose new surface area and evoke a complete phase transformation. This uncommon procedure was necessary due to the slow chemical conversion of the powders which arose from preliminary XRD surveys.

5.2.1.2 Preparation and characterization of KNN HTE libraries in the Saito-plane

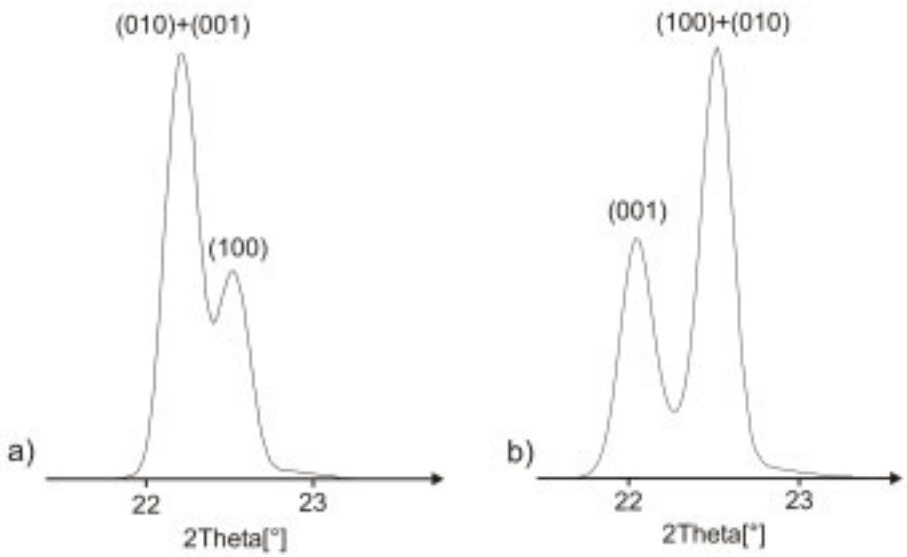

Figure 5.2: Scheme of orthorhombic (a) and tetragonal (b) XRD patterns in the system $(K_{0.5}Na_{0.5})_{1-y}Li_y(Ta_zNb_{1-z})O_3$ in the 2θ range relevant for this work.

According to the procedure described in section 5.2.1.1 2 sets of masterbatches were prepared, namely $(K_{0.5}Na_{0.5})_{1-y}Li_y(Nb_{1-z}Ta_z)O_3$ with $y = z = 0$ and

$y = z = 0.1$ (MB1 and MB2) as well as $y = z = 0.0325$ and $y = z = 0.0515$ (MB3 and MB4). Using these, three libraries containing 22 (LTKNN1 and 3) and 20 (LTKNN2) samples were prepared by again layering the respective powder fractions in five parts alternately on top of each other and subsequently mixing them in parallel for 10 minutes at 80 rpm. Shaping was conducted cold-isostatically at 400MPa for 2 minutes. Heat-treatment was performed with a dwelling time of 1 hour at 1075 °C and heating as well as cool-down at 10 K/min.

Six XRD-patterns were recorded on different areas of each sample in the range of 21-24° 2θ (detector distance 30 cm) yielding (110)-, (010)- and (001)-peaks of the tetragonal and orthorhombic phases expected from [SHT+04] and [ST06] (see figure 5.2).

	$(K_{0.5}Na_{0.5})_{1-y_i}Li_{y_i}(Nb_{1-z_i}Ta_{z_i})O_3$	
Library	**Masterbatches**	**Stoichiometric coefficients**
LTKNN1	MB1 and MB2	$y_i = z_i = \frac{0.1}{21} \cdot (i-1), i = 1, ..., 22$
LTKNN2	MB1 and MB2	$y_i = z_i = \frac{0.019}{19} \cdot (i-1) + 0.0325, i = 1, ..., 20$
LTKNN3	MB3 and MB4	$y_i = z_i = \frac{0.019}{21} \cdot (i-1) + 0.0325, i = 1, ..., 22$

Table 5.2: Three preliminary HTE KNN-libraries in Saito-plane. For graphical representation refer to figure 5.3.

Subsequently, each sample's patterns were summed up to minimize signal-to-noise ratio and to form a pattern mean over the sample surface. Finally, a normalization step was performed over the highest peak to achieve direct comparability between the summed patterns.

5.2.2 Results and discussion

Figure 5.4 shows the XRD patterns of LTKNN1 graphically assembled one behind the other. To allow for an easier comparison between the individual patterns, they were normalized over the larger of the two peaks respectively. The phase change could clearly be deduced from the peak switch that is marked with arrows.

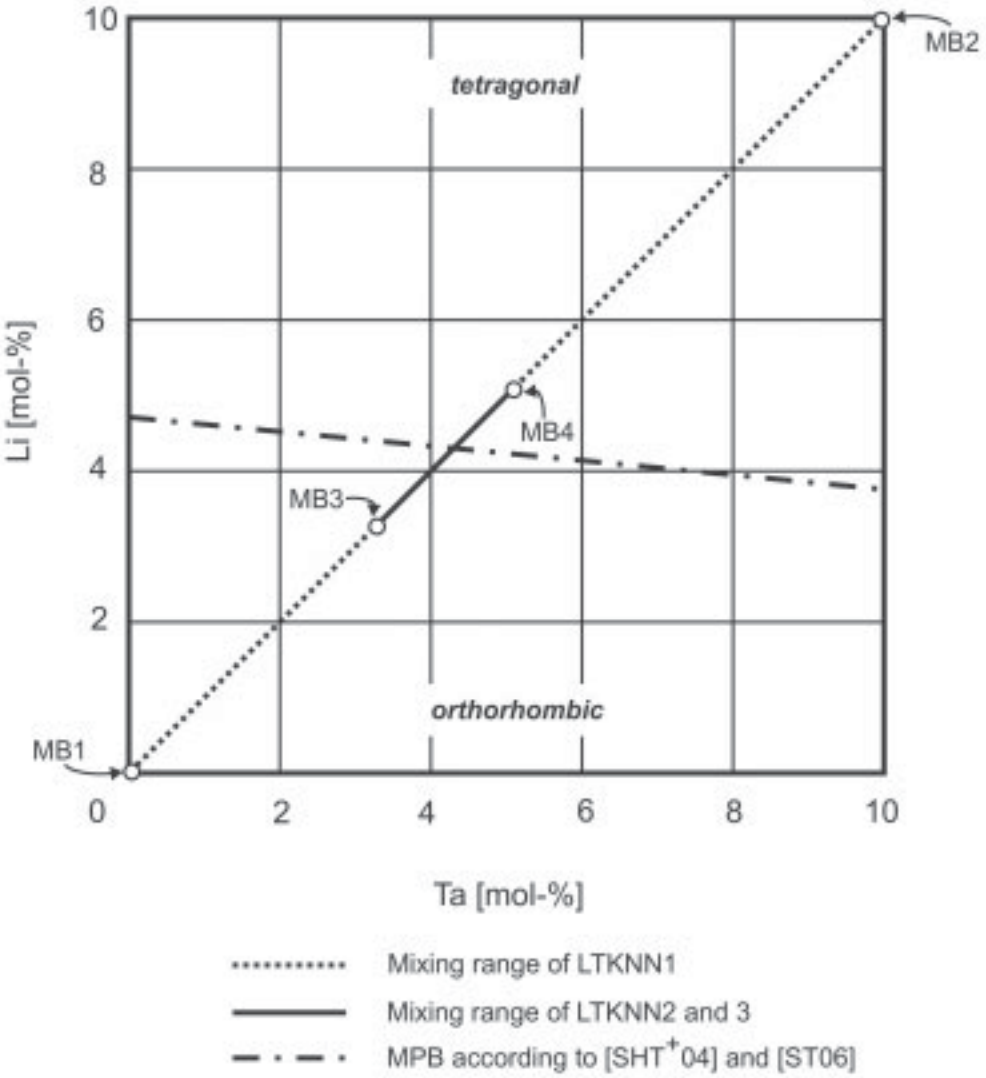

Figure 5.3: Scheme of the sampled concentration axis in a section of the phase diagram for Li- and Ta-modified KNN adapted from [SHT+04].

For LTKNN1 this phase change occurred sharply on one of its samples, namely sample no. 9 which is equivalent to a Li/Ta-concentration of 3.72 mol-%.

For LTKNN2 the phase transition was not as clear. The transition here occurred not on one sample but rather in a concentration range marked by a group of samples. The extent of this range was marked by fluctuating peak ratios and in the case of LTKNN2 could be limited by samples no. 8 (3.95 mol-% Li/Ta) and

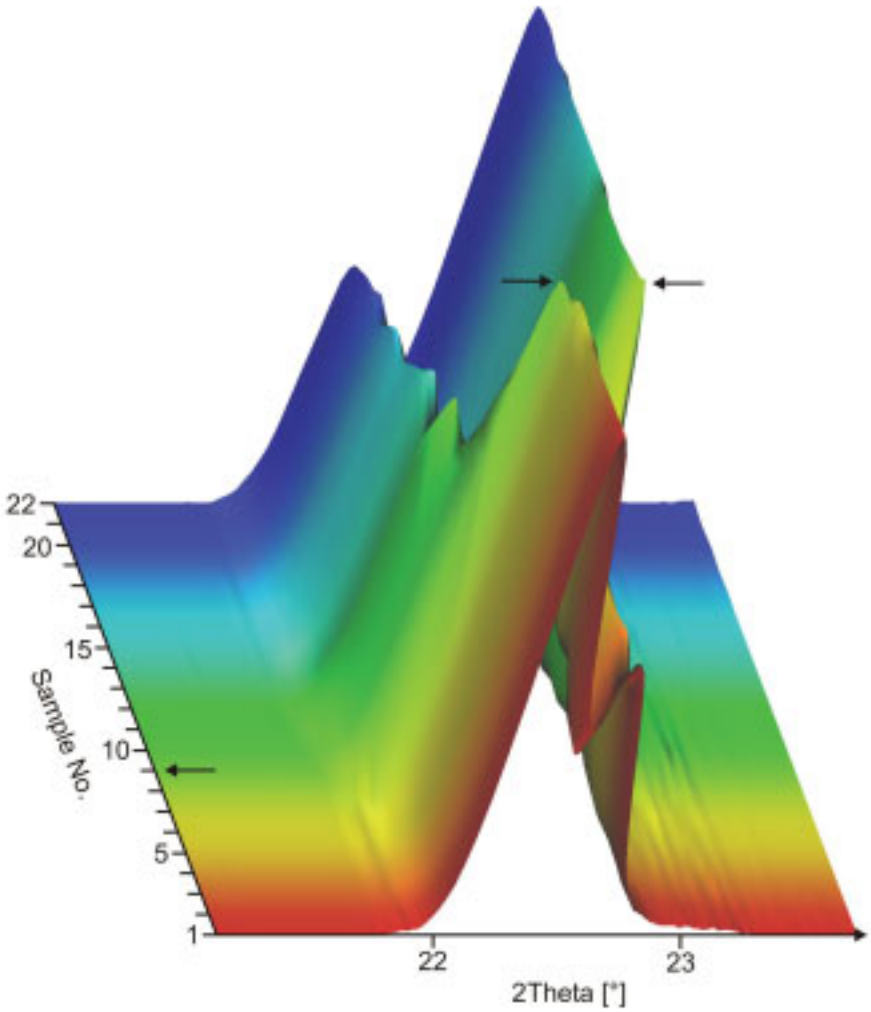

Figure 5.4: XRD patterns of 20 samples of library LTKNN1. Note the phase change marked by arrows.

no. 12 (4.35 mol-% Li/Ta), hence spanning 0.4 mol-%.

In the library LTKNN3 the concentration resolution was comparable to the one featured in LTKNN2. Nevertheless, the phase transition range in this case was a lot narrower being restricted between sample no. 12 (4.15 mol-% Li/Ta) and no. 13 (4.24 mol-%) which was equivalent to a width of 0.1 mol-%.

From the course of the MPB postulated by Saito *et al.* and its junction with the sampled concentration axis it is evident that the phase change for LTKNN1-3

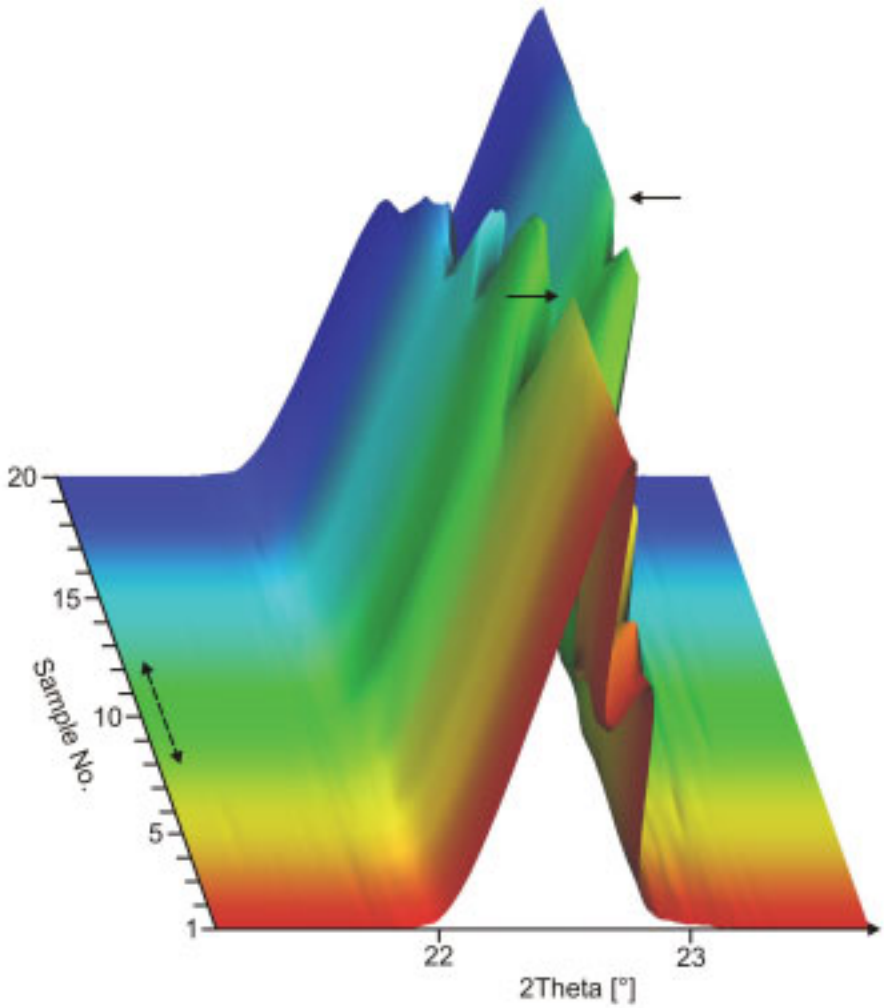

Figure 5.5: XRD patterns of 20 samples of library LTKNN2. Note the phase change marked by arrows.

should occur approximately at a concentration of 4.2 mol-% Li and Ta, which was missed in the case of LTKNN1 by merely 0.5 mol-%. For LTKNN2 4.2 mol-% was found approximately in the middle of the suggested phase transition range. For LTKNN3 finally, the phase boundary as proposed by Saito *at al.* at 4.2 mol-% was one side of the transition range indicated by the XRD results.

The different setups of the three libraries allowed one to study the influence of three different factors in the HTE experimental design on the homogeneity of the final samples as shown in the broadness of the phase transition range (precision) as

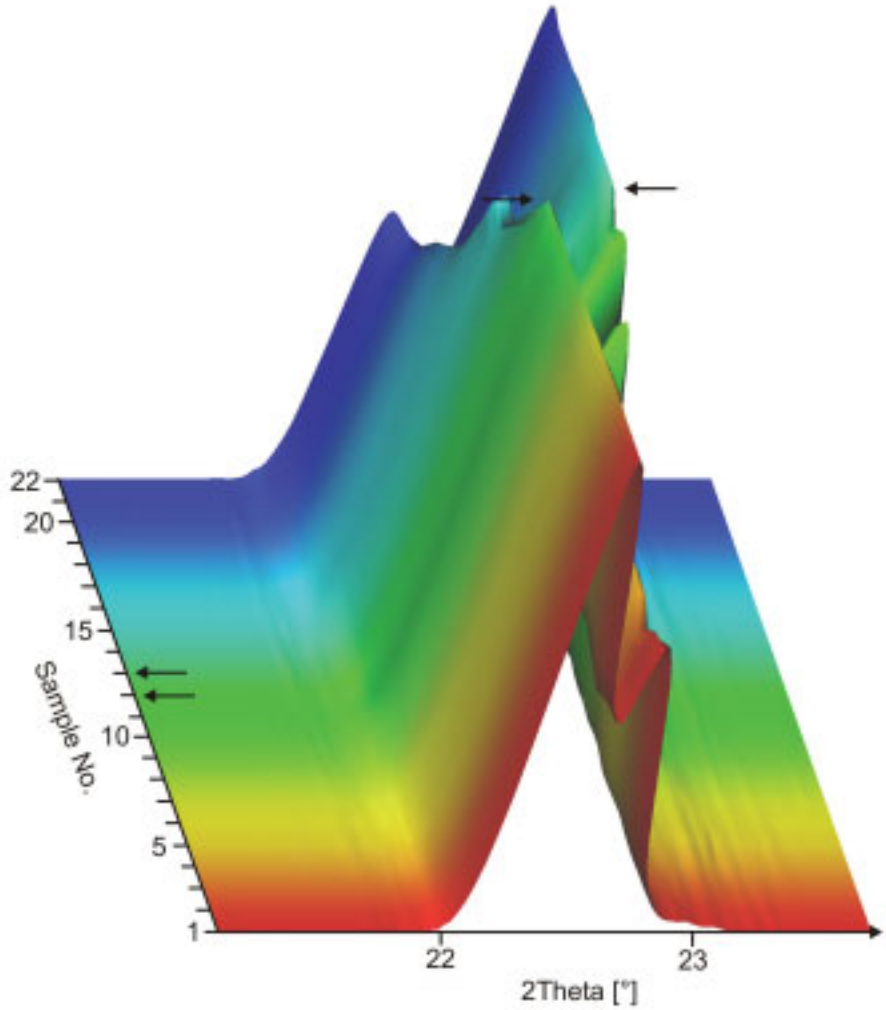

Figure 5.6: XRD patterns of 20 samples of library LTKNN3. Note the phase change marked by arrows.

well as in the degree of accordance with the data known from [SHT+04] and [ST06] (accuracy). Those three factors were the mixing range (i.e. the concentration difference spanned by the library), the masterbatch range (i.e. the concentration difference between the masterbatches used) and the library's resolution (i.e. the concentration difference between two library members). The factor values for the three libraries are given in table 5.3.

With respect to the precision of the studied phase change it was obvious that LTKNN1 and LTKNN3 showed better results in terms of sharp phase transition

Library	Mixing range	Masterbatch range	Resolution
LTKNN1	10 mol-%	10 mol-%	0.5 mol-%
LTKNN2	1.9 mol-%	10 mol-%	0.1 mol-%
LTKNN3	1.9 mol-%	1.9 mol-%	0.1 mol-%

Table 5.3: Experimental design factors for three preliminary KNN libraries.

even though they varied in all of the three factors given in table 5.3. The ratio of masterbatch range to resolution however, was the same for both libraries namely approximately 20 whereas it was a lot higher (approximately 100) for LTKNN2.

In terms of accuracy LTKNN2 and 3 showed better results than LTKNN1. Both of them featured concentration ranges for the phase change that bordered the phase boundary concentration as suggested in [SHT+04] and [ST06] whereas LTKNN1 showed a transition that deviated by 0.5 mol-%.

These results help to identify the efficiency boundaries of the parallelized mixing procedure. Firstly, the ratio of masterbatch range to resolution of the HTE library affects the precision of the final results. The findings presented in chapter 4.3 made clear that the magnitude of concentration difference between the masterbatches influences the degree of inhomogeneity in the green body. The subsequent heat treatment is capable of inducing further homogenization in the respective sample. However, depending on the concentration difference of the masterbatches there will still be inhomogeneities present in the respective library member. These inhomogeneities will show in analysis when the resolution of the library is too small.

Secondly, the mixing range of the library seems to affect the accuracy. However, the result suggesting this is somewhat ambiguous, since the concentration difference between the phase boundary in LTKNN1 and the one suggested by Saito *et al.* is in the same order of magnitude as the library's concentration resolution.

Obviously, the masterbatch range/resolution ratio of 20 $\frac{\text{mol}-\%}{\text{mol}-\%}$ is not an absolute value that can be used for any further work on the presented HTE-setup. The affinity for a ceramic bulk sample to show a homogeneous structure at the end of

the process chain is dependent on the powder properties (agglomeration, flowability) and of course on the diffusivity during heat treatment. Hence, a critical ratio has to be determined for every new material system investigated. However, it is evident that ratio is crucial and it should be observed that at a given masterbatch range the resolution may not be refined carelessly or, vice versa, if a distinct resolution is wanted a critical masterbatch range my not be exceeded.

5.3 HTE experiments in previously unknown concentration space

5.3.1 Experimental

5.3.1.1 Preparation and characterization of KNN HTE libraries in previously unknown concentration space

Since the preliminary experiments showed encouraging results it was decided to vary the system with one more degree of freedom, namely the K/Na-ratio. This was equivalent with expanding the Saito-plane previously worked in into a concentration volume as depicted in figure 5.7 by a library of 125 samples (LTKNN4) of 600mg in the system $(K_xNa_{1-x})_{1-y}Li_y(Nb_{1-z}Ta_z)O_3$ where the mixing procedure was conducted exactly as described in section 5.2.1.1. The samples were again equidistant in concentration due to the variation of the stoichiometric coefficients x=[0.4, 0.45, 0.5, 0.55, 0.6], y=[0, 0.025, 0.05, 0.075, 0.1] and z=[0, 0.05, 0.1, 0.15, 0.2]. The concentration volume was chosen such that it could be covered with approximately 100 samples, a degree of throughput that seemed realistic after the preliminary endeavours. Six masterbatches were prepared according to the procedure outlined in 5.2.1.1 with the concentrations $(K_{0.6}Na_{0.4})NbO_3$ (MB5), $(K_{0.4}Na_{0.6})NbO_3$ (MB6), $K(Nb_{0.65}Ta_{0.35})O_3$ (MB7), $Na(Nb_{0.65}Ta_{0.35})O_3$ (MB8), $(K_{0.75}Li_{0.25})NbO_3$ (MB9) and $(Na_{0.75}Li_{0.25})NbO_3$ (MB10).

It is evident that in the case mentioned above finding the concentration of each masterbatch for the respective samples was not trivial. Hence, an algebraic model was derived from both the chemical element balance and boundary conditions for this ABO_3-type material. From the six equations resulting out of a complete

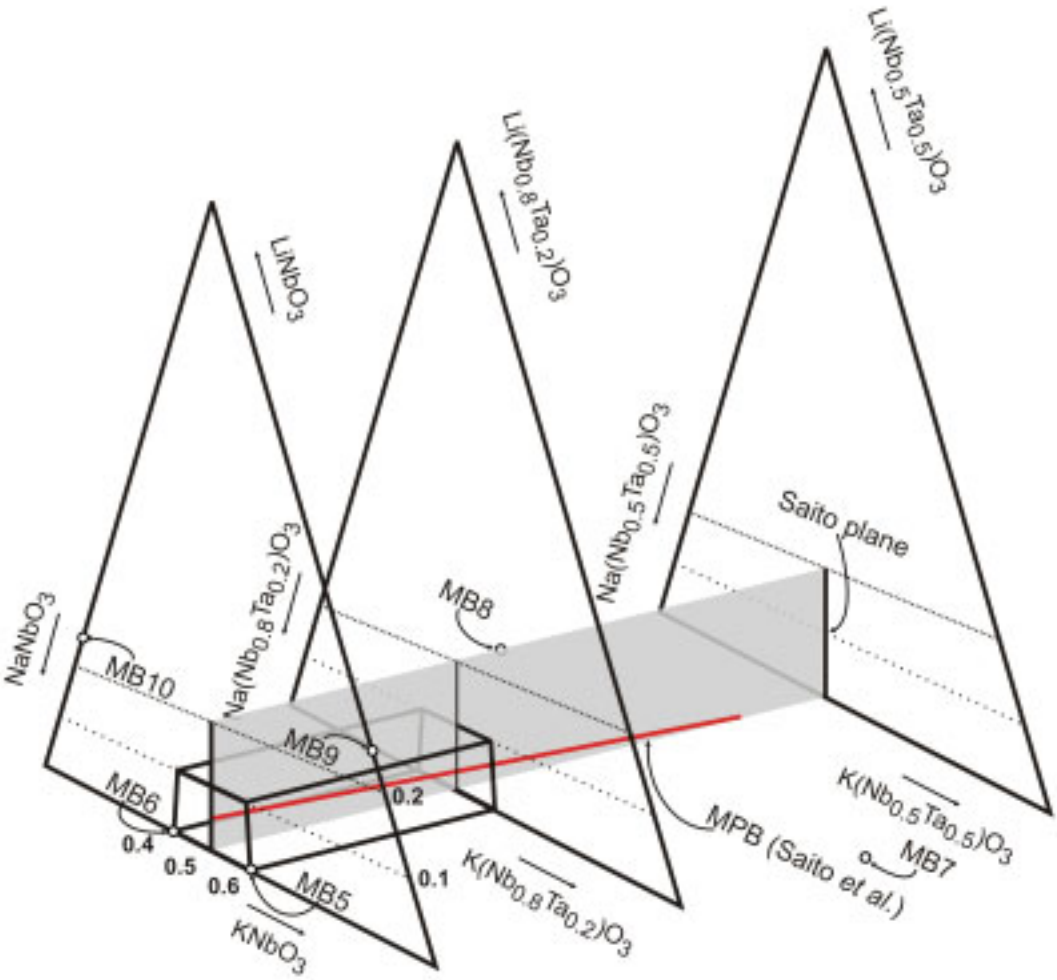

Figure 5.7: Scheme of ternary phase diagram of $(K_xNa_{1-x})_{1-y}Li_y(Nb_{1-z}Ta_z)O_3$. The shaded area is the concentration plane examined in [SHT+04] and [ST06] termed Saito-plane in this work. The red line shows the approximate progression of the known morphotropic phase boundary. The dots labeled MB5-10 are the masterbatches used in high-throughput synthesis of the library. The volume depicted between the two ternary systems $RNbO_3$ and $R(Nb_{0.8}Ta_{0.2})O_3$ with $R = K, Na, Li$ is the experimental space investigated.

balance for the six elements in $(K_xNa_{1-x})_{1-y}Li_y(Nb_{1-z}Ta_z)O_3$, three (one per stoichiometric coefficient) were linear dependent. Nevertheless, six equations were needed to solve for six masterbatch concentrations. The K- and Na-contents ($[K]$ and $[Na]$) in the final material resulted directly from the concentration ratio of masterbatch pairs MB5-6, MB7-8 and MB9-10 respectively. These pairs had to be

dosed in a proportion dictated by the respective stoichiometric coefficient $\frac{x}{(1-x)}$. For example

$$\frac{\hat{c}_5}{\hat{c}_6} = \frac{x}{(1-x)} \Rightarrow \frac{x}{(1-x)} \cdot \hat{c}_6 - \hat{c}_5 = 0 \tag{5.2}$$

with $\hat{c}_i$ being the molar fractions of the respective masterbatches. Hence, in total three boundary conditions of the form

$$\frac{[K]}{[Na]} = \frac{x}{(1-x)} = \frac{\hat{c}_5}{\hat{c}_6} = \frac{\hat{c}_7}{\hat{c}_8} = \frac{\hat{c}_9}{\hat{c}_{10}} \tag{5.3}$$

could be used.

The three linear independent element balances could be formulated such that there was one equation for the A-, B- and O_3-site of the molecule respectively. E.g. the Nb-balance could expressed as

$$1 - z = \hat{c}_5 + \hat{c}_6 + 0.65 \cdot (\hat{c}_7 + \hat{c}_8) + \hat{c}_9 + \hat{c}_{10}. \tag{5.4}$$

In

$$\begin{pmatrix} 1 & 1 & 1 & 1 & 0.75 & 0.75 \\ 1 & 1 & 0.65 & 0.65 & 1 & 1 \\ 1 & 1 & 1 & 1 & 1 & 1 \\ -1 & \frac{x}{(1-x)} & 0 & 0 & 0 & 0 \\ 0 & 0 & -1 & \frac{x}{(1-x)} & 0 & 0 \\ 0 & 0 & 0 & 0 & -1 & \frac{x}{(1-x)} \end{pmatrix} \begin{pmatrix} \hat{c}_5 \\ \hat{c}_6 \\ \hat{c}_7 \\ \hat{c}_8 \\ \hat{c}_9 \\ \hat{c}_{10} \end{pmatrix} = \begin{pmatrix} 1-y \\ 1-z \\ 1 \\ 0 \\ 0 \\ 0 \end{pmatrix} \tag{5.5}$$

the first three equations are the element balances for $K + Na$, Nb and O_3 respectively. The second three equations are formulations of the $\frac{[K]}{[Na]}$-ratios of the three masterbatch pairs mentioned above (see equation 5.3).

Solving for $\hat{\mathbf{c}}$ with the respective set of stoichiometric coefficients x, y and z yielded the molar fractions of the six masterbatches for that sample where

$$\sum_{i=5}^{10} \hat{c}_i = 1. \tag{5.6}$$

The samples were processed in 5 groups of 25 samples, where each sample in one group shared the same x value with the x values being randomized. y in turn, was completely randomized within x and z within y. It is important to note that the sample group with $x = 0.5$ in fact represented a section of the Saito-plane.

All samples were sintered in air for 8 hours at 990 °C with heating as well as cool-down being 10 K/min. This divergence in sintering temperature with respect to the previous work in the Li- and Ta-modified KNN (see section 5.2.1.2) was justified by unsatisfactory results of precursory sintering experiments. Higher temperatures lead to melting of substantial parts of some samples as can be seen in figure 5.8. Hence the sintering temperature had to be lowered gradually until uniform bulk samples could be sintered at 990 °C. With increasing number of masterbatches to be mixed in one sample the difficulties in homogenization of each sample already mentioned in 4.2.3 most likely increased, leaving macroscopic agglomerates or even groups of agglomerates in contact within the sample. If these were low-melting, instead of participating in a solid-sate reaction to densify the sample (sintering) they could have melted and caused the insufficient structure shown in figure 5.8.

Figure 5.8: HTE samples in the KNN system sintered with temperatures higher than 990 °C (1075 °C). Note the substantial mass loss due to melting.

Again six independent XRD-patterns were recorded per sample in the range of 15-70° 2θ (detector distance 15 cm) and subsequently added for reasons mentioned

above. Since a visual inspection of this multitude of patterns was no longer possible the clustering feature of the already mentioned software tool PolySNAP (see page 20) was used to structure the patterns.

As a basis for the clustering PolySNAP produced a 125×125 matrix holding a weighed mean of Pearson and Spearman correlation coefficients. For the clustering result the correlation coefficients were transformed into normalized Euclidean distances with values between 0 (i.e. two patterns are completely dissimilar) and 1 (i.e. two patterns are the same). PolySNAP used these similarity values for the clustering and reported the results in form of a dendrogram with a cut-off similarity resulting out of the best estimate of several eigenvalue operations. The cut-off line was flanked by confidence intervals derived from the highest and the lowest estimate of said eigenvalue operations.

The cut-off line could be moved manually and it was thus possible to increase or decrease the amount of clusters. This procedure was used such that in the Saito plane ($x = 0.5$) the cluster boundary best mirrored the MPB known from [SHT+04] and [ST06]. It was assumed that when doing so, the progression of the cluster boundaries through the investigated concentration volume would mirror the progression of the MPB and possibly even reveal previously unknown phase boundaries.

5.3.1.2 Comparison of the inner homogeneity to the library homogeneity

In the course of the clustering work the question arose, how much signal variance existed within one sample, i.e. how "different" were patterns recorded on one sample and hence how insecure the structural information gained from the clustering analysis of summed XRD patterns described in 5.3.1.1 was. Insight was to be gained from inspection of the six single patterns of each sample without them being summed up.

For the analysis, first an artificial zero-pattern (XRD pattern with zero intensity over the whole 2θ range) was generated. Subsequently, for each HTE-sample of LTKNN4 the six sample patterns were processed against the zero pattern by

PolySNAP yielding in total $125 \times 6 = 750$ correlation coefficients. As a reference, six patterns recorded on the same spot of one randomly chosen sample (sample no. 91: $(K_{0.55}Na_{0.45})_{0.925}Li_{0.075}NbO_3$) were processed against the zero pattern. Furthermore, variances of each of the groups of six correlation coefficients were determined (1 reference and 125 samples) and in the following 125 F-Tests were performed to test for heterogeneity of variance (heteroscedasticity) between the reference and the samples respectively (Null hypothesis $H_0 : \sigma_0^2 = \sigma_i^2$, alternative hypothesis $H_A : \sigma_0^2 \neq \sigma_i^2$). The statistical test was again performed on a level of significance of α=0.05 and was implemented in a script using the numerical software tool MATLAB. For a schematic of the testing procedure mentioned above the reader is referred to figure 5.9.

5.3.2 Results and discussion

As described on page 66 it was possible by manual adjustments to the dendrogram reported by PolySNAP to mirror the the MPB in the Saito-plane ($x = 0.5$) by a cluster boundary. This procedure yielded two different outcomes with respect to the rest of the investigated system ($x \neq 0.5$), namely a total of three and a total of two clusters.

In figure 5.10 a) the clustering result yielding two clusters can be seen. Unfortunately, PolySNAP only delivers poorly resolved graphical output. Nevertheless, the thick yellow cut-line is obvious. The numerical report of the respective clustering analysis gave its position at a similarity of 0.836. Two dashed lines above and below mark the confidence intervals the upper one being so close to the cut-off line that it is visually not distinguishable due to the poor resolution. PolySNAP offered a possibility to simplify the visualization of the clustering by reporting per cluster one most representative pattern that featured the smallest distance to all the other cluster members (descriptively speaking, the pattern “in the middle of the cluster”) [BDG04a]. For the two clusters those patterns and their accordant sample numbers and compositions can be seen in figure 5.10 b).

Furthermore, the progression of the MPB is shown against the clustering outcome in figure 5.11 a) for the Saito-plane where clusters are colour-coded. The

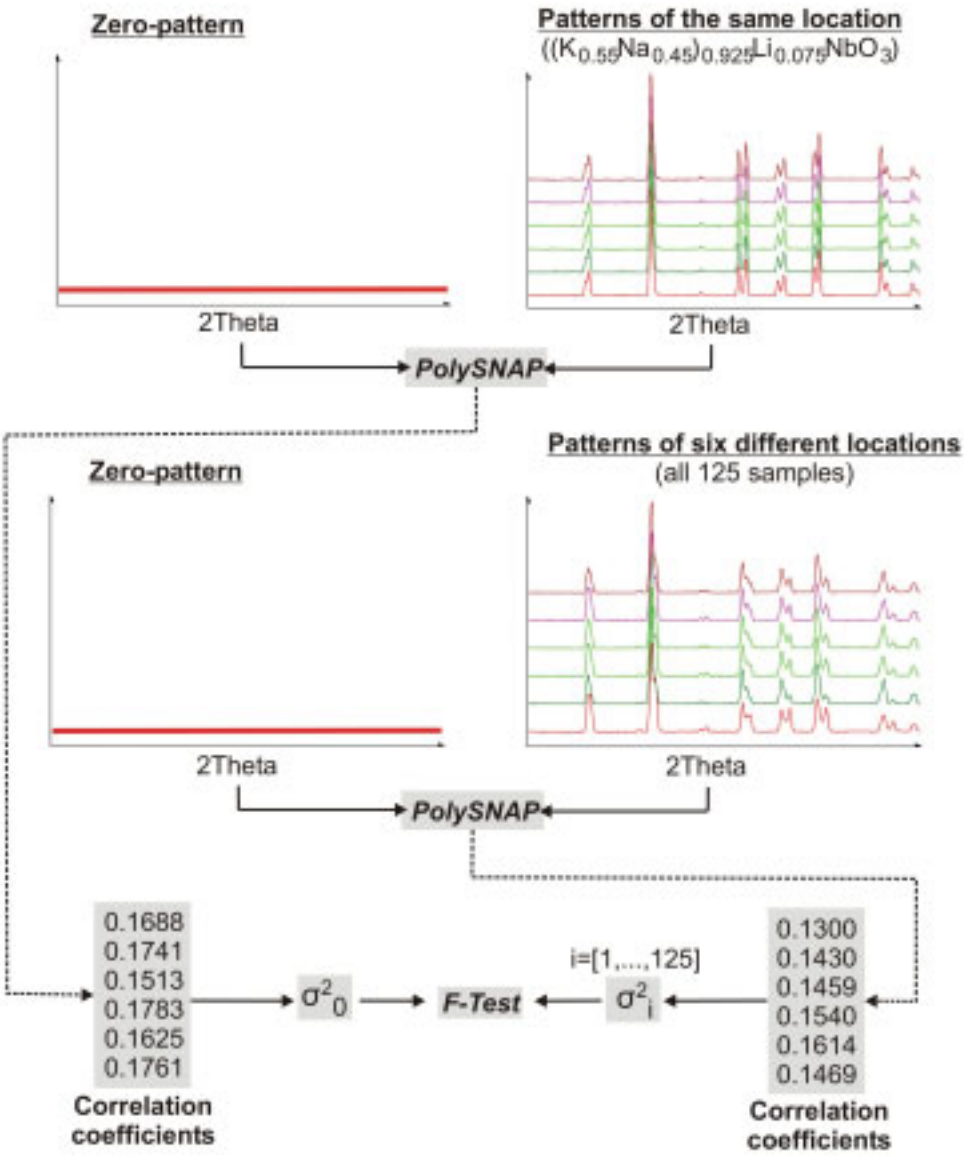

Figure 5.9: Scheme to determine inner homogeneity of samples by means of their XRD patterns. Correlation coefficients were determined using the software tool PolySNAP between a zero-pattern and six sample patterns respectively. A reference set of correlation coefficients was deduced from six patterns taken on the same spot of one sample. 125 sample variances (σ_i^2) were derived from the respective correlation coefficients and F-tested against the reference variance(σ_0^2) for heteroscedasticity.

clustering managed to reproduce the phase boundary reported in [SHT+04] and [ST06] reasonably well. Also, it was obvious that the clusters were coherent in con-

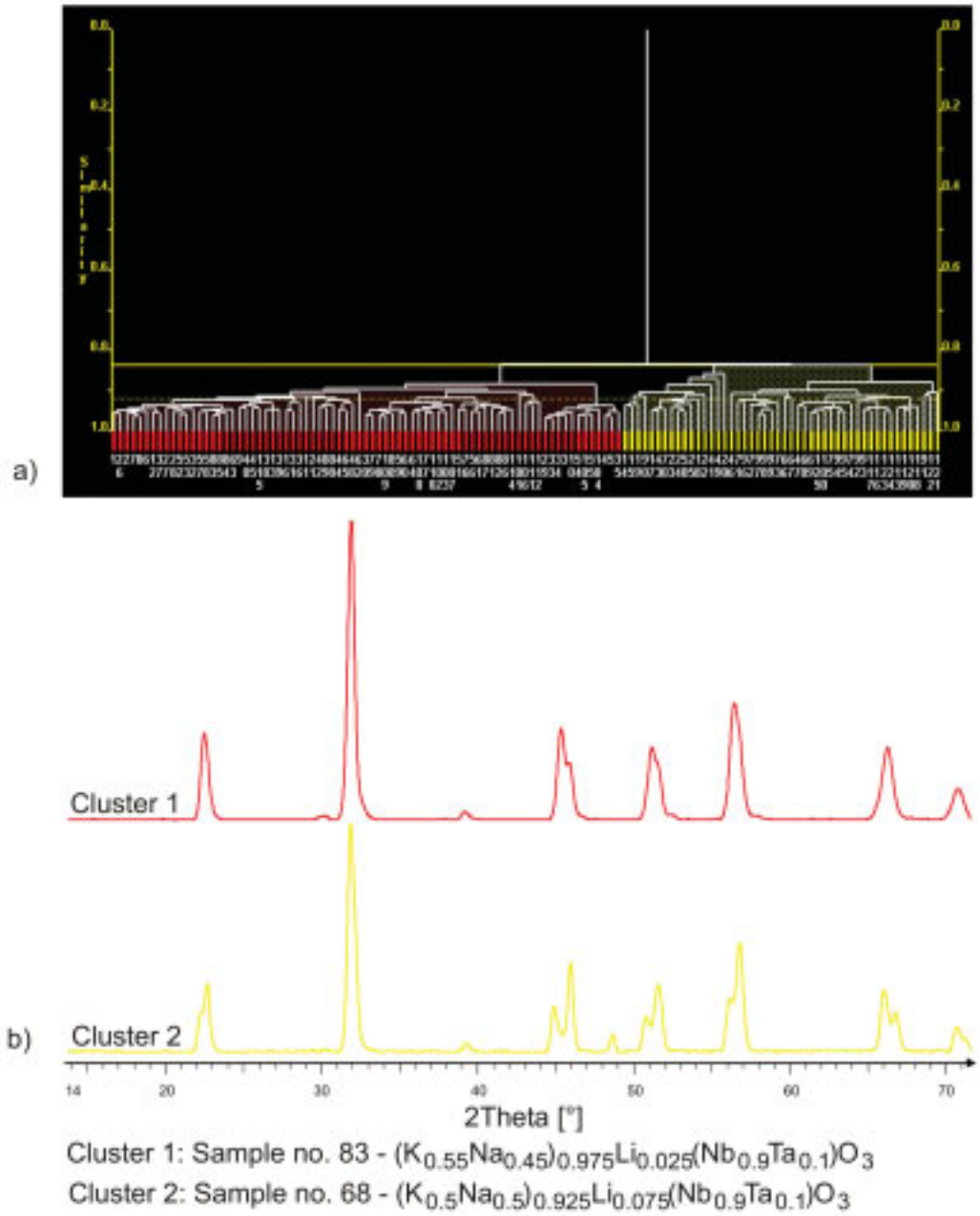

Figure 5.10: Results of clustering in colour-coding (red: cluster 1, yellow: cluster 2). a) Dendrogram as reported from PolySNAP manually restricted to two clusters. b) Most representative XRD patterns of each of the two clusters.

centration space which was the case not only for the Saito-plane visualized here but for the whole investigated concentration space. This fact lent credibility to the

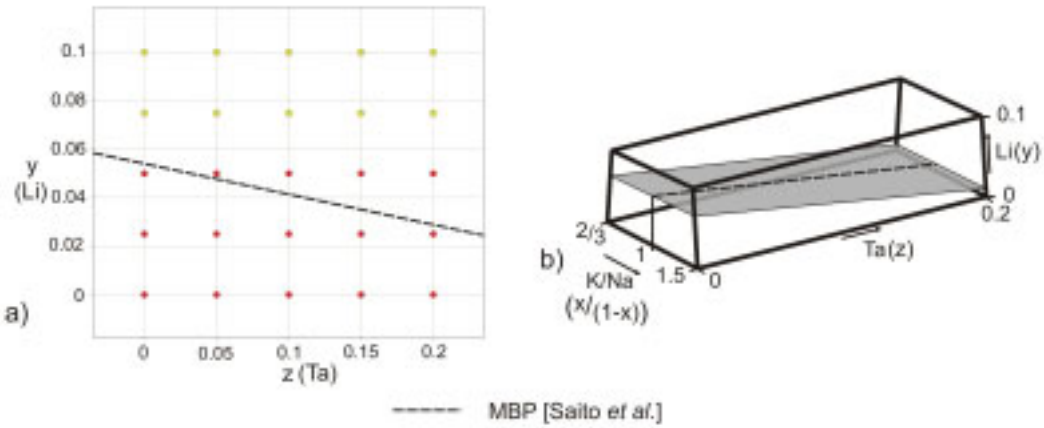

Figure 5.11: a)Representation of Saito-plane ($x(K) = 0.5$) with respective MPB (dashed line) superimposed. The coloured dots mark the samples The colours indicate the respective cluster affiliation with cluster 1 (red) identifying the orthorhombic and cluster 2 (yellow) the tetragonal phase according to [ST06]. b) Scheme of concentration volume examined. The shaded area represents the approximate progression of the cluster boundary and hence hypothetical progression of the known MPB, the known linear section of it being depicted by the dashed line.

hypothesis that clusters determined by PolySNAP could in fact serve as mappings of real phases. Nevertheless, there were obvious deviations between the PolySNAP result and the MPB that could be attributed to the parallel mixing procedure. It seemed reasonable here to correct the results suggested by PolySNAP towards the results reported by Saito *et al.* since their results are generally accepted in the concerned community. When doing so, the clustering outcome could be summarized in the scheme shown in 5.11b). Hence an MPB-area perpendicular to the Saito-plane can be expected to proceed away from the linear phase boundary section known in literature thus far.

In the second case (three clusters) that is depicted in figure 5.12 it became clear that while the clustering on the Saito-plane remained, the former cluster 2 was split into two new clusters by moving the cut-line to a similarity of 0.846. This strengthened the hypothesis of the MPB-area deduced above. The position of the third cluster is suggested in the visualization of the concentration plane yielding

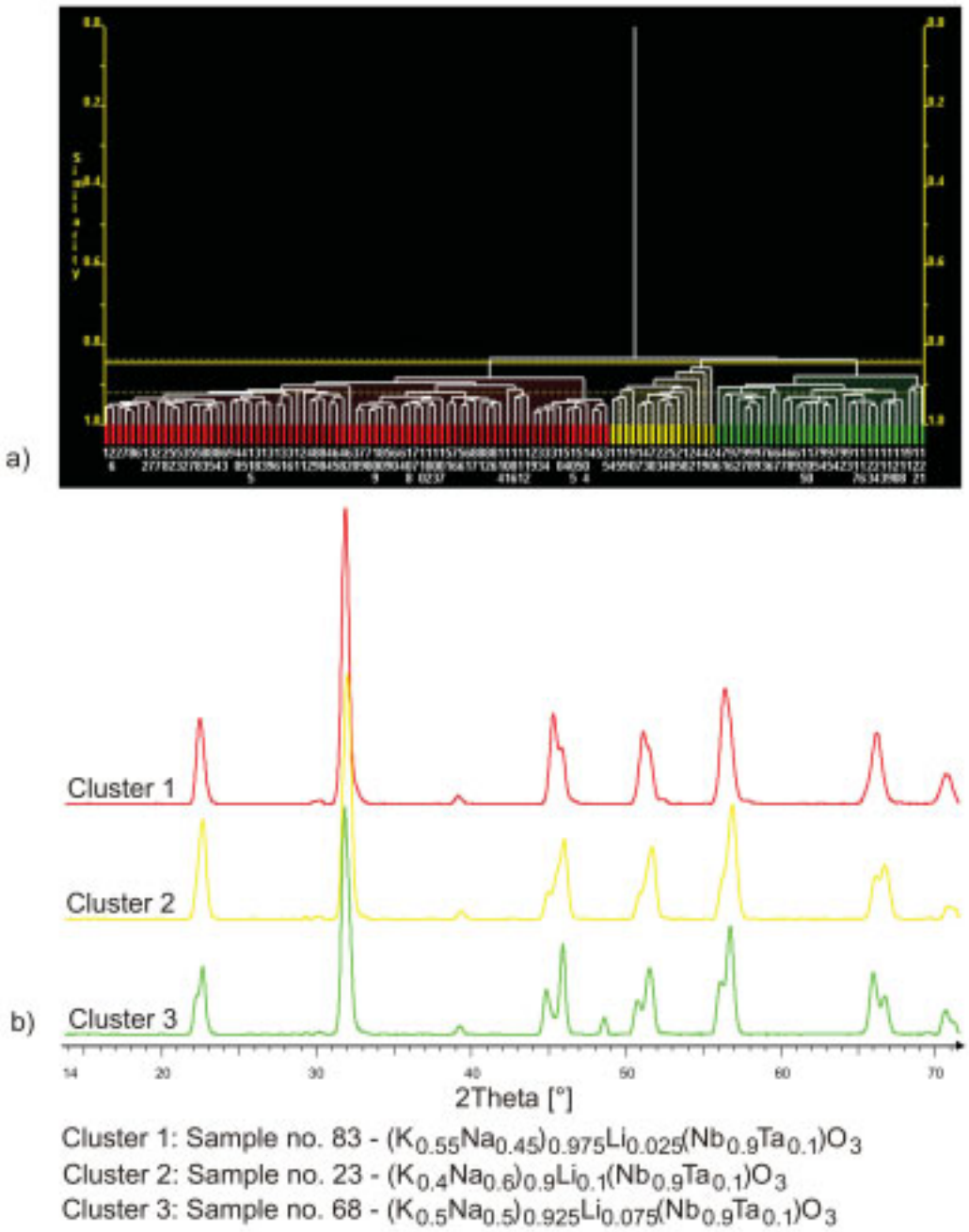

Figure 5.12: Results of clustering in colour-coding (red: cluster 1, yellow: cluster 2, green: cluster 3). a) Dendrogram as reported from PolySNAP manually restricted to three clusters. b) Most representative XRD patterns of each of the three clusters.

from the stoichiometric coefficient $x = 0.4$ in figure 5.13 a). A simplified scheme

of the PolySNAP outcome for this case can be seen in figure 5.13 b). The result hinted strongly to a third independent phase in the investigated concentration volume.

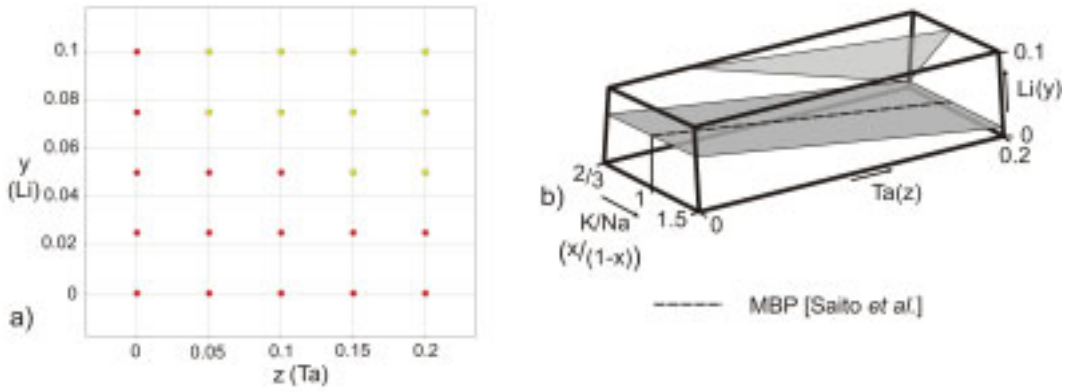

Figure 5.13: The plane given in a) corresponds to the backside of the volume shown in b) ($K/Na = 2/3$). Note the presence and location of cluster 2 (yellow). The Saito-plane was the same as in the case of two remaining clusters. b) Scheme of concentration volume examined. The two shaded areas represent the approximate progression of the cluster boundary and hence hypothetical phase boundaries. The known linear section of the MPB is again depicted by the dashed line.

	stoichiometric coefficients		
Sample No.	**x**	**y**	**z**
LTKNN4-4	0.4	0	0.15
LTKNN4-40	0.45	0.05	0.2
LTKNN4-47	0.45	0.1	0.05
LTKNN4-104	0.6	0	0.15
LTKNN4-109	0.6	0.025	0.15
LTKNN4-116	0.6	0.075	0
LTKNN4-121	0.6	0.1	0

Table 5.4: Results of statistical test for heteroscedasticity. The variance of the correlation coefficients of the sample listed here were not homogeneous with respect to the reference sample (i.e. H_0 rejected).

The results of the statistical analysis depicted in figure 5.9 fortified the plausibility of the clustering approach. It was desirable that for all or most samples the variances of the correlation coefficients were homogeneous with respect to the reference. The reference variance resulted out of six patterns recorded on the same spot of one sample and defined the smallest (systematic) variance and the F-test tested whether the null hypothesis of homogeneous variances could be maintained. Hence a maximum number of accepted H_0 was achievable and indeed only for 7 out of the 125 samples was H_0 rejected.

The rejected samples are reported in table 5.4 to show that their distribution did not follow any pattern. Specifically, they were not on or close to one of the cluster/phase boundaries. Had that been the case, it would have been conceivable that due to uneven concentration within one sample close to a phase boundary both phases were present in the same sample. Most likely, the rejected samples left the parallel mixing insufficiently homogenized.

It was beyond the used techniques to decide whether the third cluster was indeed a third independent phase. Nevertheless, the XRD pattern of the cluster pertaining to that third hypothetical phase (see figure 5.12) showed features from both of the other patterns which could also hint to a two-phase field. Such an area could in fact hold benefits analogous to those encountered along an MPB due to the biphasic nature of an MPB as mentioned in [DZZ07a].

5.4 Conclusions

In the preliminary experiments in the Saito plane reported in section 5.2 three libraries with varying mixing ranges, masterbatch ranges and resolutions were synthesized and analysed for a crystallographic phase change. The two libraries with the higher resolution of 0.1 mol-% (LTKNN2 and 3) showed good agreement with the phase information as presented in [SHT+04] and [ST06]. LTKNN2 having the higher masterbatch range featured a more fuzzy phase transition along the libraries concentration axis. The results suggested, that an important criterion when designing experiments for the HTE-setup presented here, is to keep the ratio between masterbatch range and concentration resolution low. For the Li- and Ta-modified KNN system in this work a ratio of 20 seemed to produce good results. Even though this ratio will have to be determined anew for every material system, the Li- and Ta-modified KNN in this work is known to form a liquid phase at moderate sintering temperatures [MYK+05] and hence should be prone to homogenization during heat-treatment. The ratio of 20 $\frac{\text{mol}-\%}{\text{mol}-\%}$ can thus be thought of as an upper limit and especially dry sintered systems will make lower ratios necessary.

The third library (LTKNN1) with the highest mixing range showed a sharp phase transition that lay approximately 0.5 mol-% away from the position of Saito's phase boundary. A causal connection between mixing range and accuracy could not be deduced since the difference of 0.5 mol-% could also be accounted for by the libraries lower concentration resolution. Adding to this uncertainty is the fact that a morphotropic phase boundary is in fact"*a narrow composition region with the coexistence of two different phases*" [DZZ07a]. The extension of this region for the mentioned MPB is however not known.

Another implication of this fact was that a phase transition range, as seen in LTKNN2 and 3 could be both, a physical effect due to the morphotropic nature of the phase boundary or an uncertainty resulting out of lacking experimental diligence as a result of the parallelization of synthetic process steps owing to the HTE nature of the approach. For LTKNN2, the latter option is fortified by the fact that the extension of the phase change region was clearly dependent on the above mentioned ratio between masterbatch range and resolution. For LTKNN3 the case was

not clear. Higher resolved structure analysis (e.g. applying synchrotron radiation) of the respective samples would be necessary to decide whether the HTE-setup's resolution is high enough to expose such small-scale, complex material behaviour.

The aim of this work however was not the fine structural analysis of material systems but rather to implement a workflow to speed up the materials development cycle. The discussion initiated above should thus be put into perspective. The experiments in this section required less than a week of laboratory work and created robust structural information to be fed into a subsequent conventional experimental cycle.

The second half of the works in the KNN system showed the strength of the software based clustering tool PolySNAP for simplifying and ordering high amounts of XRD data that when confronted with conventionally would have posed an insurmountable task. The plausibility of the clustering approach was strengthened further by the statistical analysis which showed clearly that the inner homogeneity of the vast majority of samples was in the order of magnitude of the deviations that were intrinsic to the experimental system. Hence a progression of the known MPB can be expected with high probability to follow the course of the phase boundary that could be detected in both clustering outcomes. For the hypothetical third phase deduced from one of the results a confirmation by a diffraction technique with higher spatial resolution is advisable. Since there was at the time of writing no access to, say, synchrotron radiation, this kind of analysis was not possible in the scope of this work. Nevertheless, this would also allow clarification of the nature of that phase (two-phase field or solid solution).

The difficulties in determining the sintering temperature indicated by the melting loss to be seen exemplified in figure 5.8 help deduce one more fundamental for designing HTE experiments using the dry powder approach which is to keep the number of masterbatches as low as possible. Of course it can be argued that it is enough to pay heed not to introduce low melting phases as masterbatches to start with. However, this general approach disregards the fact that during heat-treatment the material will not in an instant reach its final equilibrium state but will develop by means of a variety of transitional precursory phases towards a

single-phased sample. The number of possible transitional phases increases with the amount of introduced chemical elements which is also the basis for the Single-Sample-Concept by Hulliger *et al.* mentioned in 2.3.2. Assuming the amounts of chemical elements introduced into the mixture to be correlated to the amount of masterbatches necessary it becomes clear that a small number of masterbatches is necessary to allow for a controlled and reproducible heat-treatment.

The two clustering outcomes allowed one to minimize the subsequent synthetic and analytic effort in the investigated system. Specifically, the continuation of the MPB known from the works of Saito *at al.* that appeared to be mirrored in both results was cause for hope that along this phase separating plane a concentration existed that matched or surpassed the piezoelectric behaviour mentioned by Saito *et al.* and did not feature the synthesis difficulties described e.g. in [MYS+05].

From the deviations between the MPB and cluster boundary in the Saito-plane it is obvious that PolySNAP fails to picture the MPB with complete precision. Yet again, those inaccuracies have to be viewed against the savings of time due to the use of the HTE setup that allowed synthesis, characterization and evaluation of 125 samples in two weeks of work.

The work presented in this chapter is exemplary for future application fields of the HTE setup for dry powders in experimental spaces of increasing width. For library sizes exceeding 20 samples a purely visual inspection of the ensuing data is beyond question. To gain conclusive knowledge of an investigated system a software based approach is essential to structure the data. However, the information gained from such an approach is reliable only if the software tool has been previously calibrated. Evidently, the results in the second half of this chapter complement the papers by Saito *et al.* but the work that lead to these results relied on the phase diagram postulated in [SHT+04] and [ST06] as calibration data. It follows that the HTE approach presented in this work is not suitable to venture into completely unchartered terrain. It relies on some prior knowledge located somewhere in or on the boundary of compositional space to be investigated.

6 Summary and outlook

In this work a successful attempt was made to transfer high-throughput experimentation ideas to a classical solid phase synthesis procedure conventionally used at the Institute of Advanced Ceramics at Hamburg University of Technology and in many other ceramics labs around the world. The process steps of this conventional procedure had to be implemented within a HT-workflow which meant parallelizing and automatizing them as far as possible. At the heart of the setup was a commercial 4-axis laboratory robot commanding a dosing unit for dry powders. This robot premixed samples through a layered dosing of various different powders. The main mixing step took place in a planetary mill that was adapted to mix up to 40 samples at the same time. Shaping was achieved by using silicone matrices that allowed a parallel loading of a conventional cold-isostatic press. Analysis in this work was based solely on X-ray diffraction in an automated diffractometer that allowed to limit the measuring time by employment of an area detector.

The same overall procedure was followed for all the experiments in this work. A concentration range of interest was defined within the material system under investigation. Subsequently, two or more powder masterbatches were prepared using conventional powder metallurgical techniques. These masterbatches formed the feedstock for the robot that dosed powder lots of a few hundred mg with the particular concentrations. These powder lots were transformed into green bodies by way of the above mentioned parallelized mixing and shaping procedure. Finally, the samples were sintered in a conventional laboratory furnace.

It was obvious that due to the parallelized mixing inhomogeneities would possibly be carried through all the way to ready sintered sample. The X-ray diffractometer in use allowed to check for those by the capacity to scan multiple spots per sample. Furthermore, the influence of inhomogeneities on the final result could be limited by adding all patterns of one sample up, effectively forming a set of mean patterns that could be used to deduce reliable phase information.

The HTE setup's operation could be verified by a group of experiments in the well known material system Y_2O_3-ZrO_2. This material system is known to feature slow interdiffusion and has no low-melting phases. The idea of this set of experiments was to test if it was possible to produce an HTE library that was structurally comparable to a conventionally prepared group of samples of the same concentration. The HTE libraries produced had a concentration resolution of 0.5 mol-% Y_2O_3. With optimized mixing parameters an experimental error pertaining to the conventional library of merely 1 mol-% Y_2O_3 could be achieved.

Furthermore, the HTE setup was applied in a material system that at the time of writing was at center of attention at the Institute of Advanced Ceramics, namely the leadfree piezoelectric sodium potassium niobate ($K_{0.5}Na_{0.5}NbO_3$, KNN). Within this system specifically the position of the phase boundaries was of interest due to the high likelihood of superior piezoelectric properties in their vicinity. Two groups of experiments were conducted. The position of a phase boundary already known from the works of Saito *at al.* in the system $(K_{0.5}Na_{0.5})_{1-y}Li_y(Nb_{1-z}Ta_z)O_3$ was verified by an HTE approach using pure KNN and $(K_{0.5}Na_{0.5})_{0.9}Li_{0.1}(Nb_{0.9}Ta_{0.1})O_3$ as masterbatches. Libraries with a resolution down to 0.1 mol-% Li and Ta were produced and XRD analysis showed complete agreement between Saito's and the HTE data.

Subsequently, by varying the K/Na-ratio between 2/3 and 1.5 starting from the Saito-plane ($K/Na = 1$) a previously unknown concentration volume ($(K_xNa_{1-x})_{1-y}Li_y(Nb_{1-z}Ta_z)O_3$ with $x = [0.4, ..., 0.6]$, $y = [0, ..., 0.1]$ and $z = [0, ..., 0.2]$) was studied. The respective library held 125 HTE samples with a resolution down to 2.5 mol-%. A software-based clustering analysis was used to classify the samples' XRD-patterns according to their similarity. It was shown that the morphotropic phase boundary known to exist in the system $(K_{0.5}Na_{0.5})_{1-y}Li_y(Nb_{1-z}Ta_z)O_3$ expanded into a plane along the K/Na-axis. Moreover, the clustering outcome strongly hinted to a third phase existing in the investigated concentration volume with the potential benefit of an as yet unknown phase boundary.

Several experimental design principles could be deduced for future use of the setup presented in this work. The concentration difference between the masterbatches (masterbatch range) introduced inhomogeneities in the green samples by way of of powder agglomerates left intact during the parallelized mixing procedure. In case of the masterbatch ranges being too high these macroscopic overconcentrations could be equilibrated only insufficiently during heat-treatment. Hence, the masterbatch ranges should be kept to a minimum when designing experiments for the dry powder HTE setup. Furthermore, it became clear that the ratio of masterbatch range to resolution of the library was influential with respect to concentration precision of the investigated phase boundary. A masterbatch range to resolution ratio of 20 $\frac{\text{mol}-\%}{\text{mol}-\%}$ worked well for the particular KNN-system whereas a higher value created a diffuse phase transition range. Finally, when working with more than two masterbatches at the same time problems arose with low-melting phases making heat treatment impossible until the sintering temperature had been lowered substantially. When a multitude of masterbatch phases are heated together it is improbable that they form a single-phase material initially but most likely go through a series of intermediate phases while the concentrations of the respective ions slowly balance by way of diffusion. Hypothetically, this process is hampered by macroscopic inhomogeneities in the green body as mentioned above. An increasing number of masterbatches mixed in one sample adds complexity in that it becomes harder and harder to anticipate low-melting phases by means of previous knowledge, e.g. in the form of phase diagrams. It is hence advisable to start any HTE endeavour with a series of binary material libraries and if necessary add masterbatches to the setup one after another. Thus it is possible to immediately identify a problematic masterbatch and either remove it or try and add the wanted ions in another form that is more agreeable to the rest of the materials introduced.

When trying to value the presented results it is important to remember the objective of HTE in trying to systematically increase the efficiency of the examination of vast experimental spaces. The “price” is the lack of sample quality and the resulting discrepancy between HTE-samples and analogous conventionally prepared specimen. This “price” is certainly low when judging it against the benefits of the experimental paradigm change. The degree of automation involved allows for the

synthesis and analysis of material libraries uncompromised by human errors. A conventional materials laboratory dealing with comparable amounts of samples and hence individual materials necessarily employs a multitude of lab staff. Not only the changing personnel will constitute a factor in view of the experimental effects but also the extended timeframe and the consequential variance in experimental diligence. These human factors will be confounded with the regular experimental factors, like concentrations, temperatures and the like, and can potentially blur effects and hence experimental results.

The advantage of increased synthetic and analytic speed is evident and has been mentioned before. It comes about either by automation of sequential techniques where time is gained through the fact that a supervision of the respective procedure step is not necessary, or it can be achieved by parallelization, i.e. by treating several samples at once. In the latter case the degree of acceleration is determined by the degree of parallelization. In the case of this work parallelization could be determined directly from the size of the treatment units and varied due to systematic reasons between 5 (for the shaping) and 40 (for the mixing). It is against this background that the experimental error of 0.5-1 mol-% Y_2O_3 can be considered sufficiently small in order to evaluate the ZrO_2-Y_2O_3 system in this concentration range. When using the conventional powder metallurgical synthesis route that was the starting point of this work, the time to synthesize and analyse one ceramic sample is in the order of magnitude of one day. Hence in two weeks approximately 10 samples and the respective analytic results can be gained. In the same time using the dry powder HTE setup it was possible to synthesize, analyse and evaluate 125 samples in the KNN system.

Moreover, when planned and conducted thoroughly HT experiments grant systematic knowledge when compared to a high amount of disconnected conventional experiments. In an instant they allow not only statements about single samples of one library but also about property contexts within that library. This fact is reflected powerfully in the possibility to predict phase-diagram-like information as has been shown in the chapter 5.1.

According to the experimental design principles mentioned above the setup is

best suited for the examination of systems spanned by a small number (possibly two) masterbatch materials whose concentration distance should also be kept at reasonable size. In the textbook case of a high-throughput workflow with a primary cycle illuminating roughly the complete pre-defined experimental space, a secondary cycle zooming into potential lead areas of said space and a ternary cycle quasi-conventionally screening hits within those lead-areas, the presented approach could ideally be utilized as a secondary cycle.

The core of the preceding primary cycle would have to be a rapid and effective powder mixing device, e.g. a commercial laboratory tool called Speedmixer (Hauschild, Hamm, Germany). It works by means of centrifugal forces in two planes and allows for the mixing of masses of some tens of grams within minutes. Using this device it would thus be possible to produce a relative coarse concentration grid of small powder batches with a better degree of homogenization than the parallel mixing approach explained in section 3.2.2. In spite of the sequential operation of the device a significant bottleneck in the HT workflow would not be encountered due to the shortness of the mixing time. The ensuing powder batches could subsequently be tested for activity. This would decrease them only by the mass of one bulk sample (approximately 1 g). Should any of the batches show sufficient activity, they could be used directly as masterbatches in the secondary cycle - the approach presented in this work.

The batches should be chosen to initially enter the secondary cycle only in groups of two and those pairs of masterbatches could be chosen furthermore according to their position next to each other in the examined concentration space. Thus both constraints mentioned above (namely a low number of masterbatches and a small masterbatch range) could be satisfied. In an approach analogous to the one described in sections 4 and 5.2 it would be possible to define hit compositions in the vicinity of the data points acquired in the primary cycle. Finally, these hit-materials would be synthesized and analyzed conventionally in a ternary cycle for verification reasons.

Should the effort be undertaken to include the setup used in this work in a complete HTE workflow like the one outlined above, this workflow has versatile

potential in academic and industrial materials challenges. Also, since results presented here are promising for the comparatively complex material class of ceramics, a successful application towards development and optimization of metallic and polymeric materials, in part also using powders as raw materials, would stand to reason.

Bibliography

[ADKW98] D. E. Akporiaye, I. M. Dahl, A. Karlsson, and R. Wendelbo. Combinatorial approach to the hydrothermal synthesis of zeolites. *Angewandte Chemie International Edition*, 37(5):609–610, 1998.

[AKAW04] A. Apostolidis, I. Klimant, D. Andrzejewski, and O. S. Wolfbeis. A combinatorial approach for development of materials for optical sensing of gases. *Journal of Combinatorial Chemistry*, 6(3):325–331, 2004.

[AS04] N. Adams and U. S. Schubert. Software solutions for combinatorial and high-throughput materials and polymer research. *Macromolecular Rapid Communications*, 25(1):48–58, 2004.

[ASWL01] P. M. Andersson, M. Sjostrom, S. Wold, and T. Lundstedt. Strategies for subset selection of parts of an in-house chemical library. *Journal of Chemometrics*, 15(4):353–369, 2001.

[AXZ02] E. J. Amis, X.-D. Xiang, and J.-C. Zhao. Combinatorial materials science: What´s new since Edison. *MRS Bulletin*, 27(4):295–300, 2002.

[BB95] R. Bodendiek and G. Burosch. *Streifzüge durch die Kombinatorik*. Spektrum, Heidelberg, Oxford, 1995.

[BDG04a] G. Barr, W. Dong, and C. J. Gilmore. High-throughput powder diffraction II. Applications of clustering methods and multivariate data analysis. *Journal of Applied Crystallography*, 37:243–252, 2004.

[BDG04b] G. Barr, W. Dong, and C. J. Gilmore. *PolySNAP*: A computer program for analysing high-throughput powder diffraction data. *Journal of Applied Crystallography*, 37(4):658–664, 2004.

[Bri94] J. Bridgwater. Mixing. In D. Chulia, M. Deleuil, and Y. Pourcelot, editors, *Powder Technology and Pharmaceutical Processes, Volume*

9, pages 347–357. Elsevier, Amsterdam, London, New York, Tokyo, 1994.

[Caw01] J. N. Cawse. Experimental strategies for combinatorial and high-throughput materials development. *Accounts of Chemical Research*, 34(3):213–221, 2001.

[Caw03a] J. N. Cawse. The combinatorial challenge. In J. N. Cawse, editor, *Experimental Design for Combinatorial and High Throughput Materials Development*, pages 1–26. John Wiley & Sons, Inc., Hoboken, New Jersey, 2003.

[Caw03b] J. N. Cawse. The combinatorial discovery array: An overview of the chapters. In J. N. Cawse, editor, *Experimental Design for Combinatorial and High Throughput Materials Development*, pages 27–38. John Wiley & Sons, Inc., Hoboken, New Jersey, 2003.

[CBK97] Y.-M. Chiang, D. Birnie, and W. D. Kingery. *Physical Ceramics*, page 188. Wiley, New York, 1997.

[CC92] W. Cao and L. E. Cross. The ratio of rhombohedral and tetragonal phases on the morphotropic phase boundary in lead zirconate titanate. *Japanese Journal of Applied Physics*, 31:1399–1402, 1992.

[CDF+99] P. Cong, R. D. Doolen, Q. Fan, D. M. Giaquinta, S. Guan, E. W. Mc Farland, D. M. Poojary, K. Self, H. W. Turner, and W. H. Weinberg. High-throughput synthesis and screening of combinatorial heterogeneous catalyst libraries. *Angewandte Chemie International Edition*, 38(4):484–488, 1999.

[CGT+98] H. Chang, C. Gao, I. Takeuchi, Y. Yoo, J. Wang, P. G. Schultz, and X.-D. Xiang. Combinatorial synthesis and high throughput evaluation of ferroelectric/dielectric thin-film libraries for microwave applications. *Applied Physics Letters*, 72(17):2185–2187, 1998.

[CKL+07] T.-S. Chan, C.-C. Kang, R.-S. Liu, L. Chen, X.-N. Liu, J.-J. Ding, J. Bao, and C. Gao. Combinatorial study of the optimization of

$Y_2O_3 : Bi, Eu$ red phosphors. *Journal of Combinatorial Chemistry*, 9:343–346, 2007.

[CLT+03] J. M. Caruthers, J. A. Lauterbach, K. T. Thomson, V. Venkatasubramian, C. M. Snively, A. Bhan, S. Katare, and G. Oskarsdottir. Catalyst design: knowledge extraction from high-throughput experimentation. *Journal of Catalysis*, 216(1):98–109, 2003.

[Cou03] European Parliament And The Council. OJ L 37, 19, 2003.

[CTX99] H. Chang, I. Takeuchi, and X.-D. Xiang. A low-loss composition region identified from thin-film composition spread of $(Ba_{(1-x-y)}Sr_xCa_y)TiO_3$. *Applied Physics Letters*, 74(8):1165–1167, 1999.

[CWS+07] A. Cardin, B. Wessler, C. Schuh, T. Steinkopff, and W. F. Maier. High throughput expermentation for the development of new piezoelectric ceramics. *Journal of Electroceramics*, 19(4):267–272, 2007.

[DAHfM06] Katalysatoren und Formulierungen DECHEMA-Arbeitskreis Hochdurchsatzforschung für Materialien. Positionspapier Hochdurchsatztechnologien in der Materialforschung. Technical report, DECHEMA, 2006.

[DZZ07a] Y. Dai, X. Zhang, and G. Zhou. Phase transitional behaviour in $K_{0.5}Na_{0.5}NbO_3$-$LiTaO_3$ ceramics. *Applied Physics Letters*, 90:262903, 2007.

[DZZ+07b] H. Du, W. Zhou, D. Zhu, S. Qu, and Z. Pei. An approach to further imporve piezoelectric properties of $K_{0.5}Na_{0.5}NbO_3$-based lead-free ceramics. *Applied Physics Letters*, 91:202907, 2007.

[EECE01] J. R. G. Evans, M. J. Edirisinghe, P. V. Coveney, and J. Eames. Combinatorial searches of inorganic materials using the ink-jet printer: Science, philosophy and technology. *Journal of the European Ceramic Society*, 21(13):2291–2299, 2001.

[FD99] M. Falcioni and M. W. Deem. A biased Monte Carlo scheme for zeolite structure solution. *Journal of Chemical Physics*, 110(3):1754–1766, 1999.

[FKPT99] L. Fahrmeir, R. Künstler, I. Pigeot, and G. Tutz. *Statistik - Der Weg zur Datenanalyse*. Springer, Berlin, Heidelberg, 1 edition, 1999.

[FS03] Frost and Sullivan. Strategic analysis of world combinatorial chemistry markets (Report A710). Technical report, Frost&Sullivan, 2003.

[FTI+06] K. Fujimoto, H. Takahashi, S. Ito, S. Inoue, and M. Watanabe. New high-throughput material-exploration system based on combinatorial chemistry and electrostatic atomization. *Applied Surface Science*, 252(7):2446–2449, 2006.

[FTSW04] K. Fujimoto, K. Takada, T. Sasaki, and M. Watanabe. Combinatorial approach for powder preparation of pseudo-ternary system $LiO_{0.5} - X - TiO_2(X : FeO_{1.5}, CrO_{1.5}$ and $NiO)$. *Applied Surface Science*, 223(1):49–53, 2004.

[FUK04] R. Funahashi, S. Urata, and M. Kitawaki. Exploration of n-type oxides by high throughput screening. *Applied Surface Science*, 223(1):44–48, 2004.

[FW05] K. Fujimoto and M. Watanabe. Preparation of pseudo-ternary library by combinatorial robot system based on wet and dry processes. *Measurement Science and Technology*, 16:41–45, 2005.

[GBP04] C. J. Gilmore, G. Barr, and J. Paisley. High-throughput powder diffraction I. A new approach to qualitative and quantitative powder diffraction pattern analysis using full pattern profiles. *Journal of Applied Crystallography*, 37:231–242, 2004.

[GHS89a] D. J. Green, R. H. J. Hannink, and M. V. Swain. *Transformation Toughening of Ceramics*, chapter Crystallography and Phase Transformations in Zirconia and its Alloys. CRC Press, Boca Raton, FL, 1 edition, 1989.

[GHS89b] D. J. Green, R. H. J. Hannink, and M. V. Swain. *Transformation Toughening of Ceramics*, chapter Micorstructure-Mechanical Behavior of Partially Stabilized Zirconia (PSZ) Materials, pages 97–155. CRC Press, Boca Raton, FL, 1 edition, 1989.

[GN72] R. C. Garvie and P. S. Nicholson. Phase analysis in zirconia systems. *Journal of the American Ceramic Society*, 55(6):303–305, 1972.

[GNK99] M. A. Gülgün, M. H. Nguyen, and W. M. Kriven. Polymerized organic-inorganic synthesis of mixed oxides. *Journal of the American Ceramic Society*, 82(3):556–560, 1999.

[Gor81] A. D. Gordon. *Classification: Methods for the Analysis of Multivariate Data*, page 33. Chapman and Hall, London, 1981.

[HA04] J. Hulliger and M. A. Awan. A "Single-Sample Concept" (SSC): A new approach to the combinatorial chemistry of inorganic materials. *Chemistry - A European Journal*, 10:4694–4702, 2004.

[HA05] J. Hulliger and M. A. Awan. "Single-Sample Concept": Theoretical model for a combinatorial approach to solid-state inorganic materials. *Journal of Combinatorial Chemistry*, 7:73–77, 2005.

[HAHW05] S. J. Henderson, J. A. Armstrong, A. L. Hector, and M. T. Weller. High-throughput mathods to optically functional oxide and oxide-nitride materials. *Journal of Materials Chemistry*, 15(15):1528–1536, 2005.

[Han70] J. J. Hanak. The "Multiple-Sample Concept" in materials research: Synthesis, compositional analysis and testing of entire multicomponent systems. *Journal of Materials Science*, 5:964–971, 1970.

[Han03] J. J. Hanak. Mutliple-Sample Concept: The forerunner of combinatorial materials science. In X.-D. Xiang and I. Takeuchi, editors, *Combinatorial Materials Synthesis*, pages 7–34. Marcel Dekker, Inc., New York, NY, 2003.

[Har03] L. Harmon. Experiment planning for combinatorial materials discovery. *Journal of Materials Science*, 38:4479–4485, 2003.

[HBL+02] I. Hahndorf, O. Buyevskaya, M. Langpape, G. Grubert, S. Kolf, E. Guillon, and M. Baerns. Experimental equipment for high-throughput synthesis and testing of catalytic materials. *Chemical Engineering Journal*, 89:119–125, 2002.

[HDS06] J. Hulliger, L. Dessauges, and T. A. Samtleben. Analysis of compositional distributions for exploring the phase space by the Single Sample Concept in ceramic combinatorial chemistry. *Journal of the American Ceramic Society*, 89(3):1072–1078, 2006.

[HH91] C. J. Howard and R. J. Hill. The polymorphs of zirconia: phase abundance and crystal structure by Rietveld analysis of neutron and X-ray diffraction data. *Journal of Materials Science*, 26:127–134, 1991.

[HLF+03] R. J. Hendershot, S. S. Lasko, M.-F. Fellmann, G. Oskarsdottir, W. N. Delgass, C. M. Snively, and J. Lauterbach. A novel reactor system for high throughput catalyst testing under realistic conditions. *Applied Catalysis A*, 254(1):107–120, 2003.

[HS94] R. H. J. Hannink and M. V. Swain. Progress in transformation toughening of ceramics. *Annual Review Materials Science*, 24:359–408, 1994.

[HSC06] M. J. Harvey, D. Scott, and P. V. Coveney. An integrated instrument control and informatics system for combinatorial materials research. *Journal of Chemical Information and Modeling*, 46(3):1026–1033, 2006.

[HSWS08] R.-P. Herber, C. Schröter, B. Wessler, and G. A. Schneider. High throughput screening of piezoelectric response of ferroelectric thin films with automated scanning probe microscopy. *Thin Solid Films*, 516:8609–8612, 2008.

[JCJ71] B. Jaffe, W. Cook, and H. Jaffe. *Piezoelectric Ceramics*, pages 193–194. Academic, New York, 1971.

[JFK+01] Z. Jin, T. Fukumura, M. Kawasaki, K. Ando, H. Saito, T. Sekiguchi, Y. Z. Yoo, M. Murakami, Y. Matsumoto, T. Hasagewa, and

H. Koinuma. High throughput fabrication of transition-metal-doped epitaxial ZnO thin films: A series of oxide-diluted magnetic semiconductors and their properties. *Applied Physics Letters*, 78(24):3824–3826, 2001.

[JMF+00] Z. W. Jin, M. Murakami, T. Fukumura, Y. Matsumoto, A. Ohtomo, M. Kawasaki, and H. Koinuma. Combinatorial laser mbe synthesis of 3d ion doped epitaxial ZnO thin films. *Journal of Crystal Growth*, 214(1):55–58, 2000.

[JSP+99] B. Jandeleit, D. J. Schaefer, T. S. Powers, H. W. Turner, and W. H. Weinberg. Kombinatorische Materialforschung und Katalyse. *Angewandte Chemie*, 111:2648–2689, 1999.

[KBL+02] M. Kilo, G. Borchardt, B. Lesage, S. Weber, S. Scherrer, M. Schröder, and M. Martin. Y and Zr tracer diffusion in yttria-stabilized zirconia at temperatures between 1250 k and 2000 k. In *7th Conference of the European-Ceramic-Society*, pages 453–457, 2002.

[KK75] M. Kosec and D. Kolar. On activated sintering and electrical porperties of $NaKNbO_3$. *Materials Research Bulletin*, 10:335–340, 1975.

[KKMN98] D. G. Kleinbaum, L. L. Kuper, K. E. Muller, and A. Nizam. *Applied Regression Analysis and Other Multivariate Methods*. Duxbury Press, Pacific Grove, 2 edition, 1998.

[KLSM98] J. Klein, C. W. Lehmann, H.-W. Schmidt, and W. F. Maier. Kombinatorische Materialbibliothek im μg-Maßstab am Beispiel der Hydrothermalsynthese. *Angewandte Chemie*, 110(24):3557–3561, 1998.

[KSD+65] K. Kennedy, T. Stefansky, G. Davy, V. F. Zackay, and E. R. Parker. Rapid method for determining ternary-alloy phase diagrams. *Journal of Applied Physics*, 36(12):3808–3810, 1965.

[Lan82] F. F. Lange. Transformation toughening III - Experimental observations in the ZrO_2-Y_2O_3 system. *Journal of Materials Science*, 17:240–246, 1982.

[Lew00] J. A. Lewis. Colloidal processing of ceramics. *Journal of the American Ceramic Society*, 83(10):2341–2359, 2000.

[LRWE04] Q. Li, V. Rudolph, B. Weigl, and A. Earl. Interparticle van der waals force in powder flowability and compactibility. *International Journal of Pharmaceutics*, 280(1):77–93, 2004.

[ME02] M. M. Mohebi and J. R. G. Evans. A drop-on-demand ink-jet printer for combinatorial libraries and functionally graded ceramics. *Journal of Combinatorial Chemistry*, 4(4):267–274, 2002.

[MH03] A. J. Moulson and J. M. Herbert. *Electroceramics - Materials, Properties, Applications*, pages 354–358. Wiley, Chichester, 2003.

[Mor91] E. Morgan. *Chemometrics: experimental design.* Wiley, Chichester, 1991.

[MS67] N. C. Miller and G. A. Shirn. Co-sputtered $Au - SiO_2$ cermet films. *Applied Physics Letters*, 10(3):86–88, 1967.

[MSS07] W. F. Maier, K. Stöwe, and S. Sieg. Combinatorial and high-throughput materials science. *Angewandte Chemie International Edition*, 46:6016–6067, 2007.

[MYE06] M. M. Mohebi, S. Yang, and J. R. G. Evans. Compositional control in solid freeforming; fabrication of 3D FGM. *Key Engineering Materials*, 317–318:151–154, 2006.

[MYK+05] M. Matsubara, T. Yamaguchi, K. Kikuta, T. Yogo, and S. Hirano. Effect of li substitution on the piezoelectric properties of potassium sodium niobate ceramics. *Japanese Journal of Applied Physics*, 44(8):3136–6142, 2005.

[MYS+05] M. Matsubara, T. Yamaguchi, W. Sakamoto, K. Kikuta, T. Yogo, and S. Hirano. Processing and piezoelectric properties of lead-free $(K, Na)(Nb, Ta)O_3$ ceramics. *Journal of the American Ceramic Society*, 88(5):1190–1196, 2005.

[OCK+04] I. Ohkubo, H. M. Christen, P. Khalifah, S. Sathyamurthy, H. Y. Zhai, C. M. Rouleau, D. G. Mandrus, and D. H. Lowndes. Continuous composition-spread thin films of transition metal oxides by pulsed-laser deposition. *Applied Surface Science*, 223(1):35–38, 2004.

[PM07] R. A. Potyrailo and W. F. Maier. Combinatorial materials and catalysts development: Where are we and how far can we go? In R. A. Potyrailo and W. F. Maier, editors, *Combinatorial and High-Throughput Discovery and Optimization of Catalysts and Materials*, pages 3–16. Taylor & Francis Group, LLC, Boca Raton, FL, 2007.

[PT05] R. A. Potyrailo and I. Takeuchi. Role of high-throughput characterization tools in combinatorial materials science. *Measurement Science & Technology*, 16(1):1–4, 2005.

[PZC+07a] R. C. Pullar, Y. Zhang, L. Chen, S. Yang, J. R. G. Evans, and N. McN. Alford. Manufacture and measurement of combinatorial libraries of dielectric ceramics part I: Physical characterisation of $Ba_{1-x}Sr_xTiO_3$ libraries. *Journal of the European Ceramic Society*, 27(13–15):3861–3865, 2007.

[PZC+07b] R. C. Pullar, Y. Zhang, L. Chen, S. Yang, J. R. G. Evans, P. K. Petrov, A. N. Salak, D. A. Kiselev, A. L. Kholkin, V. M. Ferreira, and N. McN. Alford. Manufacture and measurement of combinatorial libraries of dielectric ceramics part II: Dielectric measurements of $Ba_{1-x}Sr_xTiO_3$ libraries. *Journal of the European Ceramic Society*, 27(16):4437–4443, 2007.

[RAM03] H. M. Reichenbach, H. An, and P. J. McGinn. Combinatorial synthesis and characterization of mixed metal oxides for soot combustion. *Applied Catalysis B*, 44(4):347–354, 2003.

[Ran90] M. Randić. Design of molecules with desired properties. In M. A. Johnson and G. M. Maggiora, editors, *Concepts and Applications of Molecular Similarity*, pages 77–146. Wiley-VCH Verlag GmbH & Co KGaA, New York, 1990.

[RCH84] M. Ruehle, N. Claussen, and A. H. Heuer. Microstructural studies of Y_2O_3-containing tetragonal ZrO_2 polycrystal (Y-TZP). In N. Claussen and M. Ruehle, editors, *Advances in Ceramics, Volume 12*, pages 352–370. American Ceramic Society, Columbus, Ohio, 1984.

[RH84] M. Ruehle and A. H. Heuer. Phase transformation in ZrO_2-containing ceramics: II, the martensitic reaction in $t-ZrO_2$. In N. Claussen and M. Ruehle, editors, *Advances in Ceramics, Volume 12*, pages 14–32. American Ceramic Society, Columbus, Ohio, 1984.

[RIL+03] U. Rodemerck, P. Ignaszewski, M. Lucas, P. Claus, and M. Baerns. Parallel synthesis and fast screening of heterogeneous catalysts. *Topics in Catalysis*, 13(3):249–252, 2003.

[RM01] H. M. Reichenbach and P. J. McGinn. Combinatorial synthesis of oxide powders. *Journal of Materials Research*, 16(4):967–974, 2001.

[RSG+98] E. Reddington, A. Sapienza, B. Gurau, R. Viswanathan, S. Sarangapani, E. S. Smotkin, and T. E. Mallouk. Combinatorial electrochemistry: A highly parallel, optical screening method for discovery of better electrocatalysts. *Science*, 280:1735–1737, 1998.

[RSR+07] D. Rende, K. Schwarz, U. Rabe, W. F. Maier, and W. Arnold. Combinatorial synthesis of thin mixed oxide films and automated study of their piezoelectric properties. *Progesss in Solid State Chemistry*, 35:361–366, 2007.

[Sch04] F. Schüth. Hochdurchsatz-Untersuchungen. In R. Dittmeyer, W. Keim, G. Kreysa, and A. Oberholz, editors, *Winnacker-Küchler. Chemische Technik: Prozesse und Produkte*, volume 2, pages 549–585. Wiley-VCH Verlag GmbH & Co KGaA, Weinheim, 2004.

[SCR84] H. Schubert, N. Claussen, and M. Ruehle. Preparation of Y_2O_3-stabilized tetragonal polycrystals (Y-TZP) from different powders. In N. Claussen and M. Ruehle, editors, *Advances in Ceramics, Volume 12*, pages 766–783. American Ceramic Society, Columbus, Ohio, 1984.

[SHT+04] Y. Saito, T. Hisaaki, T. Toshihiko, T. Nonoyama, K. Takatori, T. Homma, T. Nagaya, and M. Nakamura. Lead-free piezoceramics. *Nature*, 432(4):84–87, 2004.

[Sie98] A. Siegel. Combinatorial synthesis of advanced ceramic materials. *Canadian Ceramics Quarterly*, 67(2):17–21, 1998.

[SS07] H. Salmang and H. Scholze. *Keramik*, pages 817–834. Springer-Verlag, Berlin, 7 edition, 2007.

[ST06] Y. Saito and H. Takao. High performance lead-free piezoelectric ceramics in the $(K, Na)NbO_3$-$LiTaO_3$ solid solution system. *Ferroelectrics*, 338:17–32, 2006.

[Sta82] J. N. Staniforth. Advances in powder mixing and segregation in relation to pharmaceutical processes. *Int. J. Pharm. Tech. & Prod. Mfr.*, 3:1–12, 1982.

[Ste04] A. Steland. *Mathematische Grundlagen der empirischen Forschung*. Springer, Berlin, Heidelberg, New York, 2004.

[Sun03] T. X. Sun. Fractional masking methods in combinatorial synthesis of functional materials. In J. N. Cawse, editor, *Experimental Design for Combinatorial and High Throughput Materials Development*, pages 39–53. John Wiley & Sons, Inc., Hoboken, New Jersey, 2003.

[SWY+97] X.-D. Sun, K.-A. Wang, Y. Yoo, W. G. Wallace-Freedman, C. Gao, X.-D. Xiang, and P. G. Schultz. Solution-phase synthesis of luminescent materials libraries. *Advanced Materials*, 9(13):1046–1049, 1997.

[TE98] W. D. Teng and M. J. Edirisinghe. Development of ceramic inks for direct continuous jet printing. *Journal of the American Ceramic Society*, 81(4):1033–1036, 1998.

[TEE97] W. D. Teng, M. J. Edirisinghe, and J. R. G. Evans. Optimization of dispersion and viscosity of a ceramic jet printing. *Journal of the American Ceramic Society*, 80(2):486–490, 1997.

[TYS84] H. Toraya, M. Yoshimura, and S. Somiya. Calibration curve for quantitative analysis of the monoclinic-tetragonal ZrO_2. *Journal of the American Ceramic Society*, 67(6):C119–C121, 1984.

[vDS04] R. B. van Dover and L. F. Schneemeyer. The codeposited composition spread approach to high-throughput discovery/exploration of inorganic materials. *Macromolecular Rapid Communications*, 25(1):150–157, 2004.

[vDSFH99] R. B. van Dover, L. F. Schneemeyer, R. M. Fleming, and H. A. Huggins. A high-throughput search for electronic materials - thin-film dielectrics. *Biotechnology and Bioengineering (Combinatorial Chemistry)*, 61(4):217–225, 1999.

[VGKM04] C. J. Vess, J. Gilmore, N. Kohrt, and P. J. McGinn. Combinatorial synthesis of oxide powders with an autopipetting system. *Journal of Combinatorial Chemistry*, 6(1):86–90, 2004.

[VW01] H. J. Venables and J. I. Wells. Powder mixing. *Drug Development and Industrial Pharmacy*, 27(7):599–612, 2001.

[WAK+06] R. Wendelbo, D. E. Akporiaye, A. Karlsson, M. Plassen, and A. Olafsen. Combinatorial hydrothermal synthesis and characterisation of perovskites. *Journal of the European Ceramic Society*, 26:849–859, 2006.

[Wil68] J. C. Williams. The mixing of dry powders. *Powder Technology*, 2:13–20, 1968.

[Wil90] P. Willett. *Concepts and Applications of Molecular Similarity*, page 47. Wiley, New York, 1990.

[WW05] O. L. Warren and T. J. Wyrobek. Nanomechanical property screening of combinatorial thin-film libraries by nanoindentation. *Measurement Science And Technology*, 16:100–110, 2005.

[Xia98] X.-D. Xiang. Combinatorial synthesis and high throughput evaluation of functional oxides - An integrated materials chip approach. *Materials Science and Engineering B*, 56(2–3):246–250, 1998.

[Xia99] X.-D. Xiang. Combinatorial materials synthesis and high-throughput screening: An integrated materials chip approach to mapping phase diagrams and discovery and optimization of functional materials. *Biotechnology and Bioengineering (Combinatorial Chemistry)*, 61(4):287–241, 1999.

[XSB+95] X.-D. Xiang, X. Sun, G. Briceno, Y. Lou, K.-A. Wang, H. Chang, W. G. Wallace-Freedman, S.-W. Chen, and P. G. Schultz. A combinatorial approach to materials discovery. *Science*, 268:1738–1740, 1995.

[XT03] X.-D. Xiang and I. Takeuchi. Introduction. In X.-D. Xiang and I. Takeuchi, editors, *Combinatorial Materials Synthesis*, pages 1–6. Marcel Dekker, Inc., New York, NY, 2003.

[YE04a] S. Yang and J. R. G. Evans. Acoustic control of powder dispensing in open tubes. *Powder Technology*, 139:55–60, 2004.

[YE04b] S. Yang and J. R. G. Evans. Device for preparing combinatorial libraries in powder metallurgy. *Journal of Combinatorial Chemistry*, 6(4):549–555, 2004.

[Yos88] M. Yoshimura. Phase stability of zirconia. *Ceramic Bulletin*, 67:1950–1955, 1988.

[ZCYE07] Y. Zhang, L. Chen, S. Yang, and J. R. G. Evans. Thick film ceramic combinatorial libraries: The substrate problem. *QSAR & Combinatorial Science*, 26(10):1036–1045, 2007.

[ZFKA05] W. Zhang, M. J. Fasolka, A. Karim, and E. J. Amis. An informatics infrastructure for combinatorial and high-throughput materials research built on open source code. *Measurement Science and Technology*, 16(1):261–269, 2005.

[Zha01] J.-C. Zhao. A combinatorial approach for efficient mapping of phase diagrams and properties. *Journal of Materials Research*, 16(6):1565–1578, 2001.

[ZXS07] S. Zhang, R. Xia, and T. R. Shrout. Lead-free piezoelectric ceramics vs. PZT? *Journal of Electroceramics*, 19(4):251–257, 2007.

Appendix A

Phase analysis data

Numerical data of phase analysis in Y-TZP system described in chapter 4.2.3:

Library	**Sample**	**Y_2O_3 [mol-%]**	**mean monoclinic phase [weight-%]**
Reference	1	0	100,0
Reference	2	1	99,9
Reference	3	2	84,7
Reference	4	3	60,3
Reference	5	5	14,4
Reference	6	7,5	9,4
Reference	7	10	0,2
5 mol-%, dry	1	0,5	93,0
5 mol-%, dry	2	1	86,2
5 mol-%, dry	3	1,5	84,6
5 mol-%, dry	4	2	63,1
5 mol-%, dry	5	2,5	66,8
5 mol-%, dry	6	3	60,4
5 mol-%, dry	7	3,5	38,9
5 mol-%, dry	8	4	30,2
5 mol-%, dry	9	4,5	19,1
5 mol-%, dry	10	5	11,5
10 mol-%, dry	1	0,5	93,3
10 mol-%, dry	2	1	90,6
10 mol-%, dry	3	1,5	87,1
10 mol-%, dry	4	2	80,7
10 mol-%, dry	5	2,5	76,2

Continued on next page

Library	Sample	Y_2O_3 [mol-%]	mean monoclinic phase [weight-%]
10 mol-%, dry	6	3	68,9
10 mol-%, dry	7	3,5	58,9
10 mol-%, dry	8	4	57,0
10 mol-%, dry	9	4,5	49,5
10 mol-%, dry	10	5	38,6
5 mol-%, cyclohexane	1	0,5	94,3
5 mol-%, cyclohexane	2	1	87,4
5 mol-%, cyclohexane	3	1,5	75,7
5 mol-%, cyclohexane	4	2	68,2
5 mol-%, cyclohexane	5	2,5	60,6
5 mol-%, cyclohexane	6	3	53,6
5 mol-%, cyclohexane	7	3,5	38,1
5 mol-%, cyclohexane	8	4	29,0
5 mol-%, cyclohexane	9	4,5	22,5
5 mol-%, cyclohexane	10	5	13,7
10 mol-%, cyclohexane	1	0,5	95,0
10 mol-%, cyclohexane	2	1	89,0
10 mol-%, cyclohexane	3	1,5	78,0
10 mol-%, cyclohexane	4	2	69,8
10 mol-%, cyclohexane	5	2,5	71,1
10 mol-%, cyclohexane	6	3	69,9
10 mol-%, cyclohexane	7	3,5	65,2
10 mol-%, cyclohexane	8	4	53,3
10 mol-%, cyclohexane	9	4,5	46,6
10 mol-%, cyclohexane	10	5	36,2
5 mol-%, acetone	1	0,5	95,0
5 mol-%, acetone	2	1	88,2
5 mol-%, acetone	3	1,5	80,3
5 mol-%, acetone	4	2	77,8
5 mol-%, acetone	5	2,5	59,8
5 mol-%, acetone	6	3	55,8

Continued on next page

Library	Sample	Y_2O_3 [mol-%]	mean monoclinic phase [weight-%]
5 mol-%, acetone	7	3,5	40,6
5 mol-%, acetone	8	4	26,8
5 mol-%, acetone	9	4,5	20,0
5 mol-%, acetone	10	5	11,8
10 mol-%, acetone	1	0,5	95,5
10 mol-%, acetone	2	1	89,1
10 mol-%, acetone	3	1,5	83,8
10 mol-%, acetone	4	2	69,7
10 mol-%, acetone	5	2,5	64,6
10 mol-%, acetone	6	3	59,2
10 mol-%, acetone	7	3,5	54,0
10 mol-%, acetone	8	4	45,9
10 mol-%, acetone	9	4,5	38,2
10 mol-%, acetone	10	5	38,5
5 mol-%, ethanol	1	0,5	94,8
5 mol-%, ethanol	2	1	86,9
5 mol-%, ethanol	3	1,5	77,6
5 mol-%, ethanol	4	2	76,6
5 mol-%, ethanol	5	2,5	69,9
5 mol-%, ethanol	6	3	48,9
5 mol-%, ethanol	7	3,5	39,4
5 mol-%, ethanol	8	4	31,4
5 mol-%, ethanol	9	4,5	21,8
5 mol-%, ethanol	10	5	13,5
10 mol-%, ethanol	1	0,5	n.a.
10 mol-%, ethanol	2	1	89,7
10 mol-%, ethanol	3	1,5	86,4
10 mol-%, ethanol	4	2	81,0
10 mol-%, ethanol	5	2,5	72,9
10 mol-%, ethanol	6	3	63,7
10 mol-%, ethanol	7	3,5	55,4

Continued on next page

Library	**Sample**	**Y_2O_3 [mol-%]**	**mean monoclinic phase [weight-%]**
10 mol-%, ethanol	8	4	52,8
10 mol-%, ethanol	9	4,5	50,0
10 mol-%, ethanol	10	5	45,6

Table A.1: Numerical data of phase analysis in Y-TZP system.

Appendix B

Linear regression analysis

Linear regression analysis used in section 4.3 according to method of least squares.

Linear Model:

$$y = \beta_0 + \beta_1 \cdot x \tag{B.1}$$

Regression coefficients:

$$\beta_1 = \frac{\sum_{i=1}^{n} (x_i - \overline{x})(y_i - \overline{y})}{\sum_{i=1}^{n} (x_i - \overline{x})^2} \tag{B.2}$$

$$\beta_0 = \overline{y} - \beta_1 \cdot \overline{x} \tag{B.3}$$

Correlation coefficient:

$$r = \frac{\sum_{i=1}^{n} (x_i - \overline{x})(y_i - \overline{y})}{\sqrt{\sum_{i=1}^{n} (x_i - \overline{x})^2 \sum_{i=1}^{n} (y_i - \overline{y})^2}}, \tag{B.4}$$

where r^2 is the coefficient of determination with $r^2 = [0, ..., 1]$ being the fraction of variance in y that can be explained by the model.

Appendix C

Matlab program for homogeneity test

Matlab program used for the homogeneity test described in section 5.3.1.2 and schematically shown on figure 5.9:

```
%21.09.2008 - Tobias Stegk
clear
CalleIMP=importdata('path\NumericalResults1.txt');
%Import the data from the first column of the polySNAP-file
%containing the correlation coefficients between
%zero-pattern and all patterns.
%----%
%----%
CSelfIMP=importdata('path\NumericalResults2.txt');
%Import the data from the first column of the polySNAP-file
%containing the correlation coefficients between
%zero-pattern and six patterns of the same location.
%----%
%----%
CIMP=zeros(757,1);
%Preparation of matrix CIMP.
%----%
%----%
CIMP(1:7,1)=CSelfIMP;
CIMP(8:757)=CalleIMP(2:751,1);
%CIMP contains all correlation coefficients.
%----%
%----%
EVAL=zeros(6,126);
%Preparation of matrix EVAL.
%----%
%----%
i=1;
j=2;
```

```
while j<=757
    EVAL(:,i)=CIMP(j:j+5,1);
    i=i+1;
    j=j+6;
end
%EVAL contains the same coefficients as CIMP but ordered
%in columns where the first column holds the correlation
%coefficients of the patterns from the same location.
%----%
%----%
H=zeros(125,2);
i=1;
while i<=125
    H(i,1)=i;
    i=i+1;
end
%Preparation of matrix H for results of F-test. First
%column is numbered consecutively.
%----%
%----%
i=2;
j=1;
while i<=126
    H(j,2)=vartest2(EVAL(:,1),EVAL(:,i));
    i=i+1;
    j=j+1;
end
%Second column contains result of F-test between variance
%of correlation coefficients samples vs. zero-pattern and
%variance of correlation coefficients
%same-location vs. zero-pattern.
%0 not heteroscedastic - 1 heteroscedastic.
%----%
%----%
i=1;
j=1;
while i<=125
    if H(i,2)==1
        X(j,1)=H(i,1);
    end
    if H(i,2)==1
```

```
        j=j+1
    end
    i=i+1;
end
%Write matrix of results X containing the sample numbers of
%heteroscedastic samples.
```

Lebenslauf

Persönliche Daten

Name	Tobias Stegk
Geburtsdatum	20. Februar 1976
Geburtsort	Kronberg

Schulbildung

1982 - 1986	Grundschulen Nord und West in Brunsbüttel
1986 - 1995	Gymnasien Rheinfelden und Brunsbüttel Abschluss: Allgemeine Hochschulreife

Berufsausbildung

1996 - 1999	Warsteiner Brauerei Haus Cramer GmbH & Co KG Abschluss: IHK-Prüfungszeugnis “Brauer und Mälzer”

Studium

Okt. 1998 - April 2004	Technische Universität Hamburg-Harburg Studiengang General Engineering Science Abschluss: Bachelor of Science
Okt. 1998 - Dez. 2004	Technische Universität Hamburg-Harburg Studiengang Verfahrenstechnik Abschluss: Diplom

Berufliche Tätigkeit

Feb. 2005 - Dez. 2008	Wissenschaftlicher Mitarbeiter Institut für Keramische Hochleistungswerkstoffe Technischen Universität Hamburg-Harburg
seit Mai 2009	Post doc Risø Nationallaboratoriet for Bæredygtig Energi Danmarks Tekniske Universitet

Roskilde, den 22. Juni 2009